POLITECNICO DI MILANO

Scuola di Ingegneria Industriale e dell'Informazione

Corso di Laurea Magistrale in Ingegneria Nucleare

NEUTRON TRANSPORT IN STOCHASTIC GEOMETRIES

Benchmark calculations and study of a melted reactor core

Relatore: Giacobbo Francesca Celsa

Correlatori: Mazzolo Alain

Malvagi Fausto

Tesi di Laurea di:

SOMAINI ALICE, matricola 783515

Anno Accademico 2013-2014

Abstract

The interest in solving the equation of transport in stochastic media has continued to increase these last years. Binary stochastic mixtures are particularly studied because of their several applications (diffusion of radioactive contaminants in geological media, transport in turbolent media for the inertial confinement fusion,crossing of neutrons or γ rays throughout concrete shields, ...).

The geometries we deal with in this present thesis are assumed to be Markovian, which is never the case in usual environments, but which is a necessary approximation.

We consider a two-suite neutron transport problem for which other benchmark results (based on a stochastic geometry composed by a labelled plane filled with two alternating materials) were already performed. The geometry we use is composed by random polygons built in a plane and it is Markovian in two dimensions, thus it better represents a real stochastic geometry. The goal of our benchmark calculations is to compare and analyse the previous obtained results and to test the validity of different elaborated models of the problem.

The creation of the Markovian planar geometry is done in accordance with the process described by Switzer in 1964, which allows to construct a two-dimensional geometry with Markovian properties. For each one of the sev-

eral geometry realizations, we solve the neutron transport problem with the Monte Carlo code TRIPOLI-4, developed at CEA. Then, we average the results and we build histograms to have information also on the distributions of the sought quantities.

In the second part of the thesis, we use the same procedure of Markovian geometry creation and stochastic resolution of transport equation to simulate a melted core of a PWR reactor. In this case, we do not know the distributions of the materials composing the core and we study three cases, each one characterized by a different material mixing level. We obtain and analyze the value of k_{eff}, to see how it varies and distributes depending on the way the materials actually mix after the fusion of the core.

Sommario

Negli ultimi anni è andato crescendo l'interesse nella risoluzione dell'equazione del trasporto in mezzi stocastici. In particolare, vengono studiate le miscele binarie stocastiche, utilizzabili in molti campi (diffusione dei contaminanti radioattivi in mezzi geologici, trasporto in mezzi turbolenti per il confinamento della fusione inerziale, attraversamento di schermi di cemento da parte di neutroni e di raggi γ,..). Le geometrie che trattiamo in questo lavoro sono supposte essere markoviane, cosa che non rispecchia la realtà della maggior parte dei casi che queste geometrie cercano di simulare, ma risulta essere un'approssimazione necessaria.

Abbiamo preso in considerazione un problema di trasporto per cui si avevano già dei risultati di riferimento (ottenuti da una geometria planare composta da strati alternati di due materiali). La nostra geometria è invece composta da poligoni creati in modo casuale su un piano ed è markoviana in due dimensioni, cosa che la rende più affine e rappresentativa delle reali geometrie stocastiche. Lo scopo dei nostri calcoli di riferimento è quello di confrontare e analizzare i risultati precedentemente ottenuti e di testare la validità dei modelli del problema che sono stati elaborati.

La realizzazione della geometria markoviana è basata sul processo descritto da Switzer nel 1964 che permette di creare una geometria planare con proprietà markoviane. Per ognuna delle molte realizzazioni geometriche effet-

tuate, abbiamo risolto il problema di trasporto neutronico con il codice Monte Carlo creato al CEA, TRIPOLI-4®. Abbiamo poi mediato i risultati e costruito gli istogrammi per avere informazioni anche sulle distribuzioni delle quantità cercate.

Nella seconda parte della tesi, abbiamo utilizzato la stessa procedura di realizzazione di geometrie markoviane e di risoluzione dell'equazione del trasporto per simulare un nocciolo fuso di un PWR. Anche in questo caso, non conosciamo le distribuzioni dei materiali che compongono il core, ma solo le loro proprietà. Abbiamo analizzato tre diversi casi, ognuno caratterizzato da un certo livello di mescolanza degli elementi del nocciolo e abbiamo cercato il valore del k_{eff}, per vedere come varia e come si distribuisce quando i materiali si mescolano in modo casuale gli uni con gli altri.

Sommario esteso

Il seguente lavoro di tesi è stato realizzato durante uno stage di sei mesi presso il laboratorio LTSD (Laboratoire de Transport Stochastique et Déterministe) del centro di ricerca CEA (Commissariat à l'énérgie atomique) di Saclay.
L'argomento verte sul problema del trasporto neutronico in dominî costituiti da geometrie stocastiche. Una geometria è definita stocastica quando dei materiali costituenti si conoscono le proprietà, ma non la distribuzione. Esse hanno varie applicazioni in molteplici campi della fisica: dal trasporto di contaminanti in mezzi geologici al trasporto in mezzi turbolenti per il confinamento della fusione inerziale. In questo caso, si analizza il problema della risoluzione dell'equazione del trasporto neutronico in geometrie stocastiche.
Per affrontare questo problema ci sono più strade: la prima è concepire un modello e quindi un'equazione (o un sistema di equazioni) che tenga (tengano) conto della stocasticità del dominio.
La seconda consiste nel realizzare un elevato numero di geometrie aleatorie (tenendo conto delle proprietà statistiche dei mezzi) e risolvere per ognuna di esse l'equazione, ormai deterministica in quanto nota la geometria, per infine mediarne i risultati e ottenere le medie d'insieme.
Un ulteriore metodo di risoluzione del problema è quello di costruire un algoritmo Monte Carlo che permetta di trovare già in una sola simulazione la media d'insieme, ovviamente inglobando al suo interno l'informazione della

stocasticità del dominio.

Noi abbiamo perseguito la seconda via, realizzando dei calcoli di riferimento per un problema di trasporto neutronico noto e per cui si hanno già dei precedenti risultati di benchmark. Anche se il procedimento è uguale (realizzare un gran numero di geometrie aleatorie, risolvere l'equazione e mediare), ciò che principalmente cambia tra i primi calcoli di riferimento (a cui nella tesi ci si riferisce come Benchmark 1D) e i nostri è il tipo di geometria aleatoria. Nei calcoli di benchmark precedentemente effettuati, [1], la geometria aleatoria è una lastra piana formata da una serie di spessori di due materiali alternati l'uno con l'altro lungo l'asse x (da 0 ad L). In questo caso, la dimensione stocastica è solo una: quella lungo l'asse x. I valori degli spessori dei due materiali vengono estratti da una distribuzione esponenziale. Ogni materiale è caratterizzato da uno spessore medio, che è la media della distribuzione esponenziale e che viene chiamato anche corda media, e da una probabilità p_i di trovare il materiale i in ogni punto del dominio ($i = 0, 1$). Suddetta geometria è quindi markoviana [1] in una sola dimensione (x) e per questo i risultati sono nominati Benchmark 1D. Per ogni geometria realizzata, l'equazione del trasporto monodirezionale viene risolta con metodi deterministici [1] e vengono poi mediati tutti i risultati.

La geometria su cui abbiamo effettuato i calcoli di riferimento è diversa da quella precedentemente descritta: è un piano costituito da una serie di poligoni realizzati aleatoriamente gettando delle rette in modo randomico su un quadrato di lato L, secondo il processo descritto da Switzer, [11]. Si costruisce così una geometria con proprietà markoviane in due direzioni, x e y, che costituisce la geometria del Benchmark 2D. Per ogni realizzazione della geometria, abbiamo risolto il problema del trasporto con il codice Monte

[1] per la definizione di markovianità vedere Cap 2.2.1

Carlo TRIPOLI-4®, creato al laboratorio SERMA di Saclay.
Rispetto alla geometria planare stratificata, quest'ultima è meglio rappresentativa dei reali mezzi stocastici: per questo, i risultati ottenuti vengono considerati più affidabili di quelli di Benchmark 1D e sono utilizzati per validare e analizzare i modelli, che forniscono una soluzione meno dispendiosa in tempo ed energie, ma che necessita conferma di affidabilità.
Quindi questo lavoro, anche se lungo e complesso nella messa in atto, è indispensabile per sapere quale modello è migliore, oltre a dare informazioni non solo sui valori medi, ma anche sulle distribuzioni.
Nella seconda parte della tesi, abbiamo analizzato un altro tipo di geometria aleatoria: quella costituita dal core di un reattore che ha subito fusione. In questo caso, non si conoscono le distribuzioni dei materiali contenuti all'interno ma ne sono note le proprietà. Dopo aver realizzato molteplici geometrie markoviane e risolto il problema di criticità con TRIPOLI-4®, abbiamo analizzato il valore e la distribuzione del k_{eff} in tre casi, ognuno con un diverso grado di mescolamento dei materiali.

Contents

List of Figures

List of Tables

Chapter 1

Stochastic geometries

In the last twenty years, there has been a constant interest in solving the equation of transport in stochastic media. In particular, binary stochastic mixtures are studied because of their numerous applications, concerning the diffusion of radioactive contaminants in geologic media, the crossing of neutrons or γ rays throughout concrete shields and the transport in turbulent media for the inertial confinement fusion, as well as for high-temperature gas-cooled reactors.

In all these cases, the precise composition of the two (or more) elements inside the medium is not known and we only have a statistical description: we have informations on the inner structure of the media only in a statistical sense, even if the cross section of the constituent materials are known.

Moreover, the heterogeneity of the media affects its transport properties.

First, in a stochastic scattering medium, also the effect of bypassing obstacles has to be considered: particles can bypass "obstacles" (opaque material grains) found along their path and pass through the mixture without interacting with all materials.

This effect depends upon the properties of the elements composing the medium,

but also on its topology, which defines the possible particle paths. Since this effect is different for each physical realization of the stochastic media, the study of the transport problem deals with the average effect of heterogeneity over all possible realizations, and with its fluctuations.

Even when the inner structure of the medium is known, the transport equation is too complicated to be solved analytically: an estimate for the transport solution can be obtained using either numerical simulations or simplified models of the transport process.

The solution with numerical simulations implies the construction of a large number of stochastic realizations of the media and the solution of each of them with deterministic or Monte Carlo codes.

In this case, it is needed a way to simulate the randomly mixed materials.

One method to create the stochastic geometries is that of simulating the trajectory of the neutrons by sampling the distributions of chords in the different materials composing the medium.

Simple models of stochastic media assume that the chord length distribution inside each material is exponential: i.e., the geometry is a Markovian one.

For binary stochastic media it is often assumed that the geometry has Markovian properties, even if it is never the case in usual environments. For geometries of importance, such as those consisting of randomly placed disks in two dimensions or spheres in three dimensions, the Markovian hypothesis is not strictly valid outside the disks (or the spheres) and never inside, as recently shown [9].

However, statistical geometries are often constructed on the Markovian model.

The other approach to the transport problem in stochastic mixtures is that of using simplified models for the transport process.

In the next chapter we will analyse both the numerical simulation and the

analytical solutions and we will compare their results with our Benchmark. First, we will discuss, in a general manner, the transport problem in a stochastic media.

1.1 *Transport in statistical setting*

Starting from the integro-differential transport equation:

$$\begin{aligned}\frac{1}{v}\frac{\partial\psi(\mathbf{r},\mathbf{\Omega},E)}{\partial t}+\mathbf{\Omega}\cdot\nabla\psi(\mathbf{r},\mathbf{\Omega},E)+\sigma(\mathbf{r},E)\psi(\mathbf{r},\mathbf{\Omega},E)=S(\mathbf{r},\mathbf{\Omega},E)\\+\int_0^\infty dE'\int_{4\pi}d\mathbf{\Omega}'\sigma_s(\mathbf{r},E'\to E,\mathbf{\Omega}'\cdot\mathbf{\Omega})\psi(\mathbf{r}',\mathbf{\Omega}',E')\end{aligned}\tag{1.1}$$

we consider the time independent formulation:

$$\begin{aligned}\mathbf{\Omega}\cdot\nabla\psi(\mathbf{r},\mathbf{\Omega},E)+\sigma(\mathbf{r},E)\psi(\mathbf{r},\mathbf{\Omega},E)=S(\mathbf{r},\mathbf{\Omega},E)\\+\int_0^\infty dE'\int_{4\pi}d\mathbf{\Omega}'\sigma_s(\mathbf{r},E'\to E,\mathbf{\Omega}'\cdot\mathbf{\Omega})\psi(\mathbf{r}',\mathbf{\Omega}',E')\end{aligned}\tag{1.2}$$

with the boundary and initial conditions:

$$\psi(\mathbf{r_s},E,\mathbf{\Omega},t)=\Gamma(\mathbf{r_s},E,\mathbf{\Omega},t),\qquad \mathbf{n}\cdot\mathbf{\Omega}<0 \tag{1.3}$$

where Γ is a specified function of its arguments, $\mathbf{r_s}$ is a point on the surface, and $\mathbf{n}$ is a unit outward normal vector at this point. An important special case of Eq. (1.3) is the so-called "vacuum" or "free surface" boundary condition:

$$\psi(\mathbf{r_s},E,\mathbf{\Omega},t)=0,\qquad \mathbf{n}\cdot\mathbf{\Omega}<0 \tag{1.4}$$

This boundary condition corresponds to no particle entering the system through its bounding surface.

In the time variable, we assume that the range of interest is $0 \leq t < \infty$ and, hence, we need to specify the initial condition at $t = 0$. This is the temporal boundary condition, also called the initial condition:

$$\psi(\mathbf{r}, E, \mathbf{\Omega}, 0) = \Lambda(\mathbf{r}, E, \mathbf{\Omega}) \tag{1.5}$$

where Λ is a specified function of its arguments.

In the transport equation (1.1), $\psi(\mathbf{r}, \mathbf{\Omega}, E)$ is the angular flux, with $\mathbf{r}$, $\mathbf{\Omega}$ and E denoting the spatial, angular and energy variables, $\sigma(\mathbf{r})$ and $\sigma_s(\mathbf{r}, \mathbf{\Omega} \rightarrow \mathbf{\Omega}')$ are the macroscopic total cross section and the macroscopic differential scattering cross section, respectively, and $S(\mathbf{r}, \mathbf{\Omega}, E)$ represents an external source of particles. The time dependence is implied.

In the usual (nonstochastic) application of this equation, the cross section $\sigma(\mathbf{r}, E)$, the scattering kernel $\sigma_s(\mathbf{r}, E' \rightarrow E, \mathbf{\Omega}' \cdot \mathbf{\Omega})$ and the source $S(\mathbf{r}, \mathbf{\Omega}, E)$ are known (deterministic) prescribed functions of their arguments and it is possible to solve the Eq. (1.1), subject to the boundary and initial conditions given by Eqs. (1.4) and (1.5), for the intensity $\psi(\mathbf{r}, E, \mathbf{\Omega}, t)$.

Instead, in the stochastic setting, σ, σ_s and S are only known in some statistical or probabilistic sense, which means that, at each space point $\mathbf{r}$ and time t, these quantities have some probability to assume certain values.

Consequently, we must consider σ, σ_s, S and also the intensity ψ to be a random variables.

1.2 *Ensemble-averaged transport solution*

Assuming known the complete statistical description of the random variables σ, σ_s and S, we seek the solution for $\langle\psi\rangle$, the *ensemble-averaged* of the in-

tensity ψ.

$\langle\psi\rangle$ is the expected value of the intensity of the angular flux, computed over all possible physical realizations of the domain, accordingly to the statistical descriptions of the quantities σ, σ_s and S.

There are two ways to resolve the Eq (1.1) and find $\langle\psi\rangle$.

One consists of generating, from the presumed known statistic, a certain number of physical realization of the statistics, either deterministically or by a Monte Carlo procedure. For each realization, the transport equation describes a deterministic transport problem (geometry, value of σ, σ_s, S, boundary and initial conditions known): the solution could be, in principle, computed, numerically or analytically.

To obtain the ensemble-averaged solution $\langle\psi\rangle$, this process must be repeated for all possible physical realizations: each of them will give a particular solution to the transport equation that will be averaged over all the realizations to give the expected value of the intensity ψ. Obviously, the averaging process must take into account the probability of having each physical realization of the statistics.

In general, this method involves a very large number of deterministic transport calculations to obtain an accurate estimate of the ensemble average.

A zero error computation of the ensemble-averaged intensity $\langle\psi\rangle$ would require an infinite number of simulations of the physical realizations and, hence, an infinite number of deterministic transport calculations.

The other method to compute the ensemble average is to derive a relatively small and simple set of deterministic equations which contains the ensembled-average intensity directly as one of its unknowns.

We have here compared the results given by different resolution methods for the transport problem in stochastic mixtures for which a detailed description

will be given in the next chapters.
The methods are:

- *Atomic Mix Approximation*
- *1D Benchmark*
- *L-P Model*
- *2D Benchmark*
- *Monte Carlo Algorithms: A and B*

1.3 *Equation of transport in statistical mixtures*

To discuss the two possibilities of finding $\langle\psi\rangle$ from the transport equation (1.1) in stochastic mixtures, it is convenient to consider a simple case of time independent transport in a nonscattering medium. If we consider the term $\mathbf{\Omega}\cdot\nabla$ like a directional derivative in the direction $\mathbf{\Omega}$, the Eq. (1.1) becomes:

$$\frac{d\psi(s)}{ds}+\sigma(s)\psi(s)=S(s) \tag{1.6}$$

In this equation, in which we have omitted the energy and the angular arguments of all quantities since they are simple parameter, s is the spatial variable in the direction $\mathbf{\Omega}$. Since the transport problem does not involve scattering, the Eq. (1.6) is not coupled to the equations for other energies and directions.
Taking $0\leq s<\infty$ as the spatial region of interest, the boundary condition

can be written as:

$$\psi(0) = \psi_0 \tag{1.7}$$

where ψ_0 is the prescribed boundary data. Since we are dealing with stochastic media, all the quantities σ, S, ψ_0 and $\psi(s)$ are random variables.
Let Q be a random variable, represented as the sum of its ensemble average $\langle Q \rangle$ and its deviation $\tilde{Q}$ from the mean:

$$Q = \langle Q \rangle + \tilde{Q} \tag{1.8}$$

The characteristic of $\tilde{Q}$ is to have zero mean:

$$\langle \tilde{Q} \rangle = 0 \tag{1.9}$$

Writing all the quantities like (1.8), the Eq (1.6) becomes:

$$\frac{d\langle \psi \rangle}{ds} + \langle \sigma \rangle \langle \psi \rangle + \langle \tilde{\sigma} \tilde{\psi} \rangle = \langle S \rangle \tag{1.10}$$

with its boundary condition:

$$\langle \psi(0) \rangle = \langle \psi_0 \rangle \tag{1.11}$$

To get a closure formulation and obtain the ensemble-averaged of the intensity ψ, one needs to find an approximation of the correlation term $\langle \tilde{\sigma} \tilde{\psi} \rangle$ in function of the quantity of interest, namely $\langle \psi \rangle$. Obviously, to do this, it is necessary to know the statistics of the random variables σ and S.
The other way to find $\langle \psi \rangle$ it to consider the integral, rather than the differential, transport formulation of the problem.

The solution, always in the case of no scattering, of Eq. (1.6) and (1.7) for a given physical realization of the statistics is:

$$\psi(s) = \psi_0 \; exp \; \left[- \int_0^s ds' \sigma(s') \right] + \int_0^s ds' S(s') \; exp \; \left[- \int_{s'}^s ds'' \sigma(s'') \right] \quad (1.12)$$

From the solution given by Eq. (1.12), one can obtain $\langle \psi \rangle$ by ensemble averaging, over all physical realization of the statistics, the right-hand side of the previous equation.

Once again, to perform this average, one must know the details of the statistics. In particular, we can see that there is again a correlation term, given by the joint occurrence of ψ_0 and σ, as well as S and σ.

Chapter 2

Models and approaches for solving binary stochastic mixture transport problems

In this chapter we will show and explain the different models and methods used to solve the transport problem in the case of binary stochastic mixtures. We start with considering the most common approach to solve particle transport problem in stochastic mixtures: the *atomic mix approximation*.

2.1 *Atomic mix approximation*

The atomic mix approximation is an appealing method thanks to its simplicity and computational efficiency, but it could not be accurate enough because of using of ensemble-averaged material properties.

To find the atomic mix transport equation, we consider the case of a background material composed by two randomly mixed solids or immiscible fluids;

that is, these components can not mix at the atomic level.

We label the two components with an index k and the three quantities with $\sigma_k(\mathbf{r}, E)$, $\sigma_{sk}(\mathbf{r}, E' \to E, \mathbf{\Omega}' \cdot \Omega)$, and $S_k(\mathbf{r}, E, \mathbf{\Omega})$, with $k = \alpha, \beta$.

During its travel, the particle encounters alternating segments of the two components, each of which has known deterministic values of σ, σ_s and S. The statistical nature of the problem arises through the statistics of the fluid mixing, *i.e*, the knowledge of which fluid is present at that point $\mathbf{r}$ and time t. Indeed, the global quantities σ, σ_s, and S are considered as discrete random variables and they can assume, at any $\mathbf{r}, E, \mathbf{\Omega}, t$, one of the two sets of values characterising the two components of the mixture.

A physical example for this realization is a grainy background material composed by randomly distributed chunks of random sizes and shapes of the two components of the mixtures.

For any given realization, the particle flow through this mixture is described by deterministic linear transport equation, but what we want to find is a formulation for the ensemble-averaged intensity $\langle\psi\rangle$.

The transport equation, for a binary turbulent mixture without time dependence, is :

$$\frac{d\langle\psi\rangle}{ds} + \langle\sigma\rangle\langle\psi\rangle + \langle\tilde{\sigma}\tilde{\psi}\rangle = \langle S\rangle \tag{2.1}$$

The closure for Eq. (2.1) characterising the atomic mix approximation is the neglect of the cross correlation term $\langle\tilde{\sigma}\tilde{\psi}\rangle$.

This is possible, as shown by Pomraning [2], only if the characteristic chord length Λ_k for the fluid packets of fluid k is small compared to the mean free path l_k in fluid k, that is:

$$\frac{\Lambda_k}{l_k} = \sigma_k \Lambda_k \ll 1, \quad k = \alpha, \beta \tag{2.2}$$

With this assumption, the transport equations (2.1) reduces to:

$$\frac{d\langle\psi\rangle}{ds} + \langle\sigma\rangle\langle\psi\rangle = \langle S\rangle \tag{2.3}$$

where $\langle\psi\rangle$ is our unknown and $\langle\sigma\rangle$ and $\langle S\rangle$, assumed known, are two ensemble averages defined in terms of the properties of the two mixture elements, namely:

$$\langle\sigma(s,t)\rangle = p_\alpha(s,t)\,\sigma_\alpha(s,t) + p_\beta(s,t)\,\sigma_\beta(s,t), \tag{2.4}$$

$$\langle S(s,t)\rangle = p_\alpha(s,t)\,S_\alpha(s,t) + p_\beta(s,t)\,S_\beta(s,t) \tag{2.5}$$

where $p_k(s,t)$ is the probability of finding material k at position s at time t. The sum of the two probability p_k is unity.

$$p_\alpha(s,t) + p_\beta(s,t) = 1 \tag{2.6}$$

The atomic mix transport equation, including scattering, derived from the averaging of Eqs. (1.1), (1.3) and (1.5) and neglecting the cross correlation term $\langle\tilde{\sigma}\tilde{\psi}\rangle$ and $\langle\tilde{\sigma_s}\tilde{\psi}\rangle$ is:

$$\begin{aligned}\boldsymbol{\Omega}\cdot\nabla\langle\psi(E,\boldsymbol{\Omega}\rangle + \langle\sigma(E)\rangle\,\langle\psi(E,\boldsymbol{\Omega})\rangle &= \langle S(E,\boldsymbol{\Omega})\rangle \\ &+ \int_0^\infty dE' \int_{4\pi} d\boldsymbol{\Omega}'\langle\sigma_s(E'\to E, \boldsymbol{\Omega}'\cdot\boldsymbol{\Omega})\rangle\langle\psi(E',\boldsymbol{\Omega}')\rangle\end{aligned} \tag{2.7}$$

with the corresponding boundary and initial conditions:

$$\langle\psi(\mathbf{r_s}, E, \boldsymbol{\Omega}, t)\rangle = \langle\Gamma(\mathbf{r_s}, E, \boldsymbol{\Omega}, t)\rangle, \quad \mathbf{n}\cdot\boldsymbol{\Omega} < 0, \tag{2.8}$$

$$\langle\psi(\mathbf{r}, E, \boldsymbol{\Omega}, 0)\rangle = \langle\Lambda(\mathbf{r_s}, E, \boldsymbol{\Omega})\rangle \tag{2.9}$$

The quantities σ, σ_s, S, Γ and Λ in Eqs. (2.7),(2.8) and (2.9) are random variables, generally described as:

$$\langle Q \rangle = p_\alpha \, Q_\alpha + p_\beta \, Q_\beta \tag{2.10}$$

that is the definition always used for binary stochastic mixture transport problem. It does not depend upon the approximation for the cross correlation term.

The name " atomic mix " for this description of the transport problem arises from the approximation done in Eq. (2.2), which means that small chunks vanish in the mixture (the mean free path l_k is bigger than the mean chord length Λ_k in material k, so the particle does not see, during its travel, the chunks spread in the background). Physically, the smallest chunk size possible is a single atom.

2.1.1 *Remarks*

As we have already seen, the atomic mix model is characterised by the neglect, in the transport equation (1.1), of the cross correlation term, *i.e.*, of statistical effects.

This assumption, that makes the model so attractive and simple to use, can lead to large errors in its prediction of $\langle \psi \rangle$ if Eq. (2.2) is not satisfied. This is the case when the chunks composing the mixture are not small compared to the particle mean free path.

In general, the atomic mix approximation underestimates transmission through a random mixture.

To see it, we can consider time independent transport problem in a source-

free, no scattering medium, composed by optically thin packets of element α ($\sigma_\alpha \Lambda_\alpha \ll 1$) and optically thick packets of element β ($\sigma_\beta \Lambda_\beta \gg 1$), assumed sparse, *i.e.*, with $p_\beta \ll 1$.

The mean physical realization is, then, constituted for the most part of element α, a near vacuum interspersed with very few fluid packets of infinite optical thickness.

Physically, the particle incident upon a piece of this mixture will, on the average, pass through the medium without interacting with the few sparse absorbing packets of material β.

On the other hand, according to the theoretical model, neglecting the cross correlation term $\langle \tilde{\sigma}\tilde{\psi} \rangle$ in Eq. (1.10), the behaviour of $\langle \psi \rangle$ will be an exponential one, with a scale length $1/\langle \sigma \rangle$.

The term $\langle \sigma \rangle$ will be very large, because σ_β is large; thus, the ensemble-averaged intensity $\langle \psi \rangle$ will be very small.

The atomic mix approximation will then lead to virtually no transmission through the mixture, that is not physical.

Also in our Benchmark calculations, we will see that the results are closed to those given by the atomic mix approximation only in cases where the mean physical realization is similar to an homogeneous one (pieces of elements α and β are small and it is possible to describe the mixture with its average properties).

2.2 *Analytical models : the Levermore Pomraning model*

2.2.1 *The Markovian statistics*

Before writing the equation for the *Levermore-Pomraning model*, we introduce and explain Markovian statistics.

A Markov process, named after the Russian mathematician Andrey Markov, is a " memoryless " process: the evolution of its present state does not depend upon the previous states, that are all independent.

Such an approximation is very useful, in particular for neutron transport problem: the particle history can be seen as composed by different independent steps that can be treated separately.

In our case, also the geometry is Markovian: given Λ_α, the conditional probability, supposed we are in material α at some space-time position s, of being in an other material β at $s + ds$ in direction $\mathbf{\Omega}$ is expressed by ds/Λ_α. This probability of transition between different materials is dependent only upon the fixed parameter of the statistics, Λ_α, and on the space interval ds travelled in that step.

Λ_α is called *Markovian transition probability* and it is the mean chord length in direction $\mathbf{\Omega}$ of packets of material α.

The Markovian statistics is a renewal one in which the distribution of the chord length x in a material α is exponential:

$$f_\alpha(x) = \frac{1}{\Lambda_\alpha} e^{-x/\Lambda_\alpha} \tag{2.11}$$

and the mean chord length Λ_α is given by :

$$\Lambda_\alpha = \int_0^\infty dx\, x\, f_\alpha(x) \tag{2.12}$$

Considering a binary stochastic geometry, made by two elements α and β, we define two mean chord lengths Λ_α and Λ_β, whose relation gives the probability p_k of finding material k at any given point in the spatial domain :

$$p_k = \frac{\Lambda_k}{\Lambda_\alpha + \Lambda_\beta} \tag{2.13}$$

with $k = \alpha, \beta$.

The p_k is the volume fraction of material k in the problem :

$$V_k = \frac{V_k}{V_\alpha + V_\beta} \tag{2.14}$$

and the sum of p_ks is unity.

Having defined these quantities, we can now write the expression of the distributions $f_\alpha(x)$ and $f_\beta(x)$ in function of p_k and Λ, the mean chord length in the " uncoloured " geometry[1], supposed to be Markovian. In fact, we can say that the random variables f_α and f_β, describing the chord length in material α and material β respectively, follow an exponential distribution of parameter Λ_α and Λ_β or equivalently of parameters $\Lambda/(1-p_\alpha)$ and Λ/p_α [2].

[1] a geometry made by random chunks in a background of the same material, or a planar one with slabs of different width

[2] Given $f(x)$ a random variable representing chord lengths in a mixture without colour, p_α the probability of finding material α in the domain ($p_\beta = 1-p_\alpha$) and f_α and f_β random variables describing the chord length in material α and β, we have that, if $f(x)$ follows an exponential law (for hypothesis the geometry is Markovian) of parameter Λ, then also f_α and f_β have an exponential distribution, of parameters $\Lambda/(1-p_\alpha)$ and Λ/p_α

Indicating the exponential distribution with ϵ, we have:

$$f_\alpha \sim \varepsilon\left(\frac{1}{\Lambda_\alpha}\right) = \varepsilon\left(\frac{1-p_\alpha}{\Lambda}\right) \tag{2.15}$$

$$f_\beta \sim \varepsilon\left(\frac{1}{\Lambda_\beta}\right) = \varepsilon\left(\frac{p_\alpha}{\Lambda}\right) \tag{2.16}$$

The demonstration is reported in [12].

The mean chord length Λ in the uncoloured geometry is the so called *correlation length*, given by :

$$\frac{1}{\Lambda} = \frac{1}{\Lambda_\alpha} + \frac{1}{\Lambda_\beta} \tag{2.17}$$

If the mean chord length of one material is bigger than the that of the other, the correlation length will be approximately like the smaller one.

2.2.2 *The L-P model*

Levermore-Pomraning model is an approximation of a more general one, described by the so-called Liouville master equation, widely used in particle transport involving stochastic mixtures.

The Liouville equation is generally associated with initial value problems in time and it was used in particle transport context for the first time by Van der Haegen (1986).

The master equation can fit very well the neutron transport problem, just substituting the time variable t with the space variable s.

More details and the procedure are reported in Appendix A.

As we have already seen, to find the solution of the transport problem for statistical mixtures, we have to compute the ensemble-averaged flux intensity $\langle\psi(t,\mathbf{r},\mathbf{\Omega})\rangle$, where $\psi(t,\mathbf{r},\mathbf{\Omega})$ satisfies the integro-differential transport equa-

tion (1.1), written with explicit dependence on $\mathbf{r}$, t and $\mathbf{\Omega}$, that are space, time and angular variables, respectively :

$$\left[\frac{1}{v}\frac{\partial}{\partial t} + \mathbf{\Omega}\cdot\nabla + \sigma(\mathbf{r},t)\right]\psi(\mathbf{r},\mathbf{\Omega},t) = S(\mathbf{r},\mathbf{\Omega},t) + \int_{4\pi}\sigma_s(\mathbf{r},\mathbf{\Omega}'\rightarrow\mathbf{\Omega},t)\psi(\mathbf{r},\mathbf{\Omega}',t)d\mathbf{\Omega}' \tag{2.18}$$

Eq. (2.18) is a one group transport equation: the energy variable E is not displayed: having assumed coherent scattering, it is only a parameter.
Since we are considering stochastic mixtures, the quantities $\sigma(\mathbf{r},\mathbf{\Omega},t)$, $\sigma_s(\mathbf{r},\mathbf{\Omega}'\rightarrow\mathbf{\Omega},t)$ and $S(\mathbf{r},\mathbf{\Omega},t)$ are random variables.
To describe the statistical media and get an equation for the ensemble-averaged flux $\langle\psi(\mathbf{r},\mathbf{\Omega},t)\rangle$, we need a set of states $X=\{\omega\}$, corresponding to each physical realization of the system, and a relative time-independent probability density $p(\omega)$, that respects the normalization condition:

$$\int_X p\,(\omega)\,d\omega \;= 1 \tag{2.19}$$

where $p\,(\omega)$ is the probability of observing state ω.
To each state, that is, each physical realization of the system, are associated a corresponding angular flux, $\psi_\omega(\mathbf{r},\mathbf{\Omega},t)$, and an ensemble-averaged flux, given by:

$$\langle\psi(\mathbf{r},\mathbf{\Omega},t)\rangle = \int_X p(\omega)\,\psi_\omega(\mathbf{r},\mathbf{\Omega},t)\,d\omega \tag{2.20}$$

Considering a finite set of materials $\{\alpha\}$, each characterised by non stochastic sources $S_\alpha(\mathbf{r},\mathbf{\Omega},t)$ and cross sections $\sigma_\alpha(\mathbf{r},\mathbf{\Omega},t)$ and $\sigma_{s\alpha}(\mathbf{r},\mathbf{\Omega}'\rightarrow\mathbf{\Omega},t)$, the ensemble-averaged flux is:

$$\langle\psi(\mathbf{r},\mathbf{\Omega},t)\rangle = \sum_\alpha p_\alpha(\mathbf{r},t)\langle\psi_\alpha(\mathbf{r},\mathbf{\Omega},t)\rangle \tag{2.21}$$

where p_α is the probability of finding material α at time t at position $\mathbf{r}$ and $\langle\psi_\alpha(\mathbf{r},\mathbf{\Omega},t)\rangle$ is the mean angular flux averaged over all realizations that have material α at $(\mathbf{r},t)$, that is, for all the states belonging to the subset $X_\alpha(\mathbf{r},t) = \{\omega \in X \,|\, \omega(\mathbf{r},t) = \alpha\}$. These quantities are respectively expressed by :

$$p_\alpha(\mathbf{r},t) = \int_{X_\alpha(\mathbf{r},t)} p(\omega)d\omega \tag{2.22}$$

and

$$\langle\psi_\alpha(\mathbf{r},\mathbf{\Omega},t)\rangle = \frac{\displaystyle\int_{X_\alpha(\mathbf{r},t)} p(\omega)\psi_\omega(\mathbf{r},\mathbf{\Omega},t)d\omega}{p_\alpha(\mathbf{r},t)} \tag{2.23}$$

The ensemble-averaged flux is defined as the integral of the probability density $p(\omega)$ multiplied for the probability distribution function ψ_ω, weighted by the distribution of $p(\omega)$. Inserting Eq. (2.22) in the previous one we have :

$$\langle\psi_\alpha(\mathbf{r},\mathbf{\Omega},t)\rangle = \frac{\displaystyle\int_{X_\alpha(\mathbf{r},t)} p(\omega)\psi_\omega(\mathbf{r},\mathbf{\Omega},t)d\omega}{\displaystyle\int_{X_\alpha(\mathbf{r},t)} p(\omega)d\omega} \tag{2.24}$$

The quantity $\langle\psi_\alpha\rangle$ is called α-*material* average flux because material α is present at $(\mathbf{r},t)$.

Having defined the ensemble-averaged flux $\langle\psi(\mathbf{r},\mathbf{\Omega},t)\rangle$ in function of the material fluxes, it is possible to find our unknown simply by writing equations for each of the $\langle\psi_\alpha(\mathbf{r},\mathbf{\Omega},t)\rangle$s.

Averaging the Eq. (2.18) for a two-element stochastic mixture, we obtain two coupled equations, one for $\langle\psi_\alpha(\mathbf{r},\mathbf{\Omega},t)\rangle$ and one for $\langle\psi_\beta(\mathbf{r},\mathbf{\Omega},t)\rangle$:

$$\left[\frac{1}{v}\frac{\partial}{\partial t} + \mathbf{\Omega}\cdot\nabla + \sigma_\alpha\right](p_\alpha\langle\psi_\alpha\rangle) = p_\alpha\left[\int_{4\pi}\sigma_{s\alpha}(\mathbf{\Omega}'\to\mathbf{\Omega})\langle\psi_\alpha(\mathbf{\Omega}')\rangle d\mathbf{\Omega}' + S_\alpha\right] + p_{\beta\alpha}\langle\psi_{\beta\alpha}\rangle - p_{\alpha\beta}\langle\psi_{\alpha\beta}\rangle \tag{2.25}$$

$$\left[\frac{1}{v}\frac{\partial}{\partial t} + \mathbf{\Omega}\cdot\nabla + \sigma_\beta\right](p_\beta\langle\psi_\beta\rangle) = p_\beta\left[\int_{4\pi}\sigma_{s\alpha}(\mathbf{\Omega}'\to\mathbf{\Omega})\langle\psi_\alpha(\mathbf{\Omega}')\rangle d\mathbf{\Omega}' + S_\beta\right] + p_{\alpha\beta}\langle\psi_{\alpha\beta}\rangle - p_{\beta\alpha}\langle\psi_{\beta\alpha}\rangle \tag{2.26}$$

written here omitting the arguments t, $\mathbf{r}$ and $\mathbf{\Omega}$.

In these equations new probability densities, $p_{\alpha\beta}$ and $p_{\beta\alpha}$, are introduced: they are the probabilities per unit length of trajectory of crossing an interface from material α to material β (and vice-versa) at point $(\mathbf{r}, t)$, along the direction $\mathbf{\Omega}$. Related to the transition between materials are also the fluxes $\langle\psi_{\alpha\beta}(\mathbf{r}, \mathbf{\Omega}, t)\rangle$ and $\langle\psi_{\beta\alpha}(\mathbf{r}, \mathbf{\Omega}, t)\rangle$, called *interface* average fluxes, which are the angular fluxes averaged over all states that switch from material β to material α (and vice-versa) at $(\mathbf{r}, t)$ along direction $\mathbf{\Omega}$.

Another approach to derive an equation for the material average flux is to average the integral form of the transport equation over a subset of states which have material α at position $(\mathbf{r}, t)$. With this method too we have the definition of some interface fluxes, different from the preceding ones because averaged on a different subset of states: the material average flux is here expressed in terms of average fluxes along the past trajectory in direction $-\Omega$ (that is, along points like $(\mathbf{r}', t')$, with $\mathbf{r}' = \mathbf{r} - x'\mathbf{\Omega}$ and $t' = t - x'/v$).

The equation obtained from this method is the so-called renewal-like equation:

$$\begin{aligned}\langle\psi_\alpha(t,\mathbf{r},\mathbf{\Omega})\rangle &= \psi_{bd}(t_{bd},\mathbf{r_{bd}},\mathbf{\Omega})\, e^{-\tau_\alpha(\mathbf{r_{bd}},t,\mathbf{r})} R_\alpha(\mathbf{r_{bd}},t,\mathbf{r}) \\ &+ \int_0^{x_{bd}} e^{-\tau_\alpha(\mathbf{r}',t,\mathbf{r})} \left\{ f_{s\alpha}\langle\bar{\psi}_{\beta\alpha}(t',\mathbf{r}',\mathbf{\Omega};\mathbf{r})\rangle \right. \\ &+ R_\alpha(\mathbf{r}',t,\mathbf{r})[\int_{4\pi} \sigma_{s\alpha}(t',\mathbf{r}',\mathbf{\Omega}'\to\Omega)\langle\bar{\psi}_{\alpha\alpha}(t',\mathbf{r}',\mathbf{\Omega}'\to\mathbf{r})\rangle d\mathbf{\Omega}' \\ &+ S_\alpha(t',\mathbf{r}',\mathbf{\Omega})dx'\end{aligned}$$

Independently on the formulation chosen, a problem of infinite hierarchy arises.

There are always new unknown conditional averages that appear in the equations for the material average fluxes $\langle\psi_\alpha\rangle$ and $\langle\psi_\beta\rangle$, namely, for the case in exam, $\langle\psi_{\alpha\beta}\rangle$ and $\langle\psi_{\beta\alpha}\rangle$.

This problem is correlated to the fact that we are seeking for a mean (ensemble-averaged) quantity: we average an equation to find the first order moment of a probability distribution function; to do this, we have to use its second order moment, that is unknown. So, every time a new equation in a higher order is needed to close the previous one.

It has been shown [5] that, for collisionless transport, the infinite hierarchy of equations can be reduced to a close set when the chord statistics, describing chord length on a material, are renewal ones.

Statistics are defined renewal if the probability for a chord of length z of material α is given by a predefined distribution function $f_\alpha(z)$ and it is independent of the material distribution in the past of the trajectory.

For this type of statistics the hierarchy can have a second order closure , but it is possible to close the set of equations also at the first order,using a particular type of renewal statistic: the Markovian ones, for which the distribution of the chord length z is exponential.

The closure is given by the identity :

$$\langle \psi_{\beta\alpha}(\mathbf{r}, \mathbf{\Omega}, t) \rangle = \langle \psi_{\beta}(\mathbf{r}, \mathbf{\Omega}, t) \rangle \tag{2.27}$$

which means that the interface flux is equal to the material flux. In fact, with Markovian assumption, the evolution of the current state is independent of the previous one; so, the fact that the particle is inside the material α or near to the interface does not affect the next step of its history, because it is however in material α.

Obviously, this type of closure is not possible for real transport problems, that are non-zero scattering. So, it is necessary to develop models which use some appropriate closures to truncate this infinite hierarchy of equations.

One of them is the Levermore-Pomraning model, which suggests to enforce the simple closure given by Eq. (2.27) also for arbitrary statistics and non-zero collision transport problem.

We can write, in a more synthetic way, the two coupled equations describing transport problem in scattering Markovian stochastic mixtures given by Eqs. (2.25) and (2.26), indicating with $\langle \phi_k \rangle$ the integral of the intensity $\langle \psi_k \rangle$ over the angle variable:

$$\langle \phi_k \rangle = \int_{4\pi} \sigma_{sk}(\mathbf{\Omega}' \to \mathbf{\Omega}) \langle \psi_k(\mathbf{\Omega}') \rangle d\mathbf{\Omega}' \tag{2.28}$$

and expressing the probability of transition between one material to the other, namely $p_{\alpha\beta}$ and $p_{\beta\alpha}$, in terms of the Markovian transition probabilities

Λ_α and Λ_β:

$$p_{\alpha\beta} = \frac{p_\alpha}{\Lambda_\alpha} \tag{2.29}$$

$$p_{\beta\alpha} = \frac{p_\beta}{\Lambda_\beta} \tag{2.30}$$

We obtain the following equations:

$$\left[\frac{1}{v}\frac{\partial}{\partial t} + \mathbf{\Omega}\cdot\nabla + \sigma_\alpha\right](p_\alpha\langle\psi_\alpha\rangle) = p_\alpha\left(\frac{\sigma_{s\alpha}}{4\pi}\langle\phi_\alpha\rangle + S_\alpha\right) + \frac{p_\beta\langle\psi_{\beta\alpha}\rangle}{\Lambda_\beta(\mathbf{\Omega})} - \frac{p_\alpha\langle\psi_{\alpha\beta}\rangle}{\Lambda_\alpha(\mathbf{\Omega})} \tag{2.31}$$

$$\left[\frac{1}{v}\frac{\partial}{\partial t} + \mathbf{\Omega}\cdot\nabla + \sigma_\beta\right](p_\beta\langle\psi_\beta\rangle) = p_\beta\left(\frac{\sigma_{s\beta}}{4\pi}\langle\phi_\beta\rangle + S_\beta\right) + \frac{p_\alpha\langle\psi_{\alpha\beta}\rangle}{\Lambda_\alpha(\mathbf{\Omega})} - \frac{p_\beta\langle\psi_{\beta\alpha}\rangle}{\Lambda_\beta(\mathbf{\Omega})} \tag{2.32}$$

that represent the standard approximate model.

With the first order closure we have the two coupled equations for the L-P model:

$$\left[\frac{1}{v}\frac{\partial}{\partial t} + \mathbf{\Omega}\cdot\nabla + \sigma_\alpha\right](p_\alpha\langle\psi_\alpha\rangle) = p_\alpha\left(\frac{\sigma_{s\alpha}}{4\pi}\langle\phi_\alpha\rangle + S_\alpha\right) + \frac{p_\beta\langle\psi_\beta\rangle}{\Lambda_\beta(\mathbf{\Omega})} - \frac{p_\alpha\langle\psi_\alpha\rangle}{\Lambda_\alpha(\mathbf{\Omega})} \tag{2.33}$$

$$\left[\frac{1}{v}\frac{\partial}{\partial t} + \mathbf{\Omega}\cdot\nabla + \sigma_\beta\right](p_\beta\langle\psi_\beta\rangle) = p_\beta\left(\frac{\sigma_{s\beta}}{4\pi}\langle\phi_\beta\rangle + S_\beta\right) + \frac{p_\alpha\langle\psi_\alpha\rangle}{\Lambda_\alpha(\mathbf{\Omega})} - \frac{p_\beta\langle\psi_\beta\rangle}{\Lambda_\beta(\mathbf{\Omega})} \tag{2.34}$$

2.3 *Monte-Carlo Algorithms*

Instead of seeking ensemble-averaged transport solution using an approximate set of equations, or simulating a large number of realizations and then solving each single problem to average them at the end, there is another possible way to compute the ensemble-averaged intensity: developing a Monte Carlo algorithm.

Zimmerman [8] and McCormick [7] proposed independently the use of a Monte Carlo algorithm for the solution of transport problem in binary stochastic mixtures.

We present here two algorithms: algorithm A and algorithm B. The first solves, as argued by Pomraning [6], the Levermore equations and it is, thus, equivalent to the L-P model; the second is a more accurate algorithm, thanks to its improved local material realization modelling.

Zimmerman and Adams [8] also proposed an algorithm C, that retains more memory of the particle's recent history, maintaining additional realization information: not only the current interface distance (forward and backward), but also the distance to the next interface is kept.

However, even if the realization description is more close to the real, because of the information regarding also surrounding materials, algorithm C is not feasible in multiple dimensions; thus, it will not be treated in our discussion.

2.3.1 *Monte Carlo transport theory*

2.3.2 *Algorithm A: the L-P model*

For both algorithms, the particle history begins with sampling the source particle characteristics: position, velocity and material (here material is an attribute of the particle, just like position and velocity).

Then, for a new event, three distances are introduced:

- d_b: *the boundary distance*; it is the distance to the zone boundary and it is computed using the particle current position and direction of flight and the boundaries of the spatial domain;
- d_i: *the interface distance*; it is the distance to material interface and it is sampled by material's chord length distribution (with the assumption that the particle is either on an interface between materials or located randomly inside);
- d_c: *the collision distance*; it is the distance to the next collision and it is sampled using material's total cross section;

Then the steps are:

I. sample the distance to material interface d_i
II. calculate the distance-to-boundary d_b and sample the distance-to-collision d_c
III. compute the minimum of d_i, d_b and d_c to determine which event occurs
IV. if d_b, advance the particle to the boundary: if it escapes, update the appropriate leakage tally and terminate the history, then track a new particle. If not, return to step I.
V. if d_i, advance particle and switch the material identifier (the material changes)
VI. if d_c, advance particle and sample collision type using macroscopic total and scattering cross sections for the material in which the particle exists. If the particle is absorbed, then terminate the history and track a new particle. If the sampled collision is scattering, sample the outgoing characteristics of the particle, that maintains its current material identifier. Return to step I.

We emphasize that this algorithm models a Markovian transport process, since, after each collision, the incident particle history is forgotten and the

outgoing particles are treated as " new " source particles. Following a collision, a new material interface distance is sampled: this leads to an unphysical behaviour, because in that manner the particle encounters a different material realization every time it undergoes a collision. In particular, if the particle backscatters, it can see a different medium than it traversed on its way to the collision.

Thus, algorithm A will be less accurate as scattering increases.

2.3.3 *Algorithm B: a more accurate one*

This algorithm retains partial memory of the previous particle history.

Instead of only one, two material interface distances are sampled: one in the forward direction, $d_{i,f}$, and one in the backward direction, $d_{i,b}$.

Upon crossing a material interface, a new $d_{i,f}$ is sampled and $d_{i,b}$ is set to zero. After a collision, $d_{i,f}$ and $d_{i,b}$ are kept from the incident particle, or switched if a backscatter occurs. The choice of keeping or switching the interface distance depends upon the angle between the outgoing and the incident particle directions, and on a pseudorandom number, such that forward scattered particles keep their $d_{i,f}$ and backward scattered particles switch it. Therefore, if a particle backscatters, it will see the same material it just passed through, and not a different one.

For each particle history the steps are:

I. sample the distance to material interface in the forward and in the backward direction, namely, $d_{i,f}$ and $d_{i,b}$
II. compute the distance-to-boundary d_b and sample the distance to collision d_c
III. calculate the minimum of $d_{i,f}$, d_b and d_c and determine the sampled event

IV. if d_b, initially treat as in algorithm A, step IV. Instead of resampling the distance to material interface (returning to step 1) as in Algorithm A, adjust the distance to material interface values in the forward and backward directions to account for the distance the particle was moved.Return to step II
V. if $d_{i,f}$, advance the particle of the appropriate distance, switch the material identifier, set $d_{i,b}$ to zero and sample a new forward distance $d_{i,f}$. Return to step II
VI. if d_c, treat the case as in algorithm A; instead of resampling the distance to material interface, adjust the value for the distance the particle has travelled. If the collision is a scattering, also adjust d_i in the forward and in the backward directions and, in case, switch them. Return to step II

2.3.4 *Remarks*

As we have already said, algorithm A is less accurate than algorithm B, even if, for our benchmark problem, they produce qualitatively and semi-quantitatively correct results [1], both for the ensemble-averaged quantity sought and for the material scalar flux distribution, that are quite realistic. From algorithm A to C, accuracy improves: during each history, more information about material distribution is retained. Algorithm B has a small additional complexity, but it has also smaller errors [8]. Instead, algorithm C additional complexity does not allow its use for multidimensional geometries.

2.4 *Benchmark 1D: planar geometry*

The first benchmark results obtained for the transport problem in stochastic mixtures [10] were done for a layered planar geometry, composed by alternating slabs of two different materials, under the assumption of Markovian statistics.

This calculations were achieved by simulating a large number of physical realizations, through a Monte Carlo procedure, by numerically solving the corresponding transport equation and then averaging the solutions to find the wanted ensemble-averaged quantities.

Results were also compared to those given by the standard model, written for the case of planar geometry.

2.4.1 *Transport equation in a planar layered geometry*

The Benchmark results we are referring to are those calculated by Brantley [1], who analysed two suites of the problem, one with a unity incoming partial current and one with an internal nonstochastic source. The equation describing the time-independent monoenergetic neutron scattering transport problem in a one-dimensional planar geometry, with a domain defined in x from 0 to length L, is:

$$\mu\frac{\partial}{\partial x}\psi(x,\mu)+\sigma_t(x)\psi(x,\mu)=\frac{1}{2}\sigma_s(x)\int_{-1}^{1}\psi(x,\mu')d\mu'+\frac{1}{2}q(x) \qquad (2.35)$$

$0 \leq x \leq L$, $-1 \leq \mu \leq 1$,
with the interior source:

$$q(x) = \begin{cases} 0 & \text{Suite I} \\ & \qquad 0 \leq x \leq L \\ \frac{1}{L} & \text{Suite II} \end{cases} \tag{2.36}$$

and boundary and initial conditions given by:

$$\psi(0,\mu) = \begin{cases} 2 & \text{Suite I} \\ & \qquad \mu > 0 \\ 0 & \text{Suite II} \end{cases} \tag{2.37}$$

and:

$$\psi(L,\mu) = 0, \;\; \mu < 0 \tag{2.38}$$

In equation (2.35), written in standard neutronics notation, $\psi(x,\mu)$ is the angular flux of particles at position x travelling in direction $\mathbf{\Omega}$, identified by the cosine μ to respect the x axis, $\sigma(x,\mu)$ and $\sigma_s(x,\mu)$ are the macroscopic total and scattering cross sections and $q(x)$ is an interior source of particles. The searched values are the *reflection* and the *transmission* through the layered domain corresponding to the ensemble-averaged exiting partial currents at $x = 0$ and $x = L$, given by:

$$\langle J_0 \rangle = \int_{-1}^{0} |\mu| \langle \psi(0,\mu) \rangle d\mu, \tag{2.39}$$

$$\langle J_L \rangle = \int_{0}^{1} \mu \langle \psi(L,\mu) \rangle d\mu \tag{2.40}$$

Suite I is the standard suite, treated also by Adams, Larsen and Pomraning [10], characterized by an isotropic incident angular flux at one border of the spatial domain, whereas Suite II is an interior non-stochastic spatially uni-

form source benchmark problem. The source $q(x)$ is of one neutron per unit time. For Suite I the boundary conditions represent an incident angular flux at $x = 0$ and a vacuum boundary at $x = L$. For Suite II they are, instead, of " free surface " type for both of the boundaries.
Assuming spatially homogeneous [3] Markovian statistics as description of materials composing the medium, namely α and β, each slab width can be sampled from an exponential distribution, like:

$$f_k(x) = \frac{1}{\Lambda_k} e^{-\frac{x}{\Lambda_k}} \tag{2.41}$$

with $k = \alpha, \beta$ and Λ_k the mean slab width of material k.
As previously defined, each material is also characterised by the volume fraction p_k, which is the probability of finding material k at any given point in the spatial domain:

$$p_k = \frac{\Lambda_k}{\Lambda_\alpha + \Lambda_\beta} \tag{2.42}$$

2.4.2 *Benchmark calculations*

To obtain benchmark results, the procedure is the following:

- generate one physical realization: sample the material located at the left born $x = 0$ using the probabilities p_k defined in (2.42), sample the first slab width from exponential distribution, (2.41), using the appropriate Λ_k; sample in the same manner the next slab width until the value $x = L$ is reached.

- solve the transport problem for each realization, using here discrete ordinates transport code

[3] all points in the domain have identical statistical properties

- repeat this procedure a large number of times, say M, and average the results

The ensemble-averaged quantities we are interested in are: the ensemble-averaged leakage values at $x = 0$ and at $x = L$,namely the reflection and the transmission, given respectively by:

$$\langle J_0 \rangle = \frac{1}{M} \sum_{m=1}^{M} \int_{-1}^{0} |\mu| \psi_m(0, \mu) d\mu \tag{2.43}$$

$$\langle J_L \rangle = \frac{1}{M} \sum_{m=1}^{M} \int_{0}^{1} |\mu| \psi_m(L, \mu) d\mu \tag{2.44}$$

where $\psi_m(x, \mu)$ is the solution computed for the realization m.
The transport code used by Brantley [1] employs the linear discontinuous spatial discetization with the size Δx of each mesh interval chosen such that $\sigma_k \Delta x / \mu_{min} \leq 1/10$, where μ_{min} is the minimum direction cosine in the quadrature set.

2.4.3 *The 1D model*

The standard equations (2.25) and (2.26) written for the planar geometry, sourcefree, time-independent problem under consideration is:

$$\mu \frac{\partial \psi_\alpha(x, \mu)}{\partial x} + \sigma_\alpha \psi_\alpha(z, \mu) = \frac{\sigma_{s\alpha}}{2} \int_{-1}^{1} d\mu' \psi_\alpha(z, \mu') + \frac{|\mu|}{\Lambda_\alpha} [\psi_\beta(x, \mu) - \psi_\alpha(x, \mu)] \tag{2.45}$$

$$\mu \frac{\partial \psi_\beta(x, \mu)}{\partial x} + \sigma_\beta \psi_\beta(z, \mu) = \frac{\sigma_{s\beta}}{2} \int_{-1}^{1} d\mu' \psi_\beta(z, \mu') + \frac{|\mu|}{\Lambda_\beta} [\psi_\alpha(x, \mu) - \psi_\beta(x, \mu)] \tag{2.46}$$

that, in a general form, is:

$$\mu\frac{\partial\psi_k(x,\mu)}{\partial x}+\sigma_k\psi_k(z,\mu)=\frac{\sigma_{sk}}{2}\int_{-1}^{1}d\mu'\psi_k(z,\mu')+\frac{|\mu|}{\Lambda_k}[\psi_l(x,\mu)-\psi_k(x,\mu)] \tag{2.47}$$

with boundary conditions

$$\psi_k(0,\mu)=2,\ \ \mu>0;\quad \psi_k(L,\mu)=0,\ \ \mu<0;\quad \text{with } k=\alpha,\beta \tag{2.48}$$

The ensemble average solution $\langle\psi_k(x,\mu)\rangle$ is given by the same expression as Eq. (A.19), that is, the sum, overall the materials composing the mixture, of the average flux calculated for the subset of states in which material k is present at time t and position $\mathbf{r}$ times the probability p_k of being in that material.

The equation (2.45) is obtained dividing Eq. (2.25) by p_α and then using the relationship between the p_ks and the Λ_ks: recalling the definition of the probabilities p_α and p_β in function of the mean slab width Λ_α and Λ_β:

$$p_\alpha=\frac{\Lambda_\alpha}{\Lambda_\alpha+\Lambda_\beta} \tag{2.49}$$

$$p_\beta=\frac{\Lambda_\beta}{\Lambda_\alpha+\Lambda_\beta} \tag{2.50}$$

we obtain the identity:

$$\frac{\Lambda_\alpha}{p_\alpha}=\frac{\Lambda_\beta}{p_\beta} \tag{2.51}$$

As in previous equations, in Eqs. (2.45) and (2.46), we have the usual terms of classical transport (the two terms on the left and the first on the right) and two extra terms, due to the presence of stochastic mixtures. The positive one is that corresponding to the flux getting in from material l to material k and the negative term is the flux outgoing from material k, with $l\neq k$.

Interesting here is the coupling term, $|\mu|/\Lambda_k$, that is the fraction of the cosine μ and the mean slab width in material k, Λ_k. In that case, the Markov transition probabilities, Λ_α and Λ_β, are angular dependent: the mean chord length seen by a particle travelling at an angle characterized by its cosine μ is Λ_k/μ.

Chapter 3

Benchmark problem

After having described some different methods and models to face the transport problem in stochastic geometries, we are now dealing with transport simulation in binary 2D Markovian geometries.
The procedure we have followed is:

- generate different statistical realizations of Markovian geometry, accordingly with Benchmark problem parameters
- solve the transport problem by the Monte Carlo code TRIPOLI-4 ®, developed at CEA, for each realization
- average the results and make a comparison with the results previously obtained using models or numerical simulations

Each geometry is realized in accordance with a procedure described by Switzer [11], that allows us to first build a two-dimensional Markovian geometry in the plane and then extend this geometry in the vertical direction.

3.1 *Geometry construction*

Basically, the construction of the three-dimensional geometry is a two-step process: firstly, a real Markovian two-dimensional geometry is built in a square, secondly this two-dimensional geometry is extended in the vertical direction. We now detail this procedure.

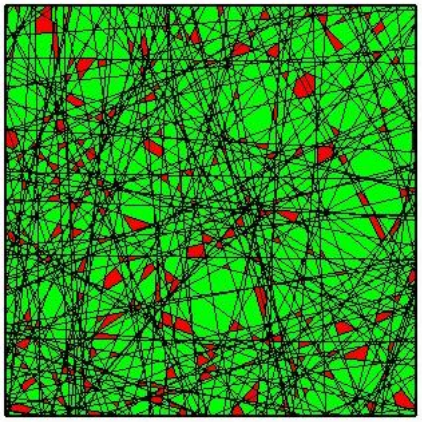

Fig. 3.1: Example of Markovian geometry formed by a set of polygons of two materials, 0 *and* 1

Its construction is done in accordance with the procedure described by Switzer [11] in 1964, that allows to realize a bidimensional Markovian geometry.

Throwing a random number of lines, following a Poisson process, on a square domain of size L, inscribed in a circle of radius r, we obtain a set of polygons that has Markovian properties.

The equation of any line in the (x, y) plane may be written as

$$\rho_i = xcos\theta_i + ysin\theta_i \quad (-\infty < \rho_i < \infty; 0 \leq \theta_i \leq \pi) \tag{3.1}$$

where ρ_i is the distance of the perpendicular from the origin O to the line and

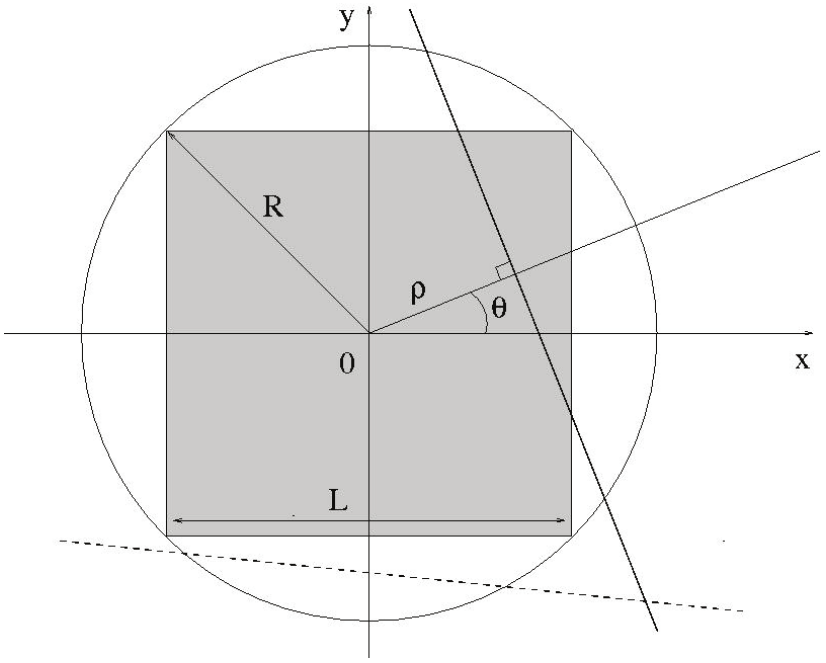

Fig. 3.2: Geometry construction: the solid line crosses the domain and serves to build the stochastic geometry. The dashed line does not cross the domain and it is rejected

θ_i is its orientation. The distances $p_0 \leq p_1 \leq p_2 \leq p_3 \leq \ldots$, with $i = 1, \ldots, n$, of the lines from point O constitute the coordinates of the events of a Poisson process, characterized by a constant density λ. It implies that, in any interval of length L, the number of random lines has a Poisson distribution, with mean λL. The probability of having n events in any interval of length L is given by:

$$p_n = \frac{(L\lambda)^n}{n!} e^{-\lambda L} \tag{3.2}$$

The lines so generated divide the square into convex polygonal cells.
One advantage property of the set of lines, called $\mathcal{L}$, is that it is homogeneous: the lines of $\mathcal{L}$ have a uniform density, of measure λ.

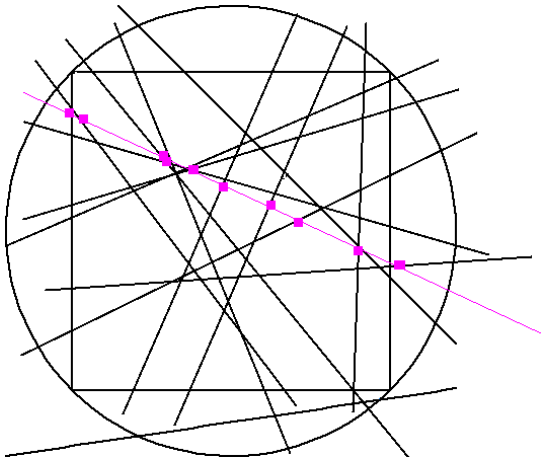

Fig. 3.3: Throwing a line test (pink line) on this geometry, it is cut in a series of segments, delimited by a group of intersection points

Seen in another way, we can say that, if we throw a line test on the geometry, the points of intersection between the line and the set of lines $\mathcal{L}$ constitute a Poisson process of density $\tau = (2\lambda)/\pi$.

So, the inverse of density, τ^{-1}, is the mean length of the segments in which the line test is cut and the lengths of these segments follow an exponential distribution of parameter $\bar{x} = \tau^{-1} = \pi/(2\lambda)$.

Being x the length of these segments, we have:

$$f(x) = \frac{1}{\bar{x}} e^{-x/\bar{x}} = \tau e^{-\tau x} = \frac{2\lambda}{\pi} e^{-(x2\lambda)/\pi} \tag{3.3}$$

Thus, the constructed geometry is a Markovian one, apart from edge effects.

To build these geometries we employed a code, developed by Thibaut Lepage at CEA, that reproduces Switzer's process.
It throws a random number of lines on a square of size L, inscribed in a circle of radius $r = L/\sqrt{2}$, in accordance with a Poisson process: if the line crosses the square domain, it is accepted; if the line crosses only the circle, it is rejected. The probability that a line crossing the circle crosses also the square is given by the perimeters ratio of the two figures:

$$\frac{4L}{(2\pi r)} = \frac{4}{(\pi\sqrt{2})} \approx 0.9 \tag{3.4}$$

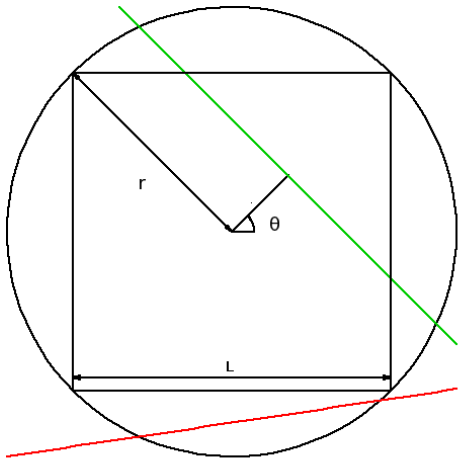

Fig. 3.4: Square domain and construction of the stochastic geometry: on a square of side L a set of lines is thrown: the green crosses the domain and it is accepted, the red does not and it is rejected

To generate the geometries, the program asks three input parameters: the *size* S , the *density* λ and the *probability* p.

- The parameter *size* is the characteristic dimension of the domain: the side L of the square. In our case, it is 10 cm

- The parameter *density* is the density of the Poisson process used to draw random lines on the plane. It has the measure of a density and it is defined as the fraction of the mean number of lines in a square of side L and the size itself:

$$\lambda = \frac{E[L]}{L} \tag{3.5}$$

This positive constant characterizes the Poisson process for the construction of the geometry and is independent of the distribution of the two materials in the medium (the quantities previously defined p_0 and p_1). We can have different realizations of the geometry with the same density and different p_i.

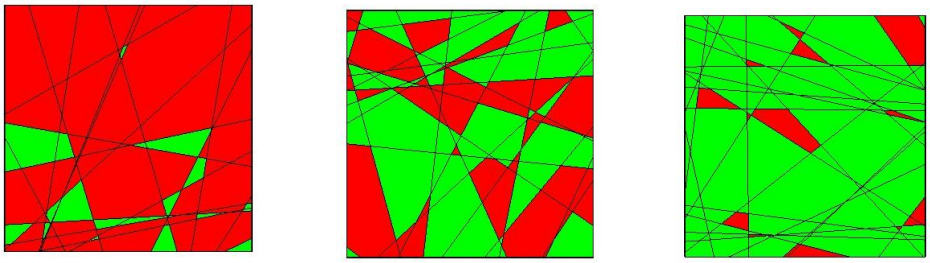

(a) $\lambda = 1.58$, $p = 0.3$ (b) $\lambda = 1.58$, $p = 0.6$ (c) $\lambda = 1.58$, $p = 0.9$

Fig. 3.5: Geometries with same density λ and different proba p_0

For our benchmark calculations, the value of λ is not given as a predefined parameter, however it can be deduced from the values of p_0 and Λ_0. In fact, it is possible to find a relationship between the density of the Poisson process, the volume fraction of one of the two materials composing the mixture and its mean chord length. Reminding the expressions of the chord length distributions in the two materials, Eqs. (2.15) and (2.16), and that of the chord length in the Markovian

geometry constructed, Eq. (2.41), we have:

$$f_0(x) = \frac{1}{\Lambda_0} e^{-x/\Lambda_0} \qquad \text{where } \Lambda_0 = \bar{x}/(1-p_0) \tag{3.6}$$

$$f_1(x) = \frac{1}{\Lambda_1} e^{-x/\Lambda_1} \qquad \text{where } \Lambda_1 = \bar{x}/p_0 \tag{3.7}$$

Here, $\bar{x}$ is the mean chord length in the geometry build up of polygons whose expression worth $\bar{x} = \pi/(2\lambda)$. Substituting this expression in Eqs. (3.6) and (3.7) we obtain:

$$\Lambda_0 = \frac{\bar{x}}{(1-p_0)} = \frac{\pi}{2\lambda(1-p_0)} \tag{3.8}$$

$$\Lambda_1 = \frac{\bar{x}}{p_0} = \frac{\pi}{2\lambda p_0}. \tag{3.9}$$

Then, given the values for p_0 and Λ_0, we can calculate the expression for the density λ:

$$\lambda = \frac{\pi}{2\Lambda_0(1-p_0)}, \tag{3.10}$$

that has a different value for each benchmark case.

- The parameter *probability* is the probability of finding one of the two materials in the domain. Given one material, the other is found thanks to the normalization condition $p_0 + p_1 = 1$.

3.2 *Benchmark problem description*

We consider a problem of transmission and partial reflection along the x axis (and conditions of mirror reflections on the other axes) through a solid, of dimensions 10x10x10 cm, composed by two materials, labeled with 0 and 1, whose parameters are given in the following tables:

Table 3.1: Material parameters for benchmark transport problem

Case	Λ_0 [cm]	σ_t^0 [cm^{-1}]	Λ_1 [cm]	σ_t^1 [cm^{-1}]	Case	c_0	c_1
1	99/100	10/99	11/100	100/11	a	0.0	1.0
2	99/10	10/99	11/10	100/11	b	1.0	0.0
3	101/10	2/101	101/20	200/101	c	0.9	0.9

Table 3.2: Ensemble-averaged material parameters

Case	$\langle\sigma_t\rangle$	$\langle\sigma_s\rangle$
1a,2a	1	10/11
1b,2b	1	1/11
3a	1	100/101
3b	1	1/101
1c,2c,3c	1	9/10

The table 3.1 contains the values for macroscopic total cross sections and mean chord lengths of the two materials composing the medium. The scattering cross section is calculated from the value of c_i, defined as the ratio between scattering and total cross section of material i : $c_i = \sigma_s^i/\sigma_t^i$, $i = 0, 1$. Giving the mean chord length Λ_i for each material is equivalent of having the volume fraction p_i, that is, the probability of finding material i in the domain :

$$p_i = \frac{\Lambda_i}{\Lambda_0 + \Lambda_1} \tag{3.11}$$

The benchmark problem is then split into three main cases, with the following values for the characteristic parameters:

Table 3.3: Three cases parameters

Case	λ	p_0
1	15.867	0.9
2	1.5867	0.9
3	0.6621	0.5

Looking at the table above, some quick considerations can be made on each case:

- **Case 1**: it can be considered the "more stochastic" case, since the mean chord lengths are small compared to the dimension 10x10cm^2 of the square. Besides the two materials are strongly mixed. The volume fractions are $p_0 = 0.9$ and $p_1 = 0.1$, respectively, so it is much more probable to find material 0 than material 1.

- **Case 2**: the total cross sections and the volume fractions are the same as in Case 1, but mean chord lengths are different: for material 0 it is 9.9 cm and for material 1 it is 1.1 cm. So, in an average sense, pieces of 0 are quite big, close to the domain size, whereas material 1 is present in small pieces.

- **Case 3**: materials in Case 3 have the same mean chord lengths, thus they are present with the same volume fraction ($p_0 = p_1 = 0.5$). Pieces are also rather big, since $\Lambda_0 = \Lambda_1 = 5.05$ cm.

For each case, there are three sub-cases, characterized by different values of scattering and absorbing cross sections for the two materials, making 9

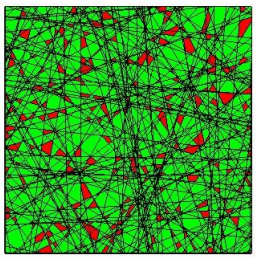

(a) Case1: $\lambda = 15.867$, $p = 0.9$

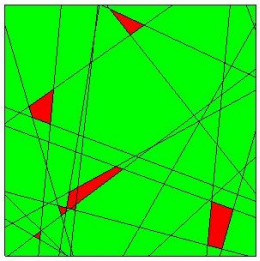

(b) Case2: $\lambda = 1.5867$, $p = 0.9$

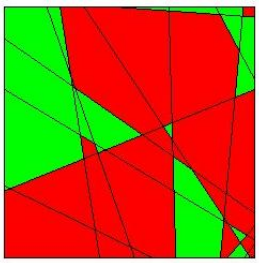

(c) Case3: $\lambda = 0.6621$, $p = 0.5$

Fig. 3.6: Examples of the three cases

cases in total. Moreover, we will analyse two different suites for the benchmark problem:

- **Suite I**: characterized by no internal source and an input current at the left side of the solid
- **Suite II**: it has an isotropic source, uniformly extended in the domain.

Since we are dealing with stochastic problem, as already mentioned, the total and the scattering cross sections are ensemble-averaged quantities, more precisely they are expressed by:

$$\langle \sigma_t \rangle = p_0 \sigma_t^0 + p_1 \sigma_t^1 \tag{3.12}$$

$$\langle \sigma_s \rangle = p_0 \sigma_s^0 + p_1 \sigma_s^1 \tag{3.13}$$

For all cases, the ensemble-averaged total cross section is unity.
The values of the different scattering cross sections, for the different cases, are given in Table 3.2.

Probability of one material geometry realization

According to the values of the material probability p_0 and p_1, we are able to calculate for the layered geometry and estimate for the bidimensional stochastic geometry the probability of having a realization completely filled with only one material.

This probability is dependent upon three parameters: p_0, the volume fraction of material 0, $\bar{x}$, the mean chord length, and L, the size of the domain.

For the geometry used in Benchmark calculations by Branltey [1], we can calculate the exact value of this probability for the three cases, using the expressions given in [13]. Instead, for the stochastic geometry composed by polygons generated with random lines, we can not have an analytical expression for this probability. We can only have a maximum.

We report the probability values in the following table, according to the expressions for P_0, P_1 and P, the probability of having, respectively, a geometry composed by only material 0, material 1 and one of the two materials, meaning, for the layered geometry:

$$P_0 = p_0 e^{-(1-p_0)L/\bar{x}} \tag{3.14}$$

$$P_1 = p_1 e^{-(1-p_1)L/\bar{x}} \tag{3.15}$$

$$P = P_0 + P_1 = p_0 e^{-(1-p_0)L/\bar{x}} + (1-p_0)e^{-p_0 L/\bar{x}} \tag{3.16}$$

and for the stochastic bidimensional geometry:

$$P_0 < p_0 e^{-2R\lambda(1-p_0)p} \tag{3.17}$$

$$P_1 < p_1 e^{-2R\lambda p_0 p} \tag{3.18}$$

$$P = P_0 + P_1 < p_0 e^{-4\sqrt{2}R\lambda(1-p_0)/\pi} + (1-p_0)e^{-4\sqrt{2}R\lambda p_0/\pi} \tag{3.19}$$

where p is the probability of random lines to intercept the square, given by $p = 4/(\pi\sqrt{2})$ and λ is the Poisson density parameter.

Table 3.4: Probability of one material geometry realization

CASE	p_0	p_1	$\bar{x}$	λ		P_0	P_1	P
1	0.9	0.1	0.099	15.867	1D	3.69E-5	3.30E-41	3.69E-5
					2D	1.52E-9	1.09E-80	1.52E-9
2	0.9	0.1	0.99	1.5867	1D	3.28E-1	1.13E-5	3.28E-1
					2D	1.19E-1	1.27E-9	1.19E-1
3	0.5	0.5	2.525	0.6621	1D	6.90E-2	6.90E-2	1.38E-1
					2D	9.53E-3	9.53E-3	1.91E-2

As we can see, the probability of having a realization filled with only one material is higher for the case of layered geometry (Benchmark 1D) than the case of a bidimensional stochastic geometry (Benchmark 2D).
In particular, this difference in the P value is more significant for Case 1, in which the Poisson density value is high. For Case 2, the value of P for the 2D-stochastic geometry is quite close to that of the layered geometry, whereas for Case 3, there is a bigger discrepancy in the calculated value for 1D-P and the estimated one for 2D-P, mainly due to the values of p_0 and p_1.

3.2.1 *The 9 cases description*

We are now analyzing in more details the nine Benchmark cases: the kind of properties materials 0 and 1, the mean chord lengths, the value of scattering cross sections.

Case 1

Case 1, as we have already said, is the more stochastic case: the Poisson density is high (15.867) compared to that of the other cases (1.5867; 0.6621). Stochastic pieces of materials 0 and 1 are little and well mixed in the domain.

- *Case a*

  Considering the values of c_0 and c_1, we can get information about the properties of materials 0 and 1:

$$c_0 = 0 \Rightarrow \sigma_s^0 = 0,\ \sigma_a^0 = \sigma_{tot}^0 \tag{3.20}$$

$$c_1 = 1 \Rightarrow \sigma_s^1 = \sigma_{tot}^1,\ \sigma_a^1 = 0 \tag{3.21}$$

  Material 0 is a pure absorber, with little absorbing cross section of 0.101 cm^{-1}, whereas material 1 has only scattering properties, with a bigger cross section (9.09 cm^{-1}).
  So, the stochastic geometry is composed by small pieces of the opaque material (mean chord length of 0.11 cm) and by bigger pieces of the transparent material (mean chord length of 9.9 cm).
  From Eqs (3.12) and (3.13) we can derive the values of the global macroscopic scattering and absorbing cross sections, that are, respectively:

$$\langle \sigma_s \rangle = \sigma_s^1\, p_1 = 0.909\,\text{cm}^{-1} \tag{3.22}$$

$$\langle \sigma_a \rangle = \sigma_a^0\, p_0 = 0.091\ \text{cm}^{-1} \tag{3.23}$$

  Of course, the sum of the two cross sections is unity. Thus, we have a mainly scattering mixing.

- *Case b*

Doing the same calculation of the previous case, we obtain:

$$c_0 = 1 \Rightarrow \sigma_s^0 = \sigma_{tot}^0,\ \sigma_a^0 = 0 \tag{3.24}$$

$$c_1 = 1 \Rightarrow \sigma_s^1 = 0,\ \sigma_a^1 = \sigma_{tot}^1 \tag{3.25}$$

This is the opposite case of Case a, because this time material 0 is the pure scattering one and material 1 is the absorbent. Since the total cross sections remain the same, we have a mixing characterized by relative small transparent pieces, with little cross section, and bigger pieces of opaque material. The total cross sections are:

$$\langle \sigma_s \rangle = \sigma_s^0\, p_0 = 0.091\,\mathrm{cm}^{-1} \tag{3.26}$$

$$\langle \sigma_a \rangle = \sigma_a^1\, p_1 = 0.909\ \ \mathrm{cm}^{-1} \tag{3.27}$$

and the mixing is mainly absorbent.

- *Case c*

  This case has the c_i parameters different from unity, so it is not composed by pure absorbent or pure scattering materials, but they have intermediate characteristics.

$$c_0 = 0.9 \Rightarrow \sigma_s^0 = 0.9\,\sigma_{tot}^0,\ \sigma_a^0 = \sigma_{tot}^0 - \sigma_s^0 \tag{3.28}$$

$$c_1 = 0.9 \Rightarrow \sigma_s^1 = 0.9\,\sigma_{tot}^1,\ \sigma_a^1 = \sigma_{tot}^1 - \sigma_s^1 \tag{3.29}$$

This leads to the following values: $\sigma_s^0 = 0.0909\,\mathrm{cm}^{-1}$, $\sigma_a^0 = 0.0101\,\mathrm{cm}^{-1}$; $\sigma_s^1 = 8.181\,\mathrm{cm}^{-1}$, $\sigma_a^1 = 0.909\,\mathrm{cm}^{-1}$.

The total scattering and absorbing cross sections of the mixture are:

$$\langle \sigma_s \rangle = \sigma_s^0 \, p_0 + \sigma_s^1 \, p_1 = 0.8999 \, \mathrm{cm}^{-1} \tag{3.30}$$

$$\langle \sigma_a \rangle = \sigma_a^0 \, p_0 + \sigma_a^1 \, p_1 = 0.1001 \ \mathrm{cm}^{-1} \tag{3.31}$$

Case 2

Case 2 is characterized by a value of λ that is ten times smaller compared to the that of the first case. The density of random lines crossing the domain is not so high and the dimension of the pieces is bigger than in Case 1, as we can see in the examples above.
Since the probability of finding materials 0 and 1 are the same as Case 1 ($p_0 = 0.9$, $p_1 = 0.1$) and the λ is ten times smaller, the corresponding mean chord lengths are ten time bigger than Λ_0 and Λ_1 for Case 1.
The total cross sections σ_{tot}^0 and σ_{tot}^1 are the same of the first case, thus also the values of scattering and absorbing cross sections of all the subcases are equal to those previously calculated.

Case 3

Case 3 has a value of λ that is not so far from that of Case 2, but the big difference between the two cases lies in the probabilities p_0 and p_1.
In this case, the probability of finding material 0 is the same of finding material 1: $p_0 = p_1 = 0.5$. Joint to the quite big values of the mean chord lengths (5.05 cm, the half of the domain size), this explains why a lot of geometry realizations are filled with only one material.
The total cross sections of the two materials are smaller than those of Case 1 and Case 2: this leads to different values for scattering and absorbing cross sections of each subcase.

- *Case a*

  Like in the other cases, material 0 is a pure absorber, with absorbing cross section equal to the total cross section, whereas material 1 has only scattering properties, with the cross section given by the total one.

$$c_0 = 0 \Rightarrow \sigma_s^0 = 0,\ \sigma_a^0 = \sigma_{tot}^0 \tag{3.32}$$

$$c_1 = 1 \Rightarrow \sigma_s^1 = \sigma_{tot}^1,\ \sigma_a^1 = 0 \tag{3.33}$$

  The total scattering and absorbing cross sections of the mixture are:

$$\langle \sigma_s \rangle = \sigma_s^1\, p_1 = 0.99\,\mathrm{cm}^{-1} \tag{3.34}$$

$$\langle \sigma_a \rangle = \sigma_a^0\, p_0 = 0.0099\ \mathrm{cm}^{-1} \tag{3.35}$$

- *Case b*

  This time, material 0 is the scattering one and material 1 is the absorbent one.

$$c_0 = 1 \Rightarrow \sigma_s^0 = \sigma_{tot}^0,\ \sigma_a^0 = 0 \tag{3.36}$$

$$c_1 = 1 \Rightarrow \sigma_s^1 = 0,\ \sigma_a^1 = \sigma_{tot}^1 \tag{3.37}$$

  and the global cross sections are given by:

$$\langle \sigma_s \rangle = \sigma_s^0\, p_0 = 0.0099\,\mathrm{cm}^{-1} \tag{3.38}$$

$$\langle \sigma_a \rangle = \sigma_a^1\, p_1 = 0.99\ \mathrm{cm}^{-1} \tag{3.39}$$

- *Case c*

  The values of scattering and absorbing cross sections of the two mate-

rials are calculated as follow:

$$c_0 = 0.9 \Rightarrow \sigma_s^0 = 0.9\,\sigma_{tot}^0,\ \sigma_a^0 = \sigma_{tot}^0 - \sigma_s^0 \tag{3.40}$$

$$c_1 = 0.9 \Rightarrow \sigma_s^1 = 0.9\,\sigma_{tot}^1,\ \sigma_a^1 = \sigma_{tot}^1 - \sigma_s^1 \tag{3.41}$$

and they are: $\sigma_s^0 = 0.01782\,\mathrm{cm}^{-1}$, $\sigma_a^0 = 0.00198\,\mathrm{cm}^{-1}$; $\sigma_s^1 = 1.782\,\mathrm{cm}^{-1}$, $\sigma_a^1 = 0.198\,\mathrm{cm}^{-1}$.

The global cross sections are:

$$\langle \sigma_s \rangle = \sigma_s^0\,p_0 + \sigma_s^1\,p_1 = 0.89991\,\mathrm{cm}^{-1} \tag{3.42}$$

$$\langle \sigma_a \rangle = \sigma_a^0\,p_0 + \sigma_a^1\,p_1 = 0.1001\ \ \mathrm{cm}^{-1} \tag{3.43}$$

that are the same of cases 1c and 2c.

The resuming table of the different nine cases parameters is reported in the following page.

Table 3.5: Parameters of the nine cases analysed

CASE 1									
λ	Λ_0	Λ_1	σ_t^0	σ_t^1		σ_s^0	σ_a^0	σ_s^1	σ_a^1
15.867	0.99	0.11	0.101	9.09	a	0	0.101	9.09	0
					b	0.101	0	0	9.09
					c	0.0909	0.0101	8.181	0.909
CASE 2									
λ	Λ_0	Λ_1	σ_t^0	σ_t^1		σ_s^0	σ_a^0	σ_s^1	σ_a^1
1.5867	9.9	1.1	0.101	9.09	a	0	0.101	9.09	0
					b	0.101	0	0	9.09
					c	0.0909	0.0101	8.181	0.909
CASE 3									
λ	Λ_0	Λ_1	σ_t^0	σ_t^1		σ_s^0	σ_a^0	σ_s^1	σ_a^1
0.6621	5.05	5.05	0.0198	1.98	a	0	0.0198	1.98	0
					b	0.0198	0	0	1.98
					c	0.01782	0.00198	1.782	0.198

3.3 *Benchmark calculations*

We will now describe the procedure to compute benchmark calculations.

We used a program that allows to generate the 2D Markovian geometry, extend the geometry in three dimensions and run the Monte Carlo code TRIPOLI-4 ® to find the searched values.

We used a program called "T4StochGeo", implemented by Thibaut Lepage in a previous stage, that generates a certain number of stochastic geometries and creates some output files, written in the characteristic language of TRIPOLI-4 ®.

It needs some input parameters:

- *size s*

- *probability p*
- *density* λ
- *geometries*: number of geometries the program builds for each triplet (size, density, proba)
- *batches*: number of simulations TRIPOLI-4 ® performed for each geometry
- *neutrons*: number of neutrons used per simulation
- *red*: name of the composition corresponding to material 0
- *blue*: name of the composition corresponding to material 1
- *homogeneous*: it allows to construct a homogeneous geometry for comparison (optional keyword)
- *origin*: used for Suite II, it realizes stochastic geometries in the domain with internal uniform source of neutrons (optional keyword)

The program requires also two other files: a composition file, that contains the list of materials simulated with the corresponding compositions, and a path file, in which are written four paths: one for the geometry program, one for the TRIPOLI-4® executable, one for its dictionary file and the last for the composition file.
It produces some output files, among which there are the datafile, directly used by TRIPOLI-4® to run the Monte Carlo simulation, and the results file, containing results and relative errors for each simulation.
For Case1, we also performed parallel calculations: for each simulation, it takes 6 hours in average and we had to do a great number of simulations to

get statistical significant results.

We will now briefly describe the Monte Carlo code TRIPOLI-4 ® and the parallel calculations.

3.3.1 TRIPOLI-4® description

TRIPOLI® is a Monte Carlo code, developed by the LTSD laboratory of CEA Saclay.

It is a three-dimensional, continuous energy computer code for particle transport that can treat neutrons, photons, electrons and positrons.

In this case, we performed neutron calculations for Benchmark problem (and criticality calculations for the k_{eff} problem- Suite III).

The scores we looked for are:

- for Suite I: the values of the outgoing currents from the domain at $x = 0$ and $x = L$, namely *reflection* and *transmission*

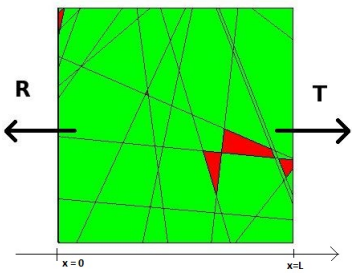

Fig. 3.7: Setup for Suite I

- for Suite II: the value of the outgoing current form the domain at $x = L$, namely the *leakage*

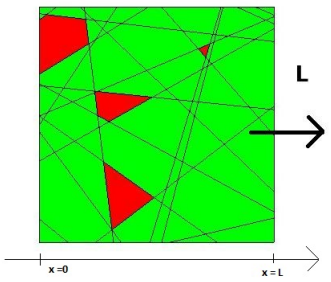

Fig. 3.8: Setup for Suite II

3.3.2 Parallel calculations

We performed parallel calculations on a cluster available at CEA.

We modified the C++ main program in order to only have a great number of stochastic geometries generated. Then, we built a series of datafile, each one recalling the geometry and the composition of one of the previous geometry simulation. Finally, we run TRIPOLI-4 ® for all the files.

For each job, we used 100 processors and we launched about 400 simulations. Each processor undertook only one simulation file at a time and, only after finished the calculation, took the next.

The mean simulation time was of 6 hours: in 24 hours, about 350 complete simulations were done. We performed 3000 calculations for each of the three subcases.

Chapter 4

Suite I Benchmark results

We are now reporting the results and the corresponding histograms for each case, with remarks and comparison to the other models and benchmark results previous described.

We show here the Benchmark calculated results for the reflection, the transmission and the absorption ($A = 1 - T - R$), together with the Benchmark results for the one-dimensional planar geometry (*Benchmark 1D*) and the results for the Markovian model (*Markovian*) and for a Monte Carlo algorithm (*Algorithm B*).

For each case, we built also a table containing the differences between the Benchmark results calculated in the 2D stochastic geometry and the other available data.

4.1 *Case 1*

4.1.1 *Case 1a*

In general, for Case 1a there is not a big discrepancy between the values calculated for our Benchmark and the results given by Benchmark 1D calculations, Markovian model and Monte Carlo algorithm B .

Table 4.1: Case 1a results

	Benchmark 2D	*Benchmark 1D*	*Markovian*	*Algorithm B*
R	0.40528	0.43634	0.37596	0.40086
T	0.018359	0.01486	0.02589	0.02202
A	0.57604	0.5488	0.59815	0.57112

However, as we can see in the table reporting the differences, the results of Algorithm B are the more similar to those calculated; in particular, they fit very well for the transmission value, for which the delta is one order smaller than the other results.

Table 4.2: Case 1a difference table

$\lvert Benchmark2D - ... \rvert$	*Benchmark 1D*	*Markovian*	*Algorithm B*
R	0.03106	0.02932	0.00442
T	0.00499	0.00753	0.00367
A	0.02756	0.0218	0.00076

We report also the histograms for the values of transmission and reflection and the corresponding errors.

Fig. 4.1: Histograms of reflection and transmission for the Case 1a

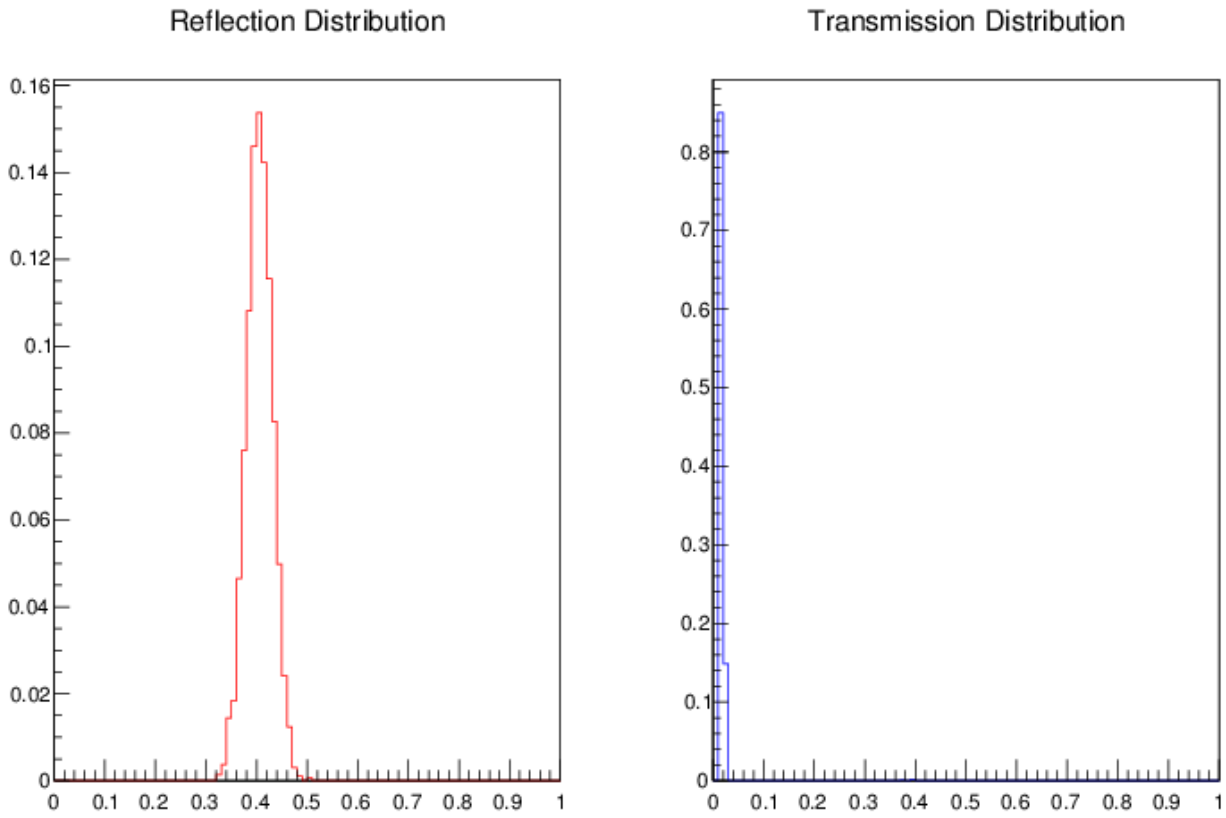

As we can see, the distributions of reflection and transmission are very peaked, even with only about 3000 simulations. This is the more stochastic case, in which pieces are well mixed and the mean chord lengths are small compared to the domain size: particles that enters the box will undergo different reactions during their travel and, in the mean, the final result is nearly the same.

Thus, it is not necessary to perform a lot of simulations: the error is already little and acceptable with this number of geometries.

Fig. 4.2: Histograms of reflection and transmission relative errors for the Case 1a

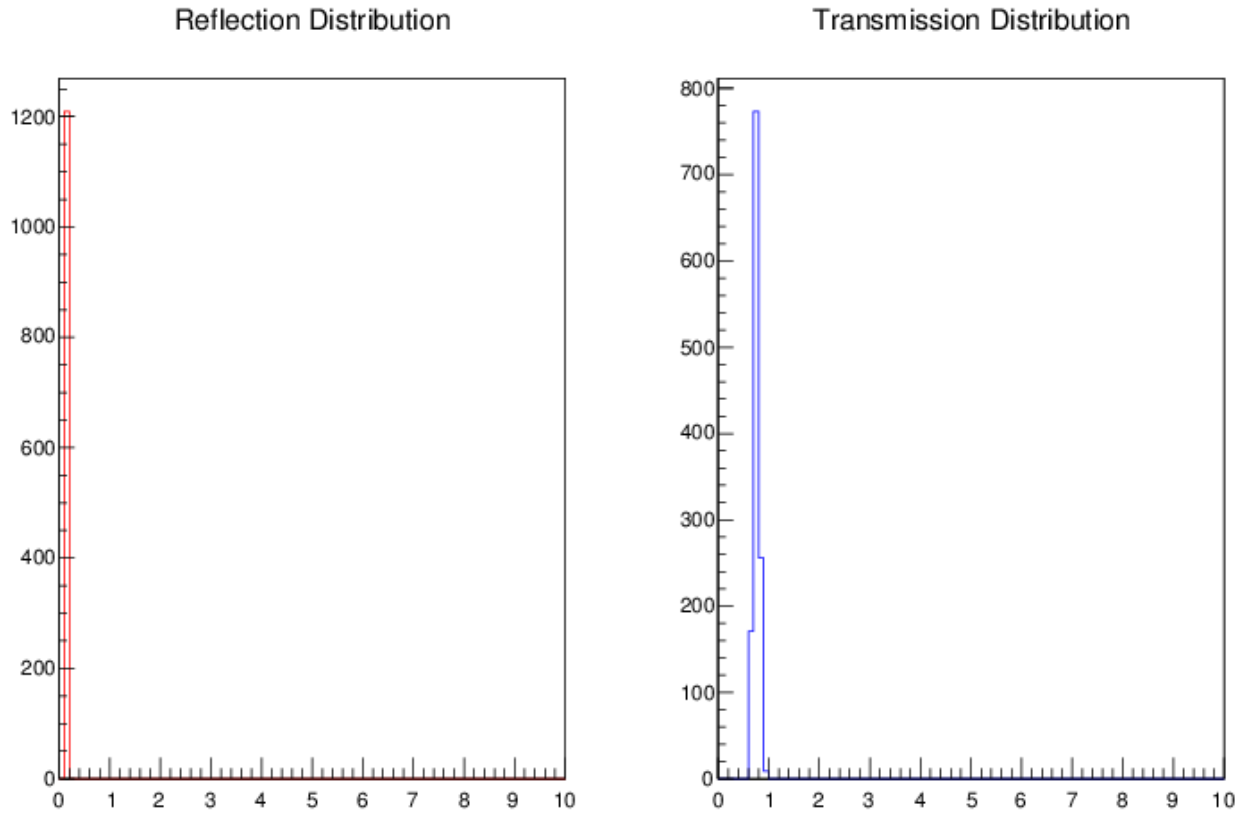

4.1.2 *Case 1b*

Table 4.3: Case 1b results

	Benchmark 2D	*Benchmark 1D*	*Markovian*	*Algorithm B*
R	0.04558	0.08549	0.05906	0.07755
T	0.001346	0.00166	0.00153	0.00164
A	0.953074	0.91285	0.93941	0.92081

In this case, the bigger difference between Benchmark results and reference values lies in the reflection. The value calculated for the reflection is very different from the value given by the Benchmark 1D.

Table 4.4: Case 1b difference table

$\lvert Benchmark2D - ... \rvert$	*Benchmark 1D*	*Markovian*	*Algorithm B*
R	0.03991	0.01348	0.03197
T	0.00031	0.00018	0.0003
A	0.04022	0.01366	0.03226

It is mainly due to the geometry configuration: in the case of planar 1D geometry, the entering particle encounters for the 90% of times a layer of scattering material, uniformly present along the y axis. At the contrary, in our geometry there is a distribution of the two materials at the inlet face: the particle can undergo a scattering reaction but also an absorbing one. Since the mean chord lengths are not only in the x direction, in our Benchmark calculations the particle can see the absorber material (in this case the 1) also at a small depth from the entrance, whereas in 1D Benchmark case it will see the first material encountered for all its x chord length.

Fig. 4.3: Histograms of reflection and transmission for the Case 1b

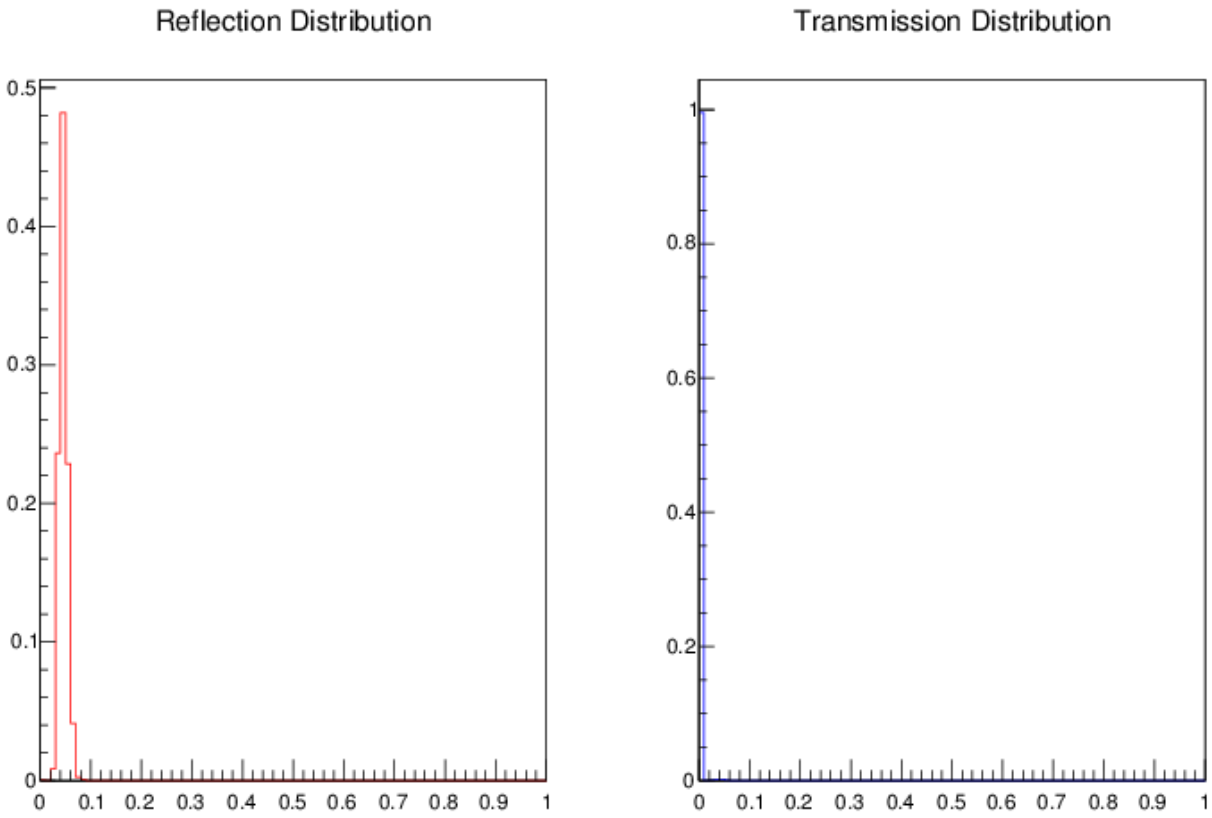

The reflection and transmission distributions are quite peaked, and it seems that only about 3500 geometries are enough to have good statistical results.

We can notice that, whereas the error distribution for the reflection is very defined, the distribution for the transmission is quite wide, because of the small mean value.

Fig. 4.4: Histograms of reflection and transmission relative errors for the Case 1b

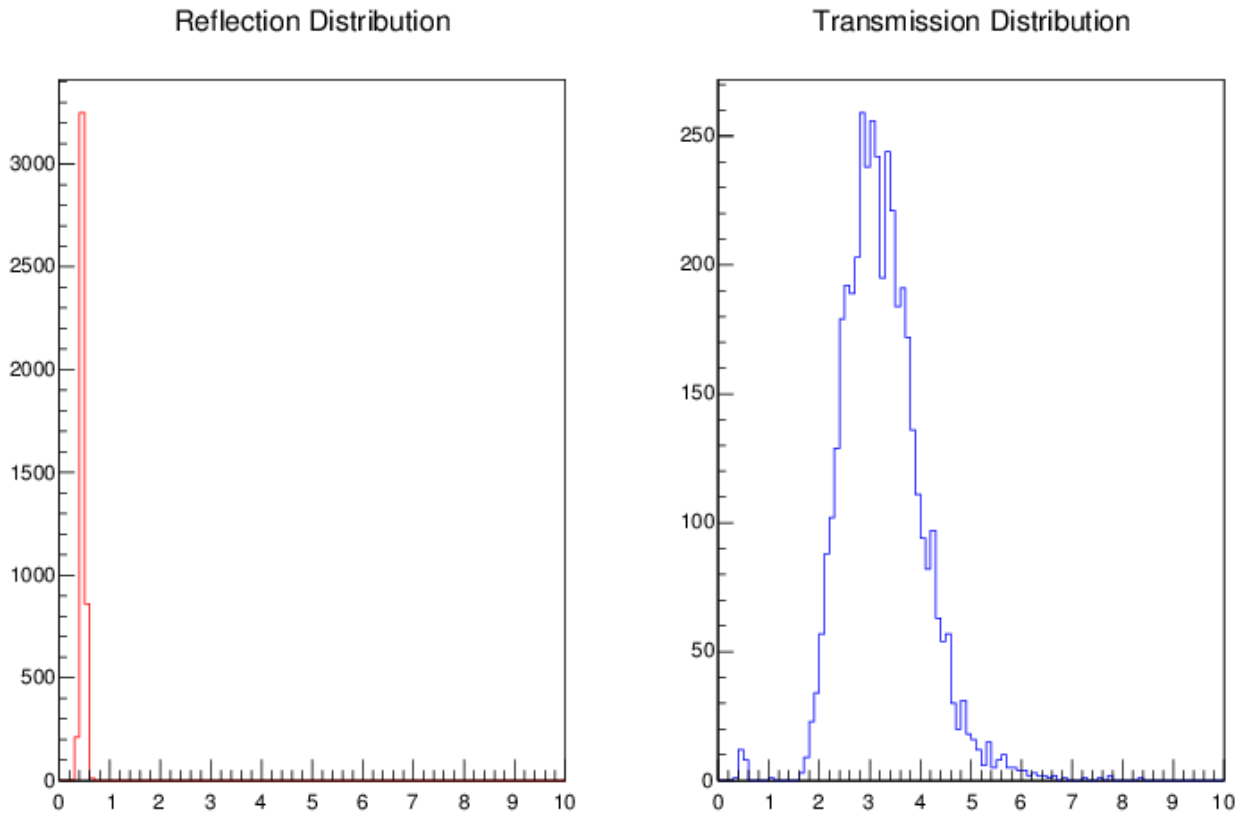

4.1.3 *Case 1c*

This is the subcase of Case 1 in which the results of the 2D Benchmark are quite close also to those of the 1D Benchmark calculations. The Markovian model does not predict very well the experimental results, while the Algorithm B gives again a good general response.

Table 4.5: Case 1c results

	Benchmark 2D	*Benchmark 1D*	*Markovian*	*Algorithm B*
R	0.47074	0.47746	0.37066	0.40690
T	0.018359	0.01609	0.02373	0.02377
A	0.51116	0.50645	0.60561	0.56933

The good agreement between the two Benchmark results might be given by the characteristics of the two materials: both material 0 and 1 have non zero absorbing and scattering cross sections, so the added stochastic dimension for the geometry does not strongly affect the results. The two materials are quite similar, because their scattering cross section is the 90% of the total cross section: thus, between a one-dimension and a two-dimension stochastic geometry there is not a great difference concerning the type of interaction a particle can undergo in the first layers of the domain (there is only a difference on the probability of interacting).

Table 4.6: Case 1c difference table

$\lvert Benchmark2D - ... \rvert$	*Benchmark 1D*	*Markovian*	*Algorithm B*
R	0.00672	0.10008	0.06384
T	0.00201	0.00563	0.00281
A	0.00471	0.09445	0.06103

The reflection and the transmission distributions, both for the mean and for the error, are peaked and the number of geometries used for this case are

less than those for case a and b: they are only 2000.

Fig. 4.5: Histograms of reflection and transmission for the Case 1c

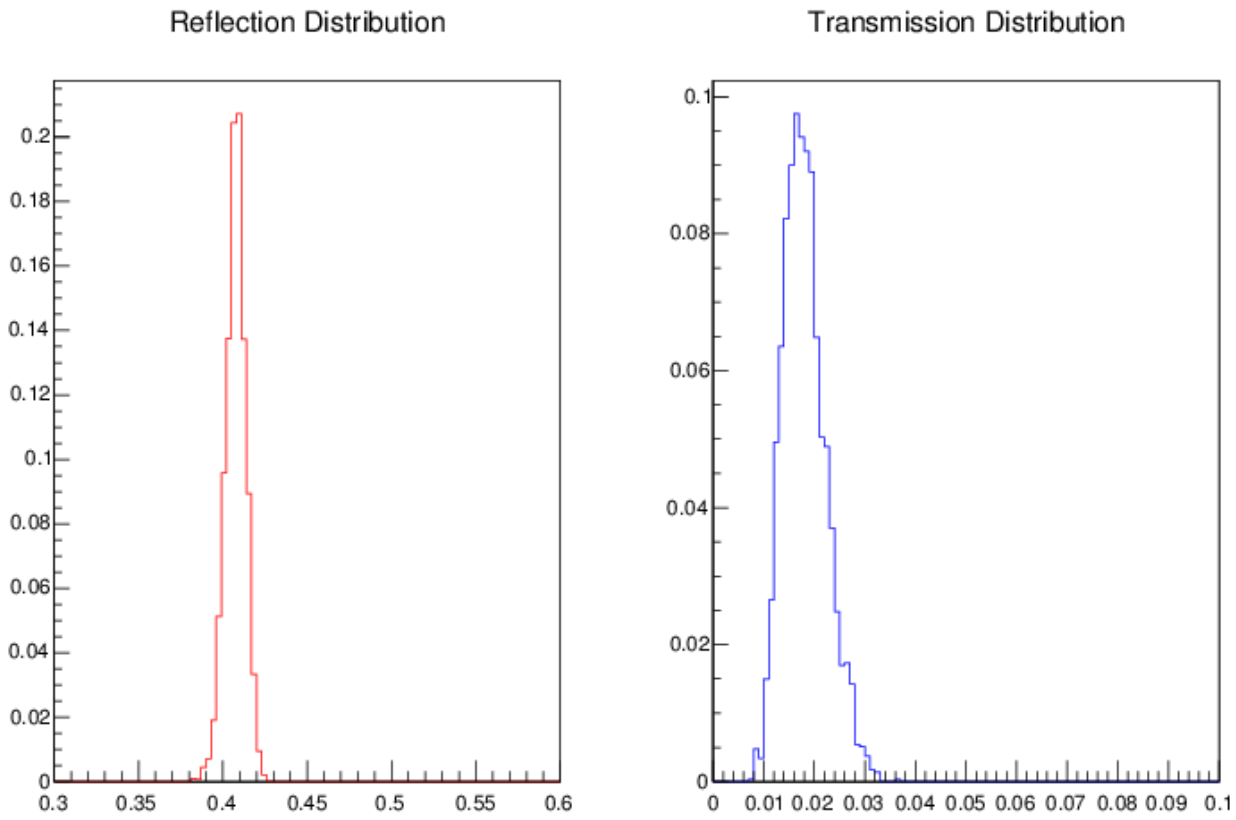

Fig. 4.6: Histograms of reflection and transmission relative errors for the Case 1c

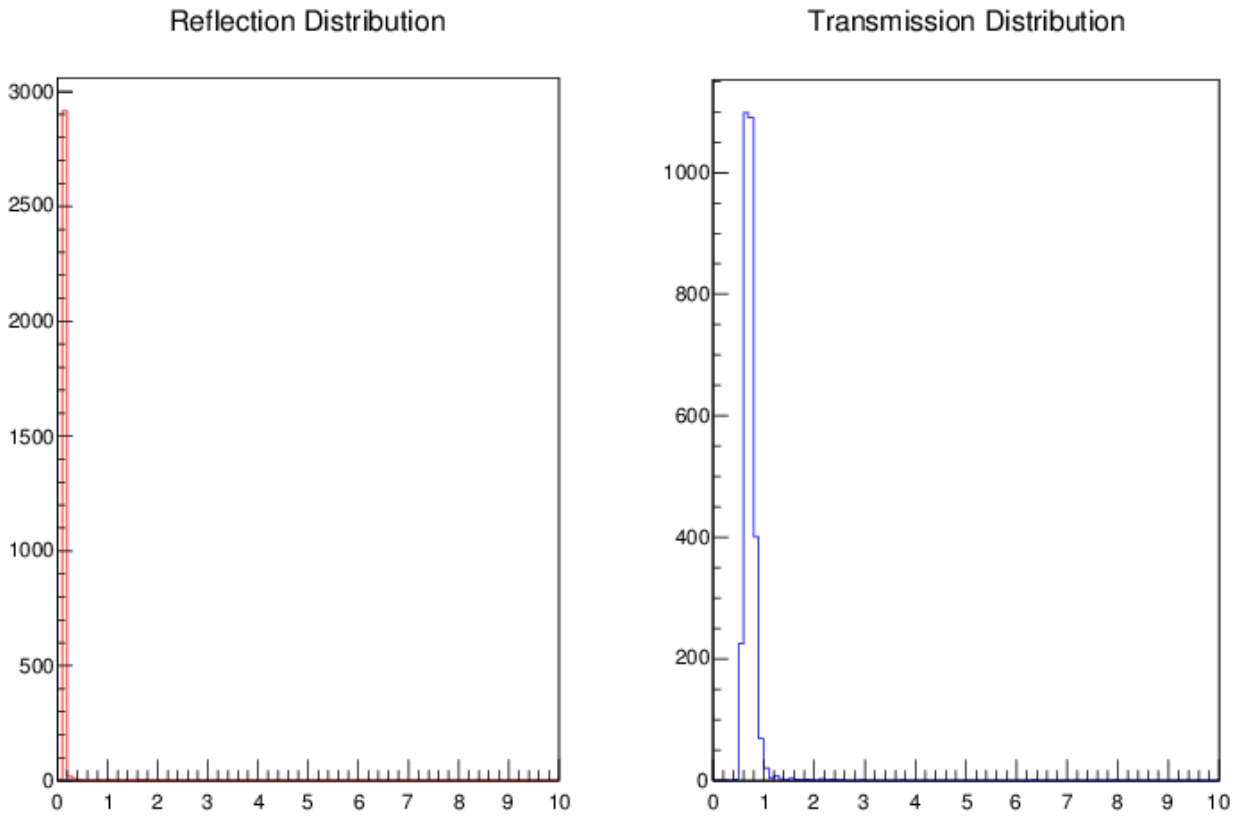

4.2 *Case 2*

4.2.1 *Case 2a*

Compared to Case 1, only the density parameter is different: it is ten times smaller, so the chunks of materials 0 and 1 in the stochastic geometry are bigger.

Table 4.7: Case 2a results

	Benchmark 2D	*Benchmark 1D*	*Markovian*	*Algorithm B*
R	0.23184	0.23723	0.17986	0.22235
T	0.09692	0.09843	0.12279	0.1006
A	0.67124	0.66434	0.69735	0.67705

Again, we can notice that Algorithm B is the one which goes closer to the 2D Benchmark results, even if for the transmission value Benchmark 1D gives a similar value.
It is remarkable that this case is less stochastic than Case 1: the results calculated for the one-dimensional geometry (Benchmark 1D) are in general not so far from ours, so a less accurate approximation of stochastic geometry could be used.
It is interesting to see that, whereas for the transmission value the result of Benchmark 1D is more close to our Benchmark, at the end regarding the absorption value, Algorithm B is the more similar.

Table 4.8: Case 2a difference table

$\lvert Benchmark2D - ... \rvert$	*Benchmark 1D*	*Markovian*	*Algorithm B*
R	<u>0.00539</u>	0.05198	0.009493
T	<u>0.00118</u>	0.03087	0.009048
A	0.0069	0.02112	<u>0.00045</u>

Even if the error distribution of the reflection is very peaked, the mean value distribution shows a spread and a Gaussian shape non completely filled.

It means that other simulations are needed in order to have good statistical results.

Moreover, we can remark that two lateral peaks begin to appear in the histograms: they correspond to the case in which the geometry is constituted by only one material. Their value on the x axis concurs exactly with the solution of the transport problem obtained considering a one-material homogeneous geometry.

The probability of having a one material realization of the geometry is not so high and, according to the values of p_0 and p_1, the probability for material 1 is smaller than the probability for material 0, as shown in Table 3.4.

Fig. 4.7: Histograms of reflection and transmission for the Case 2a

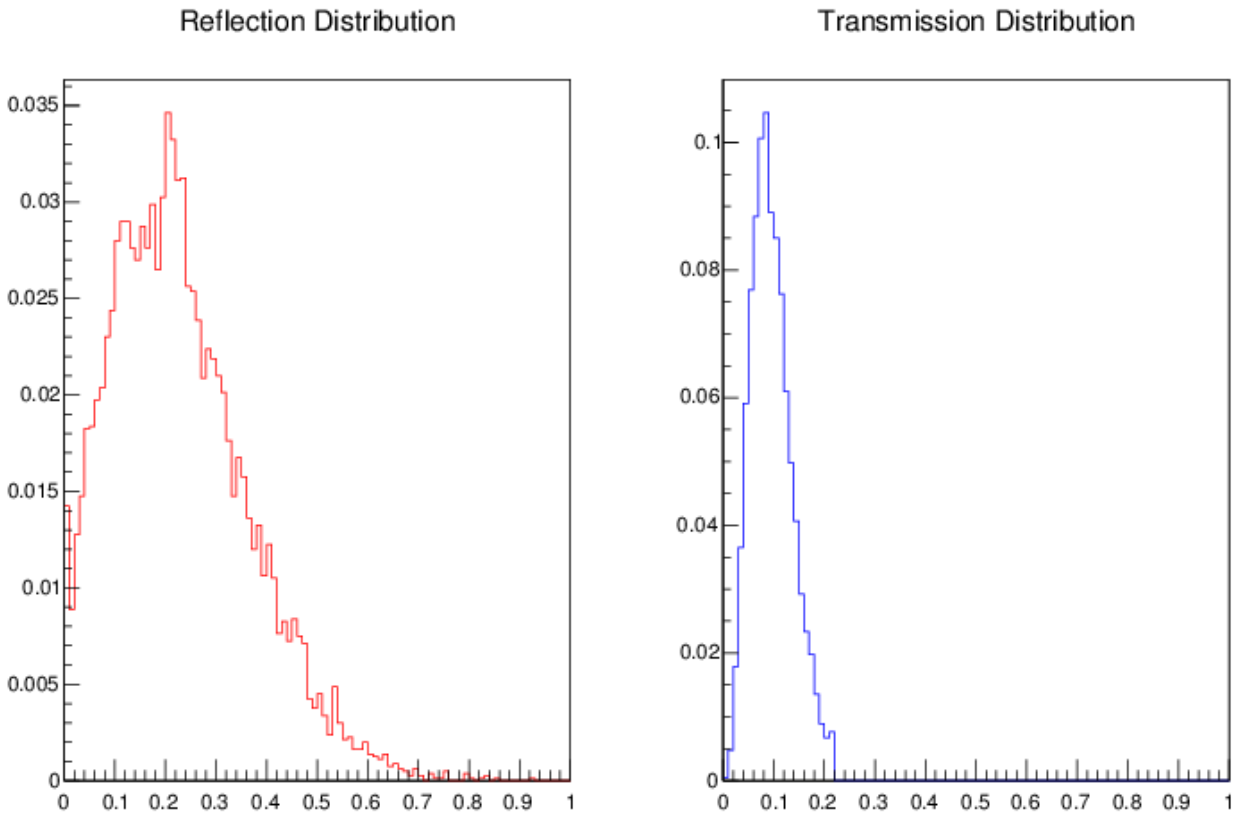

Fig. 4.8: Histograms of reflection and transmission relative errors for the Case 2a

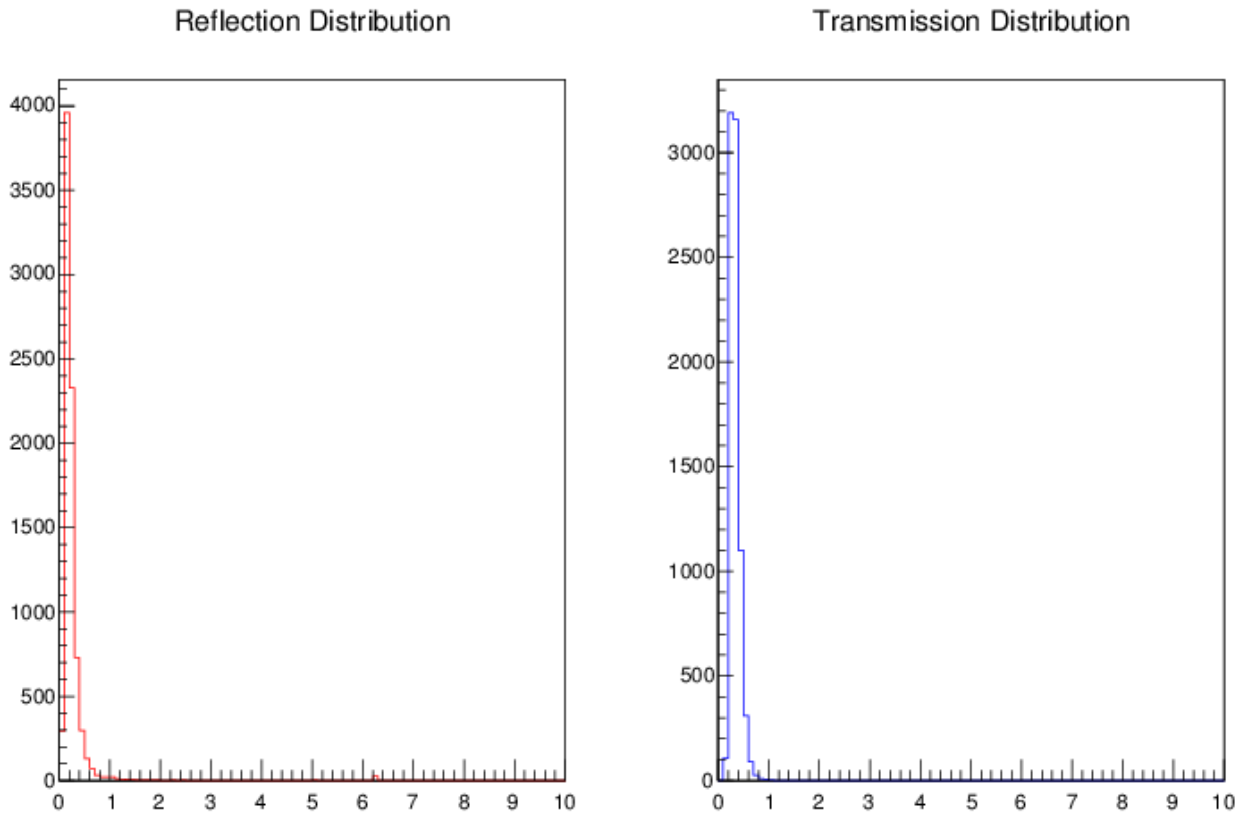

4.2.2 *Case 2b*

Results of Case 2b are quite different from those calculated in Benchmark 1D, as for the ones given by Algorithm B. Wherease, this time the Markovian model is the one which goes closer to the values we found, as we can see in Table 4.9.

Compared to Benchmark 1D, in Benchmark 2D both the reflection and the

Table 4.9: Case 2b results

	Benchmark 2D	*Benchmark 1D*	*Markovian*	*Algorithm B*
R	0.19807	0.28763	0.21928	0.28542
T	0.1436	0.19553	0.17869	0.19528
A	0.65833	0.51684	0.60203	0.5193

transmission decrease: in this case, even if the scattering material 0 is present in the 90% of the volume, the contribution of material 1 is more important: it has a greater total cross section and in the bidimensional stochastic geometry it is present in a more randomly way in all the (x, y) plane, thus the interaction can be more frequent.

Table 4.10: Case 2b difference table

$\lvert Benchmark2D - ... \rvert$	*Benchmark 1D*	*Markovian*	*Algorithm B*
R	0.08956	0.02121	0.08735
T	0.05193	0.03509	0.05168
A	0.14149	0.0563	0.13903

The reflection and the transmission distribution have a similar shape, the transmission having a more pronounced tail.

The peaks corresponding to the realization with only one material are well visible in both the histograms.

Fig. 4.9: Histograms of reflection and transmission for the Case 2b

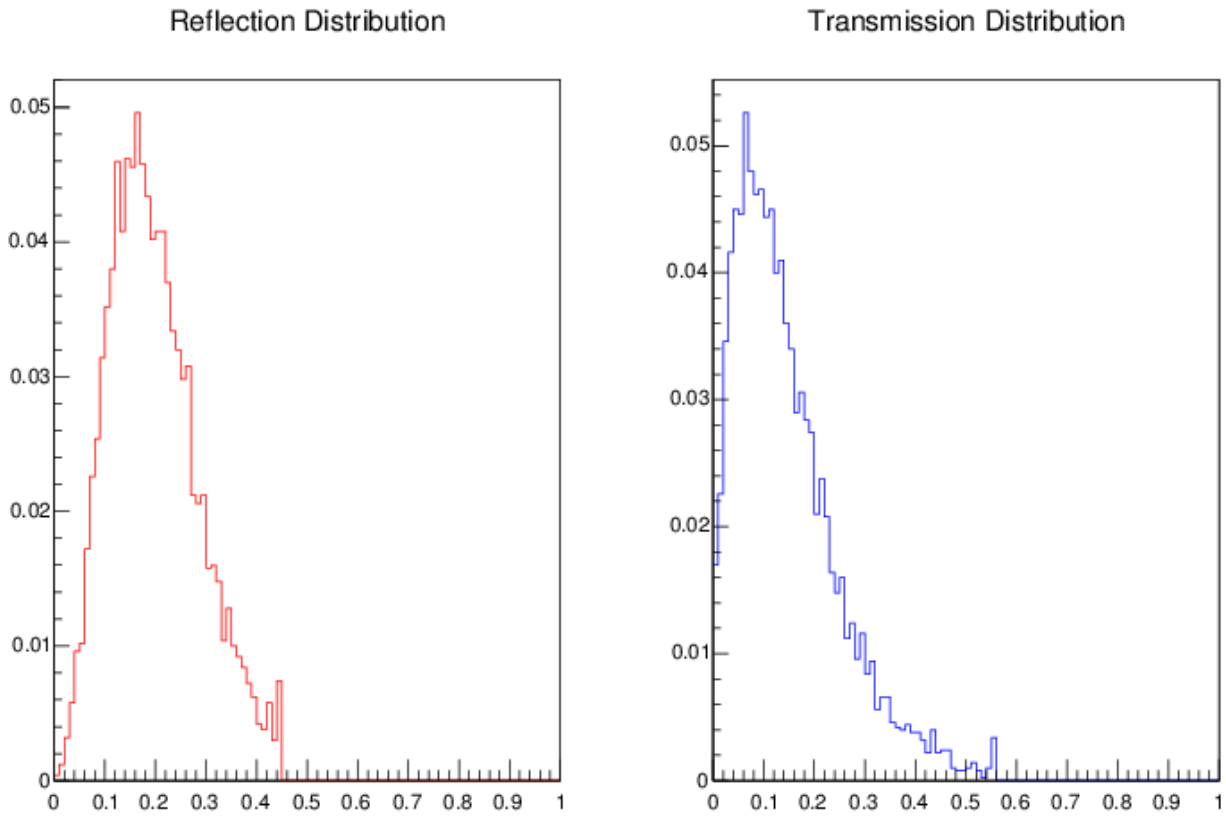

Fig. 4.10: Histograms of reflection and transmission relative errors for the Case 2b

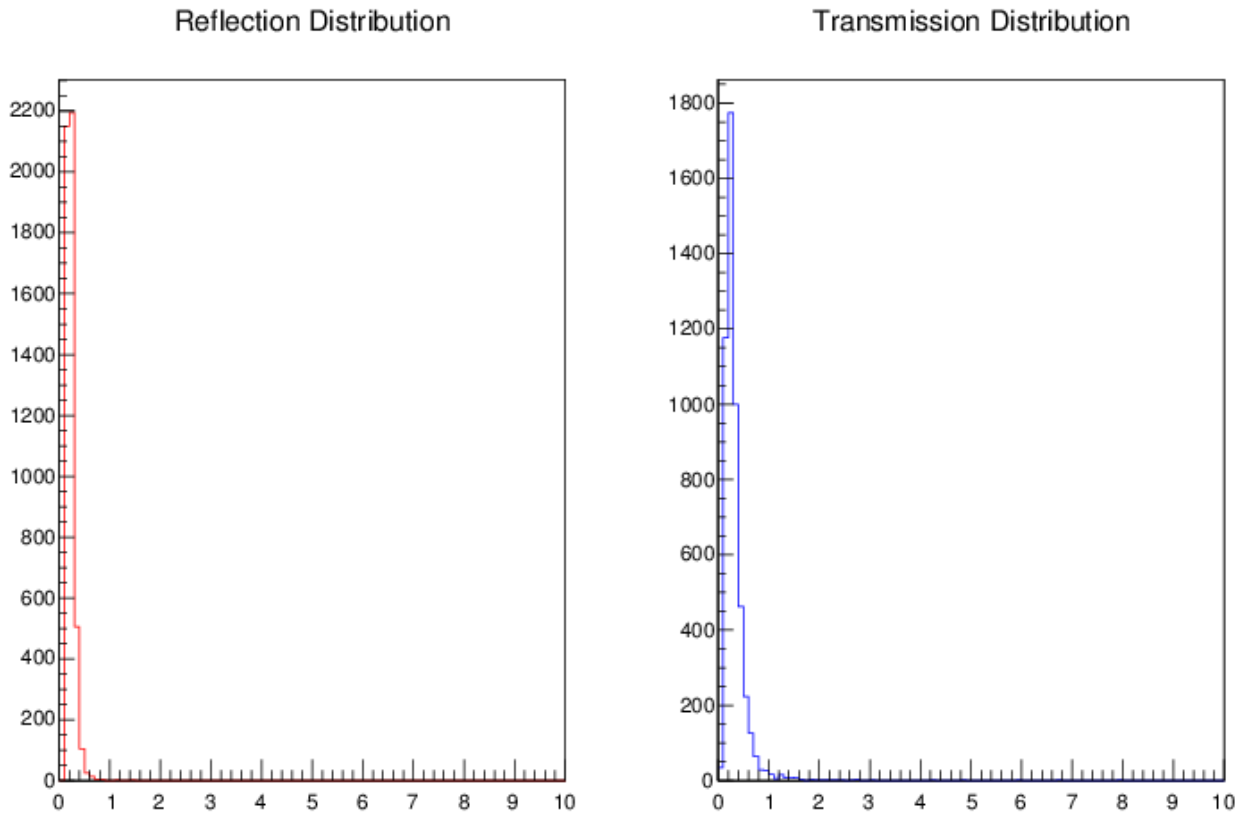

4.2.3 *Case 2c*

Compared to Benchmark 1D, the value of transmission obtained is about the same, whereas the reflections decreases. Once again, the Algorithm B is the one that produces the more similar results in relation to our Benchmark calculations.

Table 4.11: Case 2c results

	Benchmark 2D	*Benchmark 1D*	*Markovian*	*Algorithm B*
R	0.3669	0.43319	0.29092	0.40092
T	0.1814	0.1869	0.1944	0.19556
A	0.4517	0.37991	0.51468	0.40352

Table 4.12: Case 2c difference table

$\lvert Benchmark2D - ... \rvert$	*Benchmark 1D*	*Markovian*	*Algorithm B*
R	0.06629	0.07596	0.03402
T	0.00552	0.01302	0.01416
A	0.07179	0.06294	0.04818

The Markovian model shows in general a reducing accordance in opposition to Case 1, where its results are quite close to those of Benchmark 2D. Looking at the distributions, we can notice that the reflection distribution, both the mean and the error, is very peaked. The transmission shows instead a spread distribution, always with the peak of the one-material solution, meaning that more simulations are needed. In particular, the error distribution has a wide bell, even if the mean value is not so small compared to transmission in previous cases.

Fig. 4.11: Histograms of reflection and transmission for the Case 2c

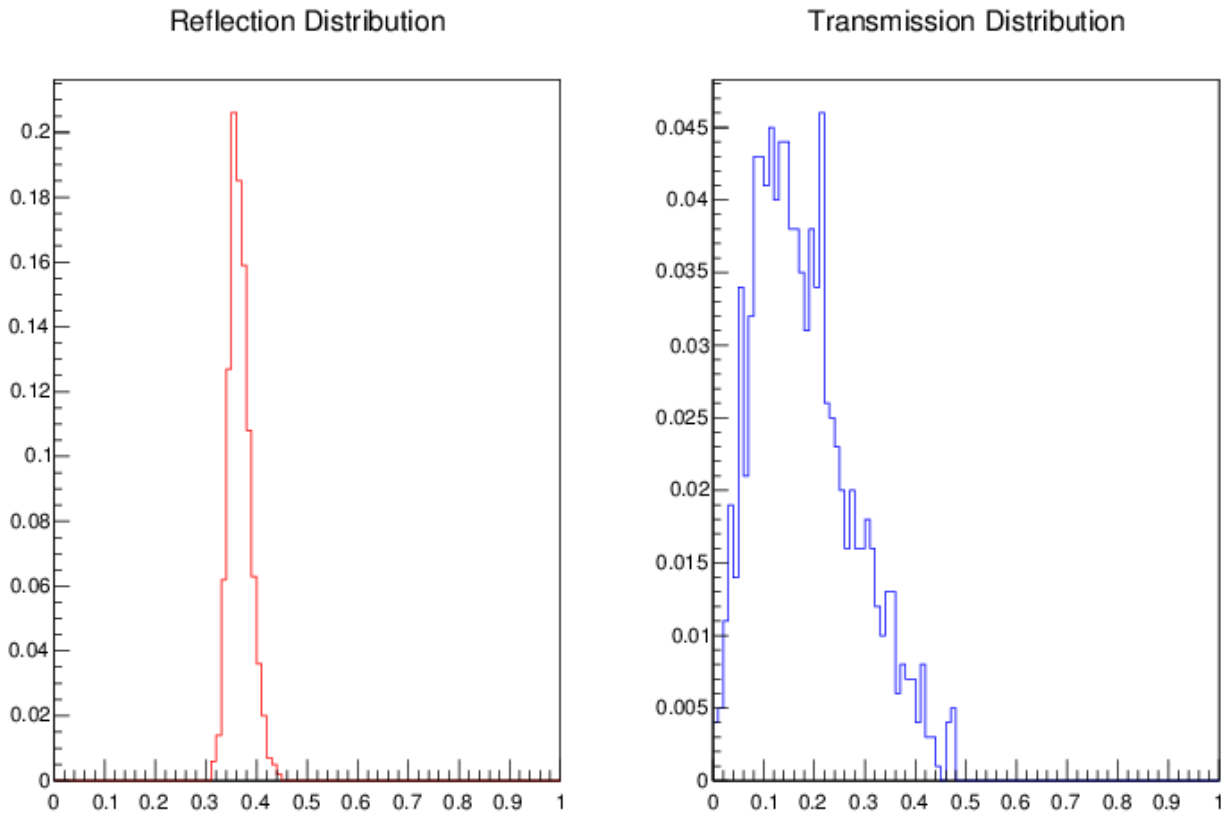

Fig. 4.12: Histograms of reflection and transmission relative errors for the Case 2c

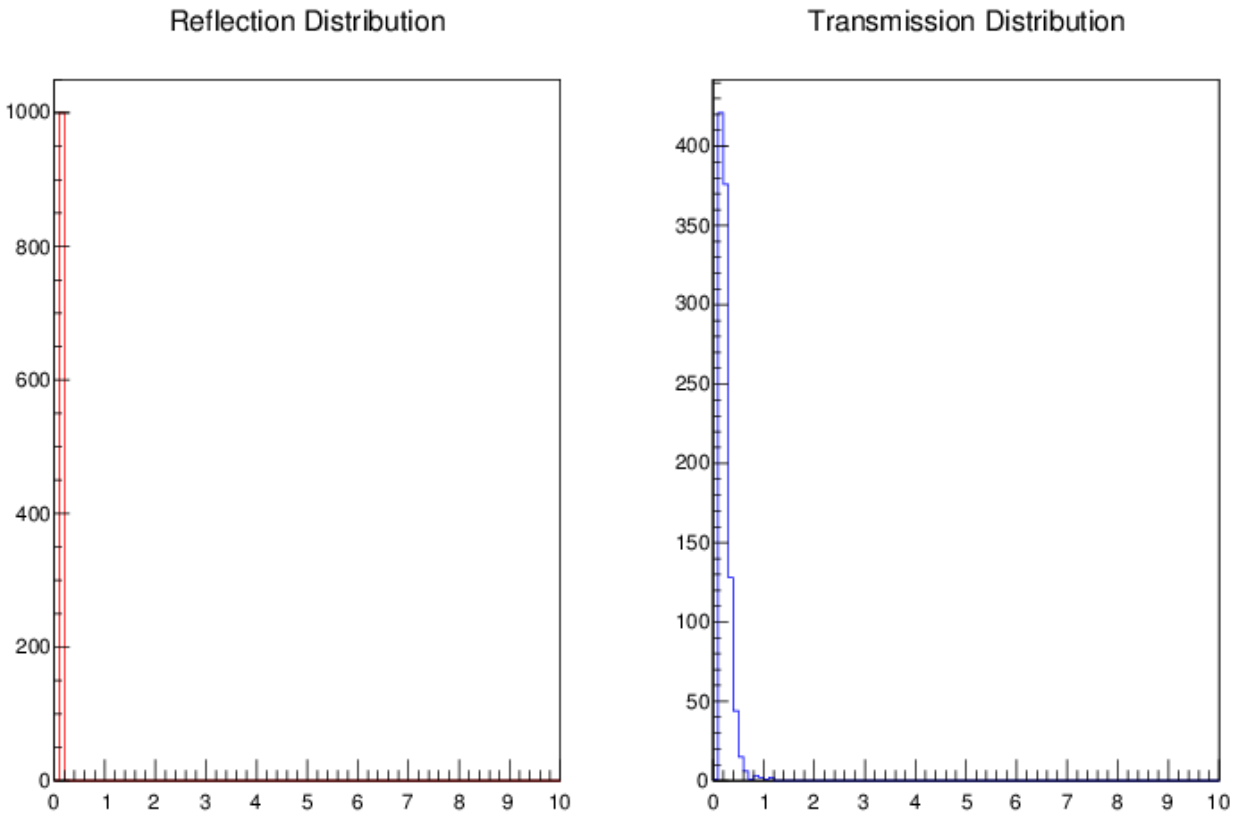

4.3 *Case 3*

4.3.1 *Case 3a*

Because of its little Poisson density λ, Case 3 is the less heterogeneous one. The probability of finding materials 0 and 1 are the same ($p_0 = p_1 = 0.5$), meaning that the mean chord lengths are almost equal to the half of the domain size. Thus, the chunks composing the geometry are very big. Also the probability of having realizations filled only with one material is higher than that for Case 1, but it remains however smaller than that of Case 2, in which the pieces have similar size, but the probability of finding material 0 is much more bigger.

According to our considerations, we can see that the results given by Benchmark 1D are very close to those obtained in calculations performed in binary stochastic geometries. In particular, for Case 3a, the values we found are in great agreement to those of Benchmark 1D.

Table 4.13: Case 3a results

	Benchmark 2D	*Benchmark 1D*	*Markovian*	*Algorithm B*
R	0.6911	0.67949	0.60694	0.65416
T	0.1635	0.16564	0.23908	0.19804
A	0.1454	0.15487	0.15398	0.1478

Table 4.14: Case 3a difference table

$\lvert Benchmark2D - ... \rvert$	*Benchmark 1D*	*Markovian*	*Algorithm B*
R	<u>0.0116</u>	0.07255	0.02533
T	<u>0.00214</u>	0.07344	0.0324
A	0.00946	<u>0.00089</u>	0.00707

The first observation regarding the histograms is that, even if the number of realizations is bigger, the distributions are more wide and spread, compared to Case 1 and also Case 2.

Secondly, the lateral peaks of the distributions corresponding to the one material realizations are well pronounced.

Although the reflection and the transmission distributions are spread, the error ones are very concentrated, meaning that the value of the variance is acceptable.

Fig. 4.13: Histograms of reflection and transmission for the Case 3a

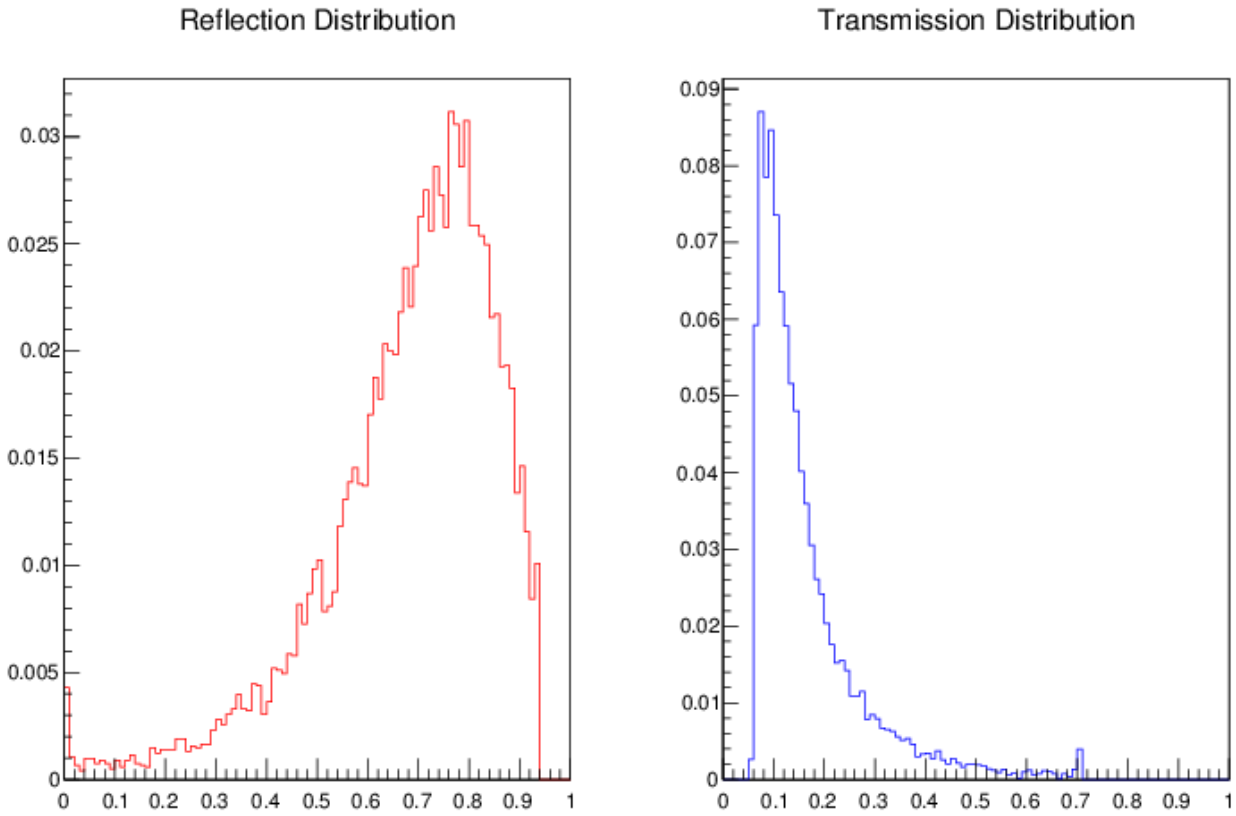

Fig. 4.14: Histograms of reflection and transmission relative errors for the Case 3a

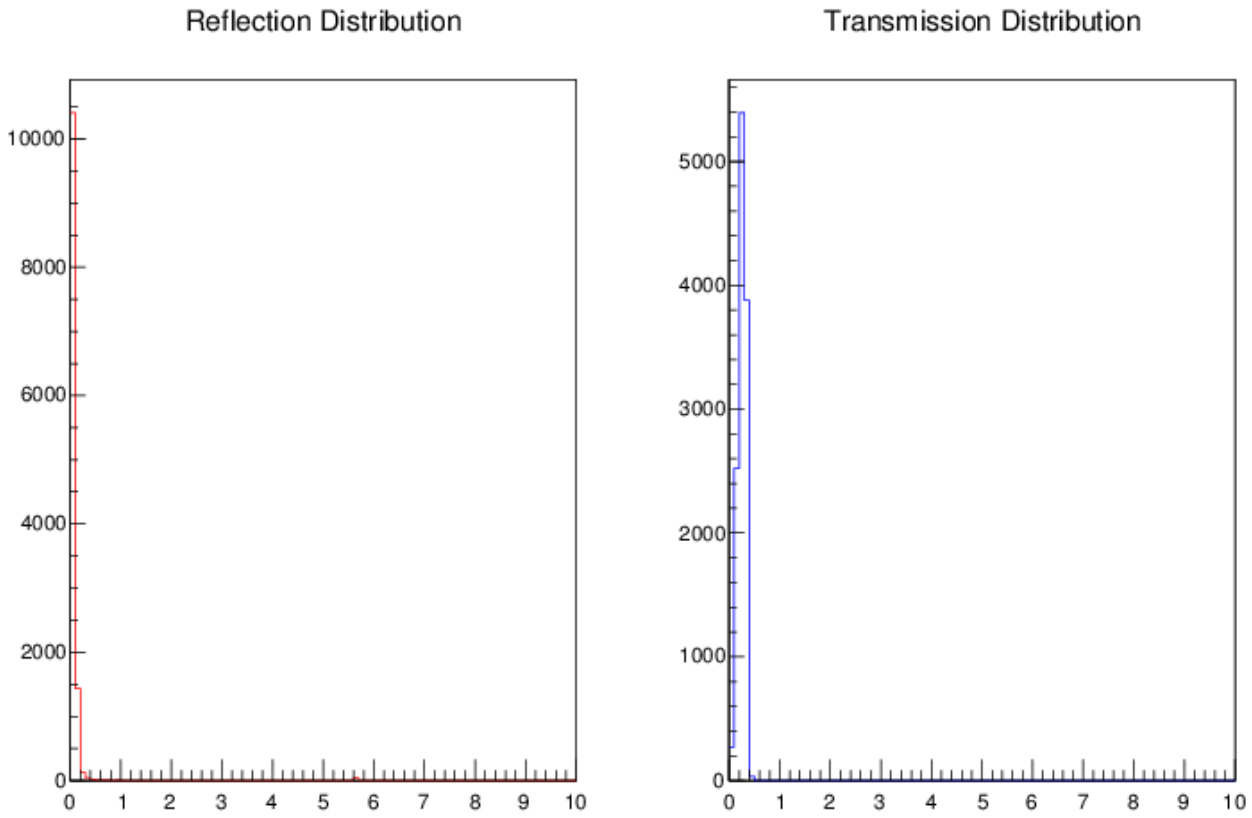

4.3.2 *Case 3b*

In this case, compared to results of Benchmark 1D, the reflection we calculated is increased, whereas the transmission is reduced.
However, we can see that in general the values obtained in Benchmark 1D are quite similar to ours, just as those from the Markovian model and the Algorithm B are.
Especially the Markovian model seems to predict the exact values for transmission and reflection of this case.

Table 4.15: Case 3b results

	Benchmark 2D	*Benchmark 1D*	*Markovian*	*Algorithm B*
R	0.020991	0.03651	0.0243	0.03598
T	0.0516	0.07678	0.07546	0.076449
A	0.92741	0.88671	0.9002	0.88757

Table 4.16: Case 3b difference table

$\lvert Benchmark2D - ... \rvert$	*Benchmark 1D*	*Markovian*	*Algorithm B*
R	0.01552	0.003309	0.01499
T	0.02518	0.02386	0.02485
A	0.0407	0.02717	0.03984

Unfortunately, the mean values of reflection and transmission are too little to have good distribution for the error histograms.
At the contrary, the mean value distributions have a well defined shape, that is also about the same for the two quantities.

Fig. 4.15: Histograms of reflection and transmission for the Case 3b

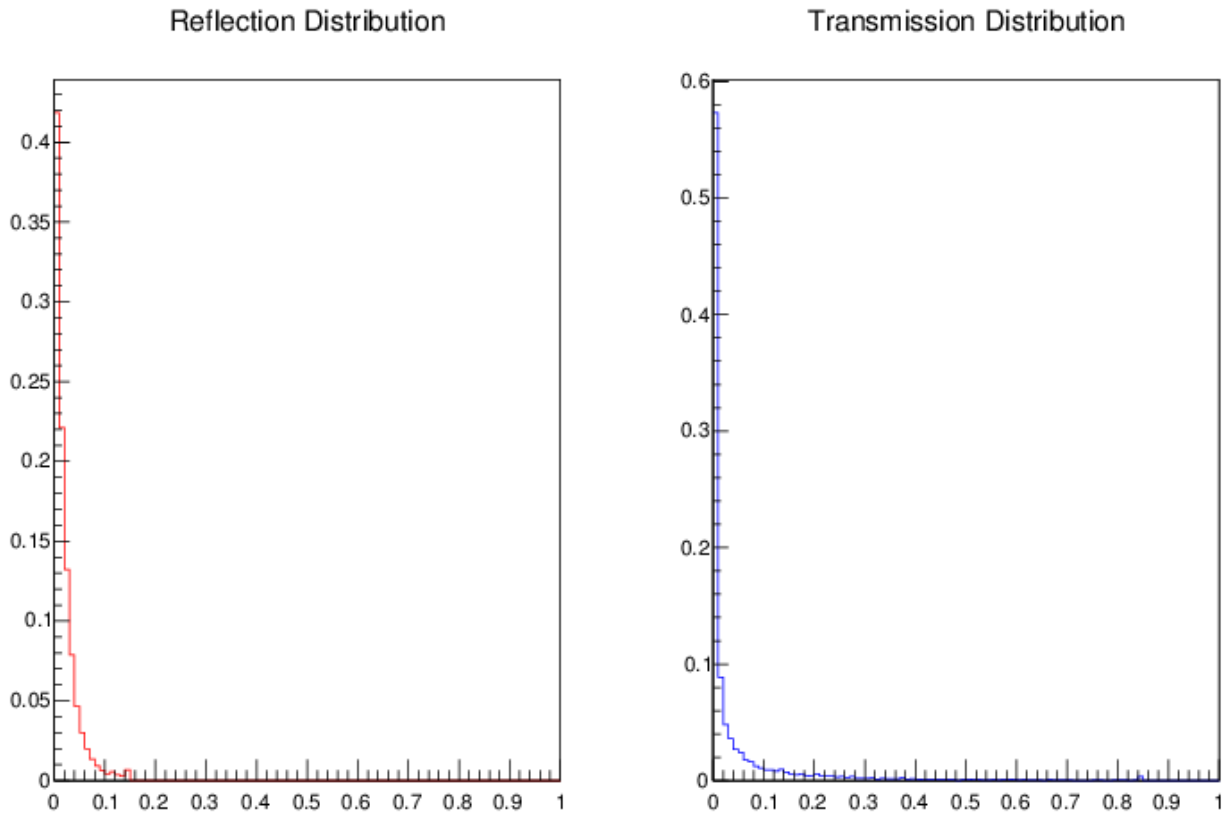

Fig. 4.16: Histograms of reflection and transmission relative errors for the Case 3b

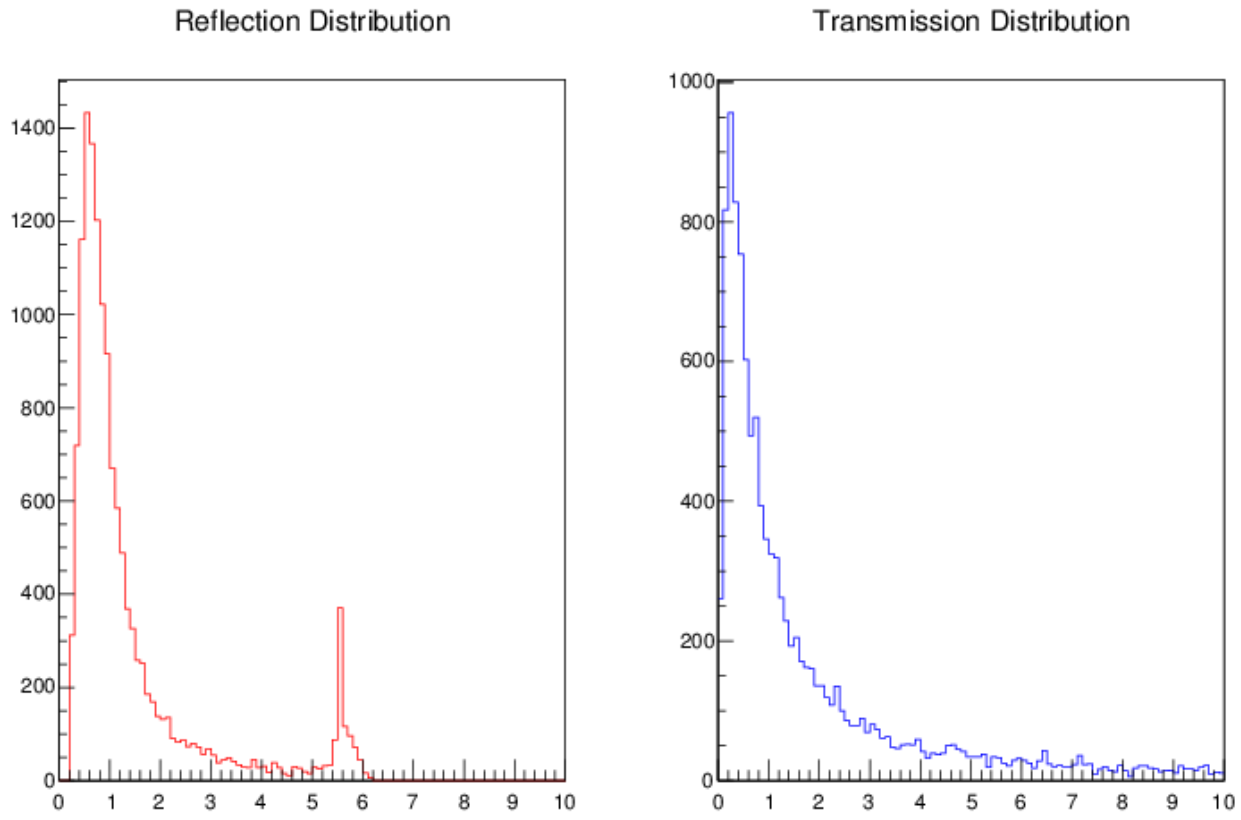

4.3.3 *Case 3c*

As for Case 2c, either the transmission and the reflection decrease compared to those of Benchmark 1D.

We can say that both the Algorithm B and the Benchmark 1D results are quite similar to the ones we obtained, whereas the Markovian model shows a reflection value that is far from the others.

Table 4.17: Case 3c results

	Benchmark 2D	*Benchmark 1D*	*Markovian*	*Algorithm B*
R	0.4116	0.44516	0.32721	0.39897
T	0.0890	0.10457	0.11946	0.11799
A	0.4994	0.45027	0.55333	0.48304

Table 4.18: Case 3c difference table

$\lvert Benchmark2D - ... \rvert$	*Benchmark 1D*	*Markovian*	*Algorithm B*
R	0.03356	0.08482	0.01306
T	0.01557	0.03013	0.02866
A	0.04913	0.0547	0.0156

Regarding the histograms, we can see that this number of geometries is sufficient to give a satisfying statistical distribution, for both the reflection and the transmission.

Concerning the reflection histogram, its shape is incomplete: it seems like the bell is cut in correspondace to the solution value for the realization with only one material. We think it is en effect due to the size of the domain considered. In fact, doing simulation of this case with a double size s, we obtain a normal shape, with the bell complete, as we can see in the added histogram.

Fig. 4.17: Histograms of reflection and transmission for the Case 3c

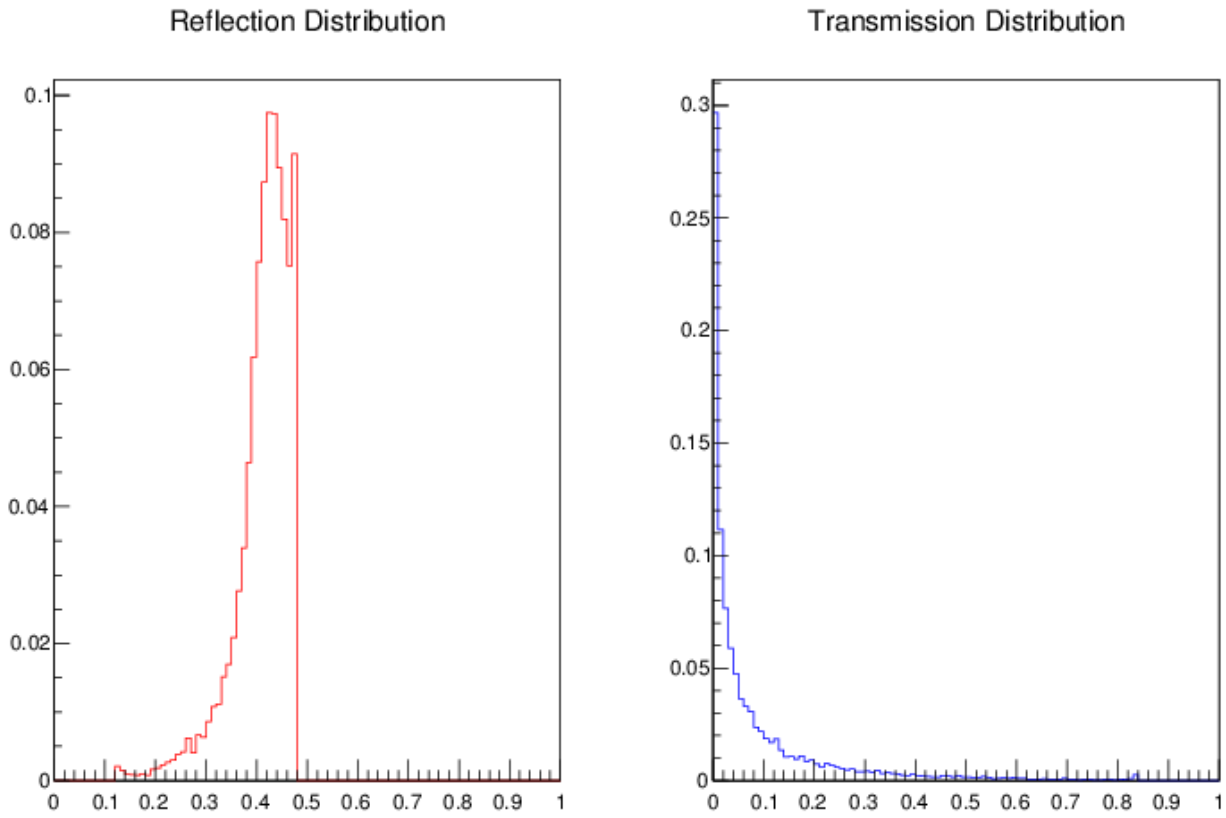

Fig. 4.18: Histograms of reflection and transmission relative errors for the Case 3c

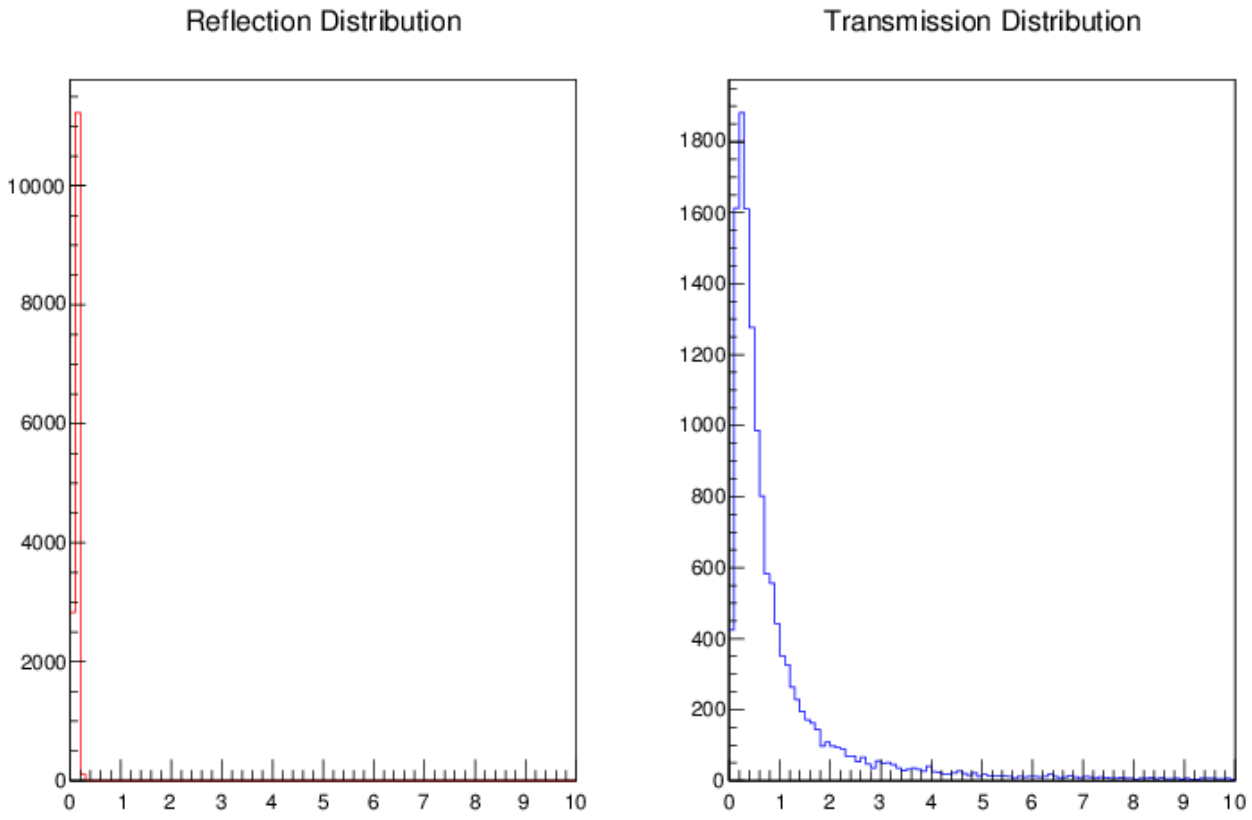

Chapter 5

Suite II benchmark results

We report here the results and the corresponding histograms for the three cases of Suite II, with remarks and comparison to the other models and benchmark results previously described.

We show the Benchmark calculated results for the outgoing neutron flux from the right side of the box, the so-called leakage value, together with the Benchmark results for the one-dimensional planar geometry (*Benchmark 1D*) and the results obtained by the two Monte Carlo algorithms (*Algorithm A* and *Algorithm B*).

For each case, we built also a table containing the differences between the Benchmark results calculated in the 2D stochastic geometry and the other available data.

5.1 *Case 1*

5.1.1 *Case 1a*

As we can see from the following tables, the result obtained from our Benchmark calculations are quite different from that of the Benchmark 1D, whereas it is more similar to the estimated one using Monte Carlo algorithms A and B.

The leakage is bigger than the one calculated in the planar geometry, once again because neutrons have more probability of finding a little piece of scattering material during their travel to the border of the domain in the bidimensional Markovian geometry.

Table 5.1: Case 1a results

	Benchmark 2D	*Benchmark 1D*	*Markovian*	*Algorithm A*	*Algorithm B*
L	0.16298	0.15268	0.16575	0.16571	0.16101

In this case, between the two algorithms, the algorithm B is the one that gives a result closer to our.

Table 5.2: Case 1a difference table

$\lvert Benchmark2D - ... \rvert$	*Benchmark 1D*	*Markovian*	*Algorithm A*	*Algorithm B*
L	0.01027	0.00277	0.00273	<u>0.001966</u>

Here we can see the histograms for the mean leakage value and the error.

Fig. 5.1: Histograms of leakage for the Case 1a

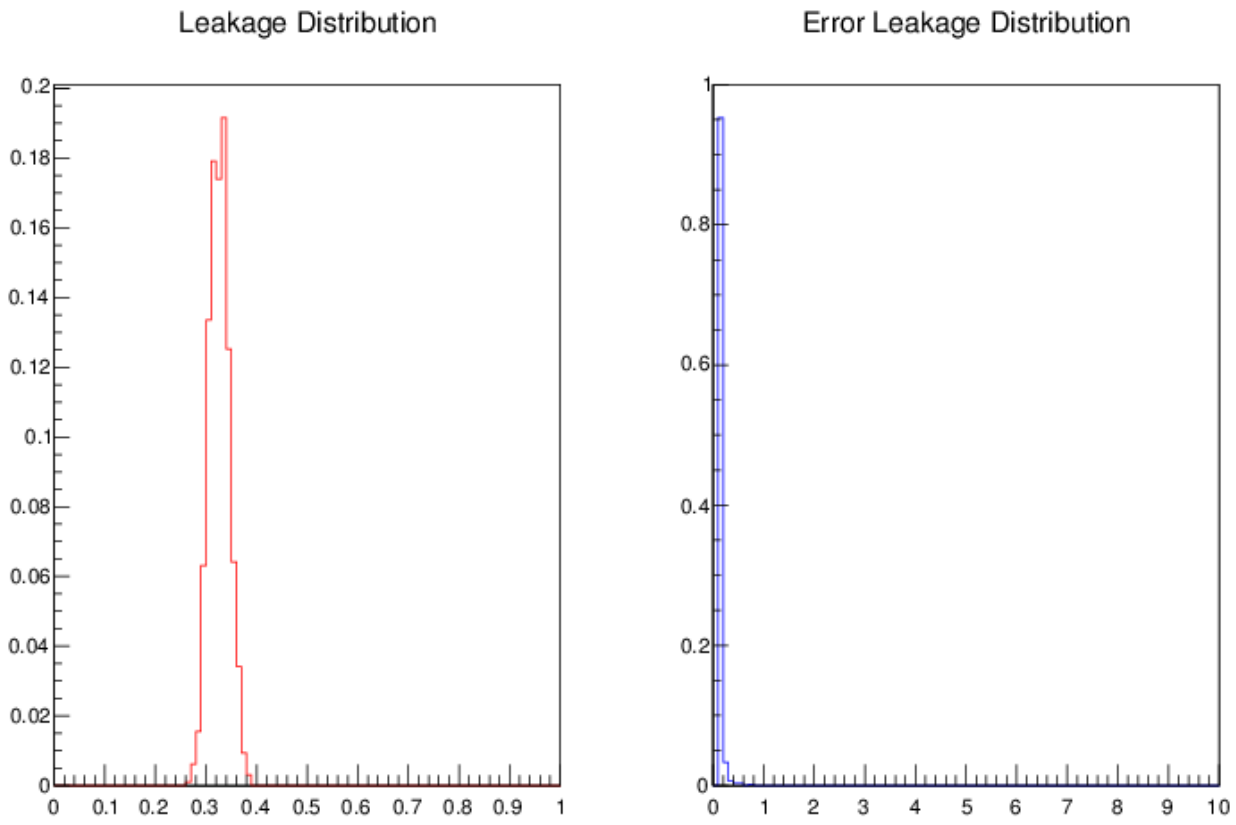

5.1.2 *Case 1b*

For Case 1b, the leakage of Benchmark 2D is close to the one given by previous benchmark calculations, but once again it has a bigger value. In this case, the scattering material (material 0) is the most present, but the total absorbing cross section is bigger than the scattering one, so the geometry characterization is not so relevant for the leakage value.

Table 5.3: Case 1b results

	Benchmark 2D	*Benchmark 1D*	*Markovian*	*Algorithm A*	*Algorithm B*
L	0.0776	0.07316	0.06934	0.06934	0.07225

In fact, the Benchmark 1D result is really close to the one we found, as the transmission value in Case 1b for Suite I.

Table 5.4: Case 1b difference table

$\lvert Benchmark2D - ... \rvert$	*Benchmark 1D*	*Markovian*	*Algorithm A*	*Algorithm B*
L	0.00444	0.00826	0.00826	0.00535

Fig. 5.2: Histograms of leakage for the Case 1b

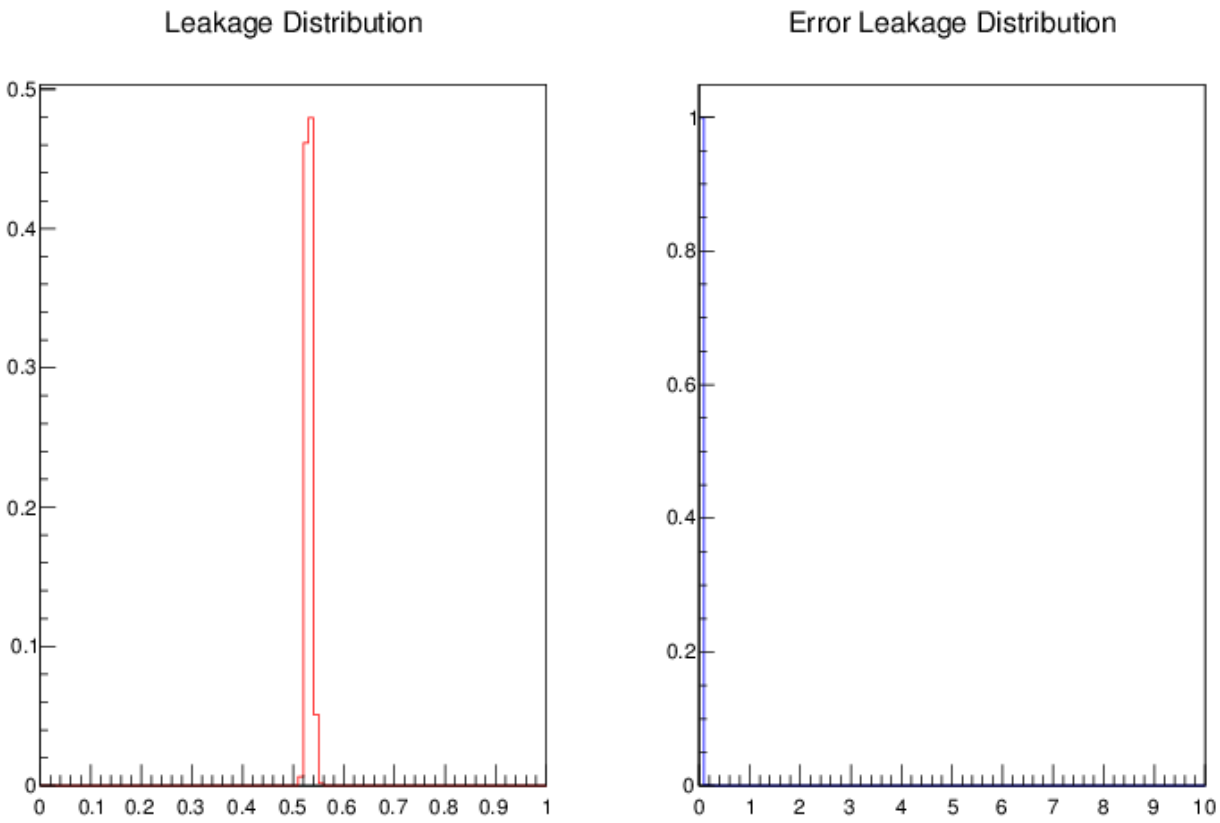

5.1.3 *Case 1c*

In this case, the calculated leakage is smaller than the other results. Once again, compared to the Benchmark 1D, we can see the influence of the geometry composition and the distribution of the materials.

Table 5.5: Case 1c results

	Benchmark 2D	*Benchmark 1D*	*Markovian*	*Algorithm A*	*Algorithm B*
L	0.16364	0.17500	0.17284	0.17286	0.17439

Between the three, the leakage estimated with the Markovian model is the one which goes closer to the result we found, even if also the value given by the Algorithm A is really similar.

Table 5.6: Case 1c difference table

$\lvert Benchmark2D - ... \rvert$	*Benchmark 1D*	*Markovian*	*Algorithm A*	*Algorithm B*
L	0.01136	<u>0.00920</u>	0.00922	0.01075

Fig. 5.3: Histograms of leakage for the Case 1c

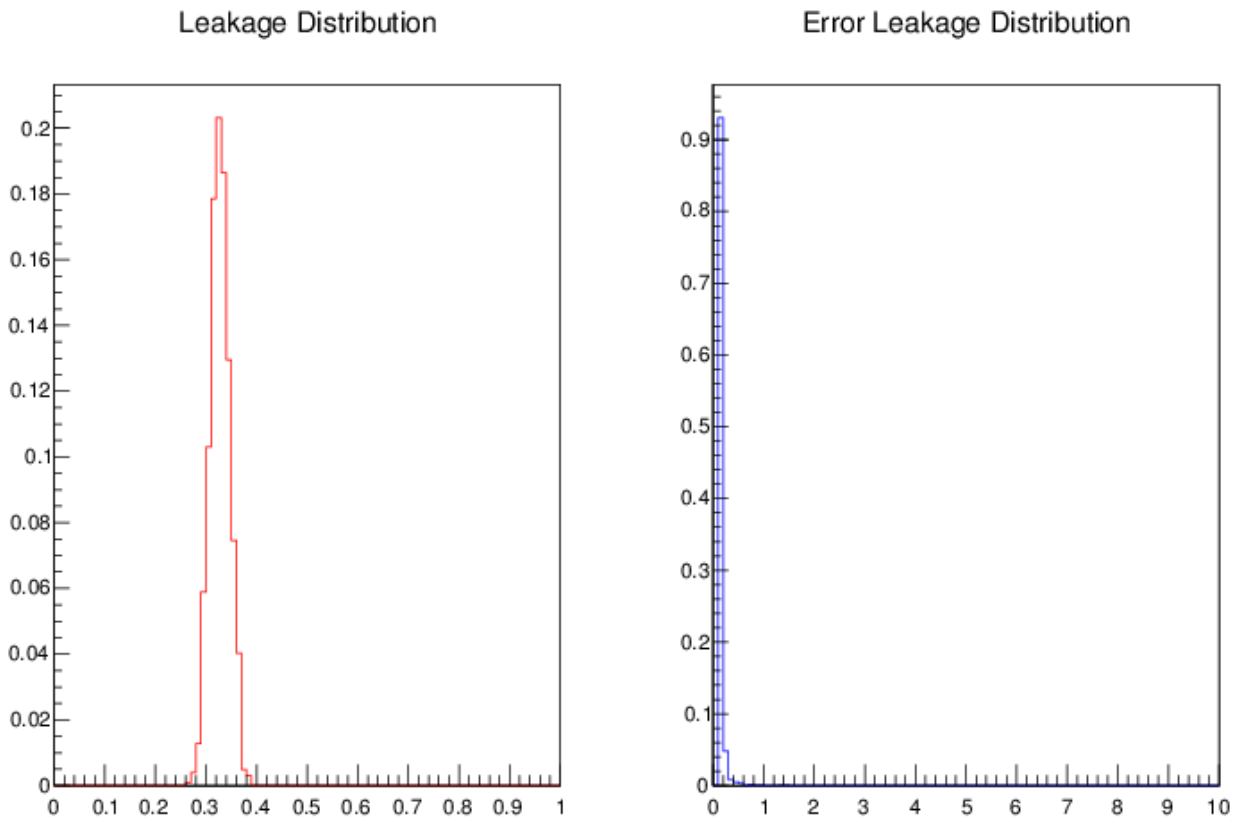

5.2 *Case 2*

5.2.1 *Case 2a*

Case 2 is the case with the same value of mean chord lengths and material cross sections of Case 1, but it shows a different value of λ, meaning that the pieces of the two materials are bigger. It is a less heterogeneous case, thus the difference between the labeled geometry is not so relevant. In fact, the calculated leakage is quite similar to the one given by Benchmark 1D.

Table 5.7: Case 2a results

	Benchmark 2D	*Benchmark 1D*	*Markovian*	*Algorithm A*	*Algorithm B*
L	0.19068	0.19077	0.9537	0.19535	0.19362

Also Algorithms A and B and the Markovian model provide leakage values close to our, with difference smaller of an order of magnitude than Case 1a. The histogram of the mean value is quite peaked, even if the number of geometries simulated is not so big.

Table 5.8: Case 2a difference table

$\lvert Benchmark2D - ... \rvert$	*Benchmark 1D*	*Markovian*	*Algorithm A*	*Algorithm B*
L	<u>0.00009</u>	0.00469	0.00467	0.00294

Fig. 5.4: Histograms of leakage for the Case 2a

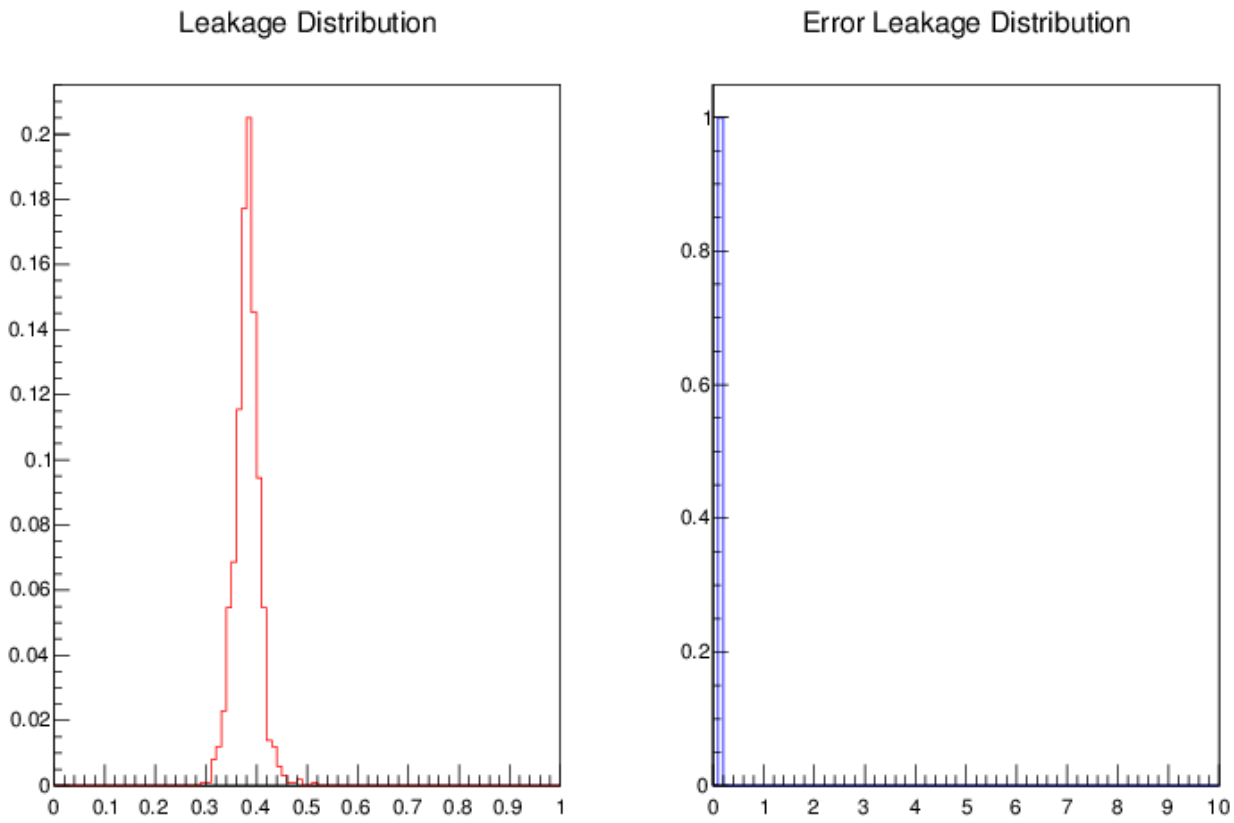

5.2.2 *Case 2b*

Also in this case, the leakage value we found is smaller than the one of Benchmark 1D, Algorithm A, Algorithm B and Markovian model. Once again, as in Case 1b, Algorithm A and the Markovian model give about the same result, which goes closer to our. For Suite II, Algorithm A is even better than Algorithm B, that fits very well results of Suite I.

Table 5.9: Case 2b results

	Benchmark 2D	*Benchmark 1D*	*Markovian*	*Algorithm A*	*Algorithm B*
L	0.22347	0.29265	0.26783	0.26787	0.29226

Table 5.10: Case 2b difference table

$\lvert Benchmark2D - ... \rvert$	*Benchmark 1D*	*Markovian*	*Algorithm A*	*Algorithm B*
L	0.06918	0.04436	0.00444	0.06879

The leakage distribution is very wide and sparse, maybe because the number of geometries simulated is not sufficient to give good statistical results (1000 geometries). However, the mean value is not really small, so the problem lies in the nature of this case, the one with material 0 as the scattering one and material 1 as the total absorbing.
A similar remark can be done for Case 2b of Suite I, for which the distributions of reflection and transmission are not too peaked as for Case 2a.

Fig. 5.5: Histograms of leakage for the Case 2b

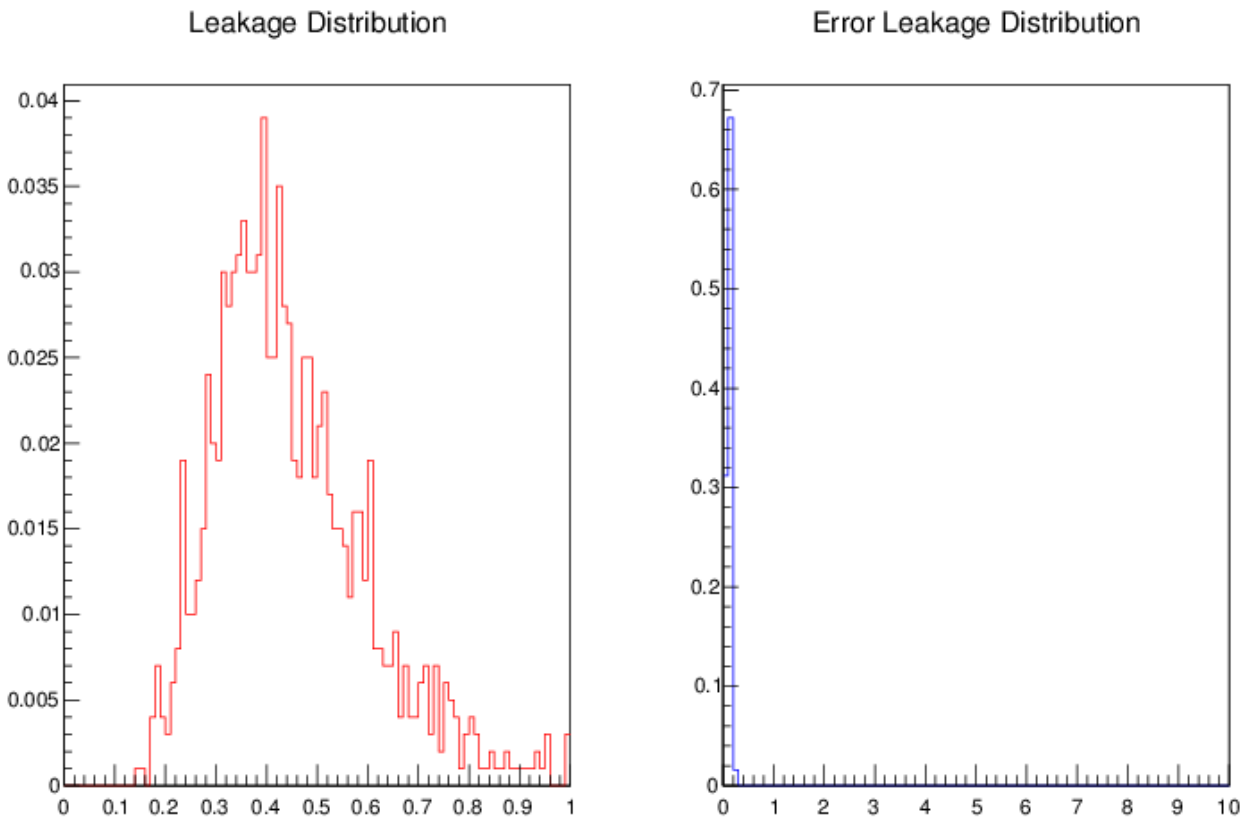

5.2.3 *Case 2c*

For this case, the calculated leakage is smaller than the one of Benchmark 1D and Algorithm B, whereas it is bigger than the one provided by the Markovian model and Algorithm A, which shows also the most little difference in values.

Table 5.11: Case 2c results

	Benchmark 2D	*Benchmark 1D*	*Markovian*	*Algorithm A*	*Algorithm B*
L	0.28716	0.31315	0.28361	0.28362	0.31199

Once again, Algorithm A goes closer to the leakage value we found, and it does of one order of magnitude compared to the other methods.

Table 5.12: Case 2c difference table

$\lvert Benchmark2D - ... \rvert$	*Benchmark 1D*	*Markovian*	*Algorithm A*	*Algorithm B*
L	0.02599	0.00355	<u>0.00354</u>	0.02483

The leakage distribution is quite spread, but it is symmetric. We can notice the appearance of the side peaks associated to the one-material realization of the geometry; the probability of having a geometry constituted by only one of the two materials is higher for this case than for the others, as we can see in Table 3.4.

Fig. 5.6: Histograms of leakage for the Case 2c

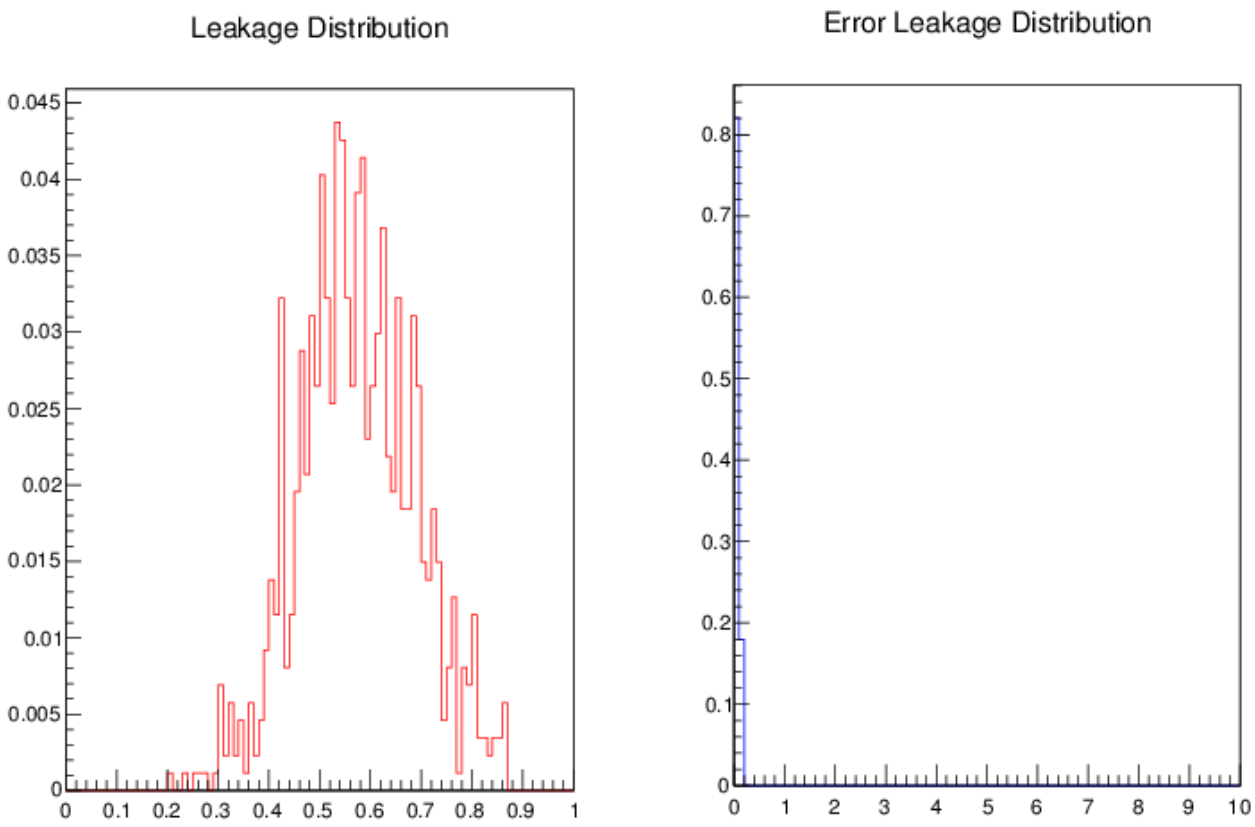

5.3 *Case 3*

5.3.1 *Case 3a*

Case 3 is the less heterogeneous one, because it has a very small Poisson density (0.6621) and the mean chord lengths are the half of the domain size. The pieces constituting the geometry are huge and in the most of the cases the realization is characterized by only one material in a big piece and a small chunk of the other one.

Table 5.13: Case 3a results

	Benchmark 2D	*Benchmark 1D*	*Markovian*	*Algorithm A*	*Algorithm B*
L	0.4100175	0.41136	0.40941	0.40933	0.4155

As we can see from this table, the results are really close one to the other, but once again the Markovian column reports the most similar leakage value to the one we performed.

Table 5.14: Case 3a difference table

$\lvert Benchmark2D - ... \rvert$	*Benchmark 1D*	*Markovian*	*Algorithm A*	*Algorithm B*
L	0.0013425	<u>0.0006075</u>	0.0006875	0.0054825

The leakage distribution is quite peaked, even if 4500 simulations are not sufficient to give a complete shape to the distribution. The peak of the one-material solution is visible.

Fig. 5.7: Histograms of leakage for the Case 3a

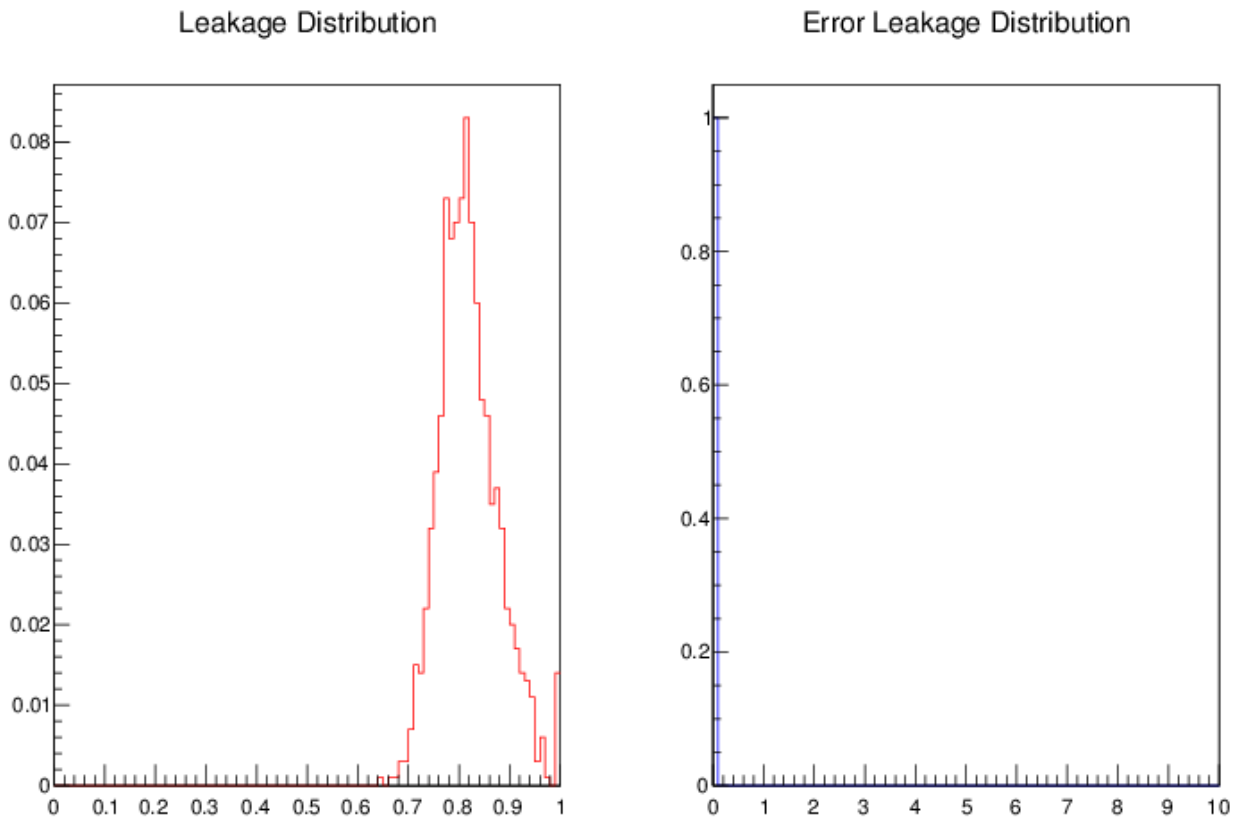

5.3.2 *Case 3b*

In this case, the leakage from Benchmark 2D is smaller than the other ones, but the value is very similar. Once again, Benchmark 1D and Algorithm B show the same difference compared to Benchmark 2D result, whereas Algorithm A and the Markovian model are the closest to our result.

Table 5.15: Case 3b results

	Benchmark 2D	*Benchmark 1D*	*Markovian*	*Algorithm A*	*Algorithm B*
L	0.09648	0.12966	0.12577	0.1258	0.12944

Table 5.16: Case 3b difference table

$\lvert Benchmark2D - ... \rvert$	*Benchmark 1D*	*Markovian*	*Algorithm A*	*Algorithm B*
L	0.03318	0.029288	0.029318	0.032958

The distribution of the leakage shows a right decreasing tale and the known one-material peak.

Fig. 5.8: Histograms of leakage for the Case 3b

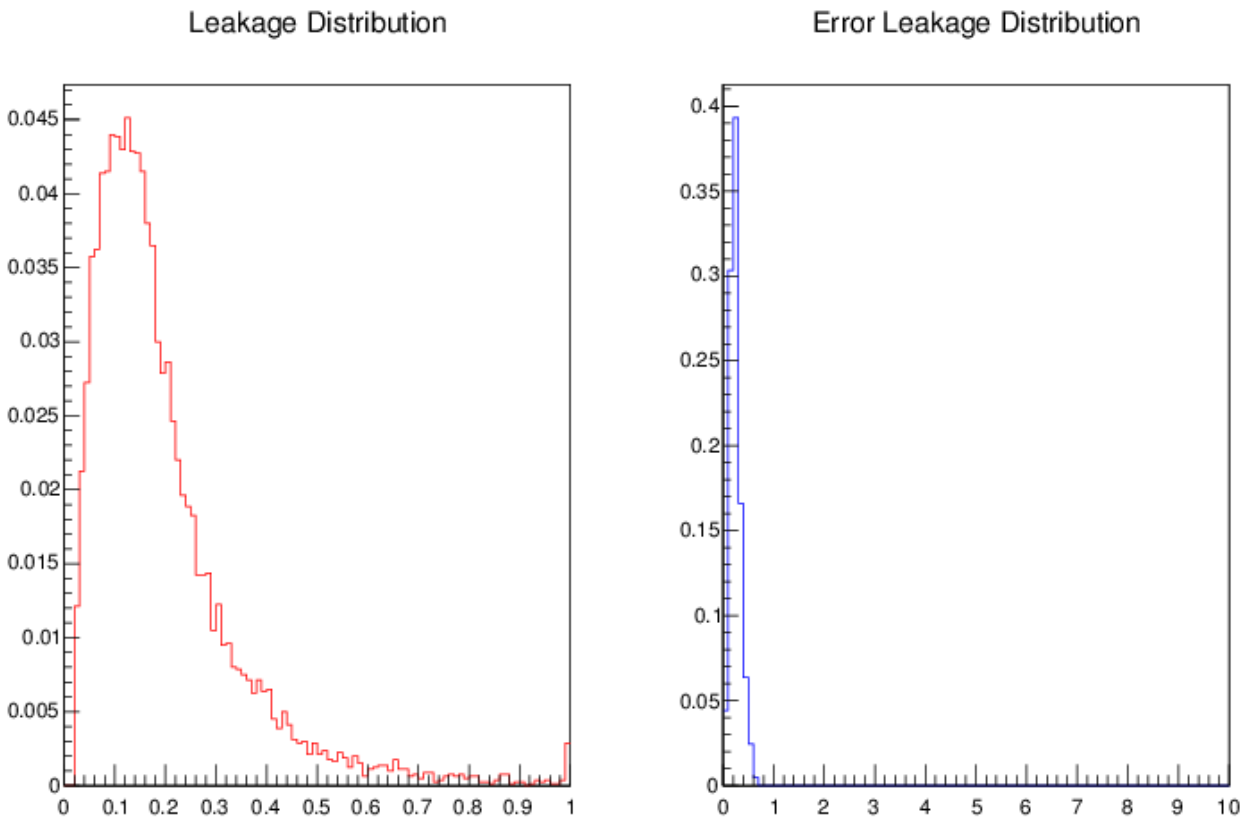

5.3.3 *Case 3c*

Concerning the numerical results, the remarks for this case are the same than those for the previous case: the leakage value we found is smaller than the other reported in the table. Algorithm A and the Markovian model provide the same numerical result, which is also the one that goes closer to our value. Algorithm B and Benchmark 1D shows the same behavior of Case 3b.

Table 5.17: Case 3c results

	Benchmark 2D	*Benchmark 1D*	*Markovian*	*Algorithm A*	*Algorithm B*
L	0.2059715	0.22563	0.21176	0.21176	0.2257

Table 5.18: Case 3c difference table

$\lvert Benchmark2D - ... \rvert$	*Benchmark 1D*	*Markovian*	*Algorithm A*	*Algorithm B*
L	0.0196585	0.0057885	0.0057885	0.0197285

The histogram is really spread, meaning the need of additional simulations (6300 until now). The two lateral picks are visible.

Fig. 5.9: Histograms of leakage for the Case 3c

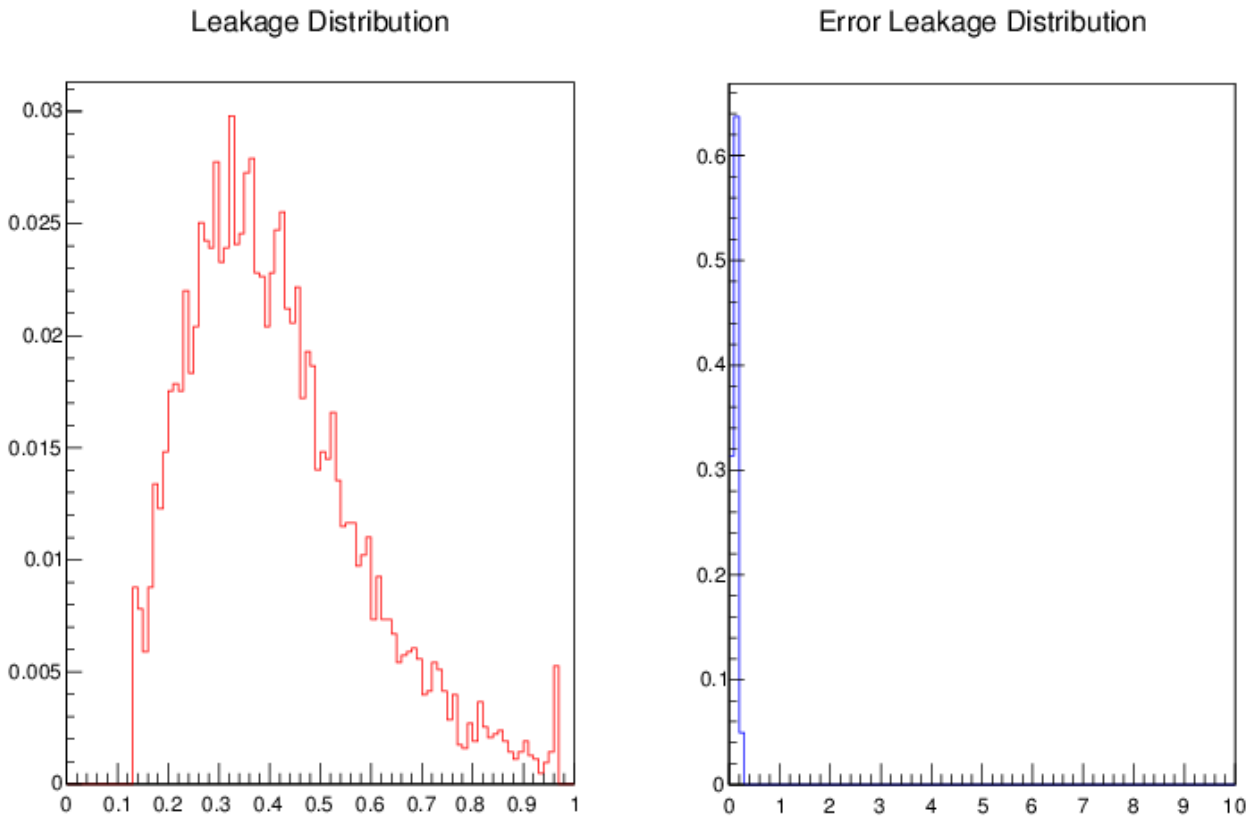

Chapter 6

K_{eff} *suite problem description*

After performing Benchmark calculations, we want to apply the stochastic geometry generation method and the neutron simulation to a domain that represents a melted nuclear reactor core.
The idea is that of studying the core in an accidental fusion event. In this situation, in fact, we do not know the distributions of the materials present in the domain and we have information only about their composition and the relative volume proportion, thus the use of the stochastic geometry simulation is justified.
The finale goal is to analyse the behavior of the effective k parameter in a 2D Markovian geometry representing the core (or a part of it) of a Pressurized Water Reactor in an accidental fusion event.
We study the k_{eff} distribution in three different cases, characterized by different levels of material mixing and so by three different values of the Poisson density parameter λ.

6.1 *Geometry construction and parameter characterization*

We consider a pin cell of a PWR, constituted by three materials: fuel, clad and buffer, which compositions are reported in Table 6.2.
A schematic representation of the real pin cell and the values of the characteristic parameters are given here.
In the picture, fuel is material C, clad is material B and buffer is material A.

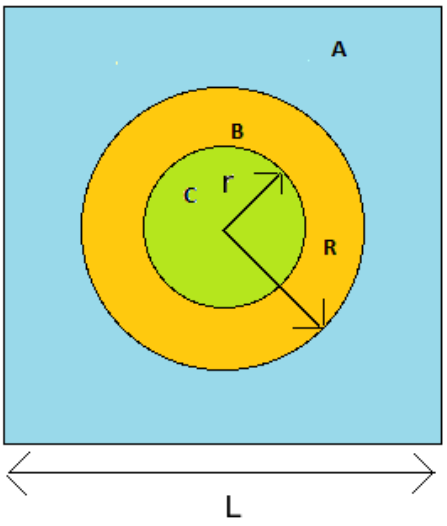

Fig. 6.1: Real pin cell representation

parameter	value
r	0.407 cm
R	0.4707 c
L	1.27 cm
h	10.01 cm
V_A	9.1778 cm^3
V_B	1.7582 cm^3
V_C	5.2092 cm^3

Table 6.1: Real pin cell characteristic values

We need to reduce our geometry to a bi-material one: material 0 is the fuel and material 1 is the so-called *bufferclad*, that is a weighted mixture of the buffer and the clad. Therefore, the atomic densities and the volumes of the new material can be calculated according to:

$$N_{AB} = N_A \cdot \frac{V_A}{V_{tot}} + N_B \cdot \frac{V_B}{V_{tot}} \tag{6.1}$$

$$V_{tot} = V_A + V_B \tag{6.2}$$

where N_A and N_B are the atomic densities of material A and material B, respectively.

Thus, from these starting values

Table 6.2: Material composition for the real pin cell

Material	Element	N [at/10^{-24}cm^3]
BUFFER	H1	0.04577
	O16	0.022885
	B10	4.5754E-6
	B11	1.8302E-5
	ZR91	0.0010492
CLAD	ZR91	0.038629
FUEL	U235	0.001136
	U238	0.021762
	O16	0.04581

we obtain those ones:

Table 6.3: Material composition for the approximate pin cell

Material	Element	N [at/10^{-24}cm^3]
BUFFER-CLAD	H1	0.03841
	O16	0.01921
	B10	3.8398E-6
	B11	1.536E-5
	ZR91	0.0070911

Its graphic representation and the characteristic values are given below.

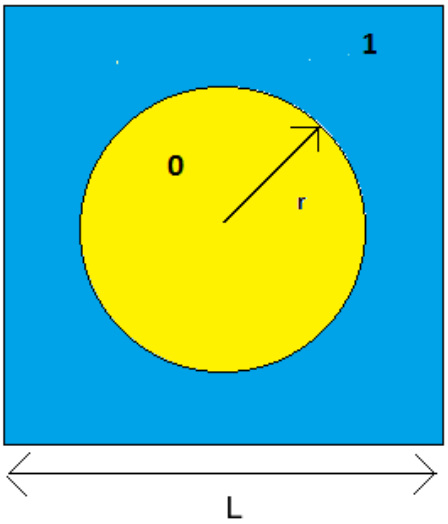

Fig. 6.2: Two-material pin cell representation

parameter	value
r	0.407 cm
L	1.27 cm
h	10.01 cm
V_0	5.20922 cm^3
S_0	25.59814 cm^2
V_1	10.9359 cm^3
S_1	50.8508 cm^2
V_{tot}	16.1451 cm^3

Table 6.4: Approximate pin cell characteristic values

Defined our geometry and its composition, we have to find the associated statistical parameters, meaning the values of the volume fraction p_0 and of the Poisson density λ.

From the two volumes V_0 and V_1 we can derive the volume fraction for material 0:

$$p_0 = \frac{V_0}{V_0 + V_1} \tag{6.3}$$

and consequently the value of p_1. They are, respectively, 0.32 and 0.68.

In order to have the other statistical parameter, λ, we have to know one of the two mean chord length. From the Cauchy's formula, we write an expression for the mean chord length in material 0, the fuel, that has a cylindrical shape.

$$\Lambda_0 = \frac{4V_0}{S_0} = 2 \cdot r \tag{6.4}$$

So, the mean chord length in material 0 is equal to the diameter of the cylinder.

The corresponding value of λ can be find using the known expression 3.10 :

$$\lambda = \frac{\pi}{2\Lambda_0(1-p_0)},$$

from which $\lambda = 2.84$.

6.2 *Three cases definition*

Like for the Benchmark calculations, we study three different cases, characterized by three different values of λ.
The first case is the one previously defined, with $\lambda = 2.84$ and $p_0 = 0.32$.
The other two cases are created in an arbitrary way, choosing the mean chord length for material 0 once as the double and once as the half of the Λ_0 calculated before.
From the value of Λ_0, meaning the value of the fuel cylinder radius, we can derive the one of the Poisson density, simply considering p_0 as a constant parameter.
Thus, Case 2 is characterized by the mean chord length in material 0, Λ_0', that is the double of Λ_0 and a Poisson density, λ', that is the half of the first case one.
For Case 3, it is a vice versa: the mean chord length in material 0, Λ_0'', is the half of Λ_0, and the density λ'' is the double of the density of the first case.
The values of the characteristic parameters are reported in the following table.

It is interesting to note the different values of L, which is the side of the pin cell in the "deterministic" configuration. For Case 2, maintaining constant p_0 and p_1, with a density $\lambda' = \lambda/2$, the side is doubled, whereas in Case

3, with $\lambda'' = 2\lambda$, the size L is the half of that of the first case.

Table 6.5: Case 2 and Case 3 parameters

Case	Λ_0 [cm]	r [cm]	$V_0[cm^3]$	$V_1[cm^3]$	$V_{tot}[cm^3]$	λ [cm^{-1}]	L [cm]
I	0.814	0.407	5.2092	10.936	16.145	2.84	1.27
II	1.628	0.814	20.837	44.279	65.116	1.419	2.56
III	0.407	0.2035	1.3023	2.7674	4.0697	5.676	0.638

This conclusion can be achieved also simply considering the relationship between the Poisson density and the size of the square domain in which lines are randomly thrown:

$$\lambda = \frac{E[N(L)]}{L} \tag{6.5}$$

where $E[N(L)]$ is the mean number of lines that cross the domain of size L.

Being $E[N(L)]$ constant (to make comparison between cases reasonable), for each value of λ we have a different value of L:

$$\lambda' = \lambda/2 \rightarrow \text{L'} = 2\ \text{L}$$

$$\lambda'' = 2\lambda \rightarrow \text{L''} = \text{L}/2$$

L is an important parameter that we have to know to perform criticality calculations in the deterministic configuration, to make comparisons also between the deterministic and the stochastic configuration for each case. Thus, for a domain size s, we can see the three corresponding both deterministic and stochastic configurations.

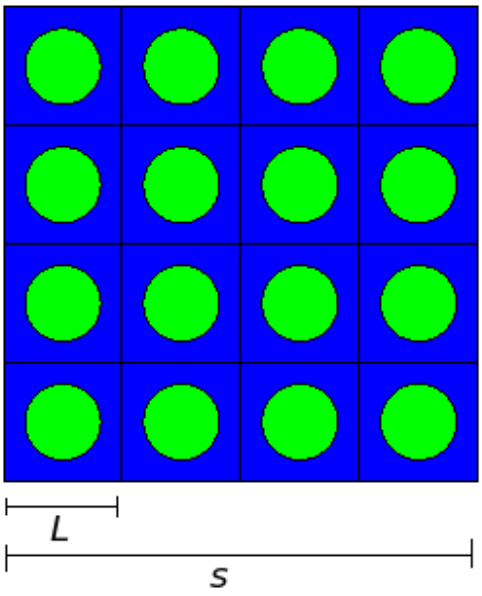

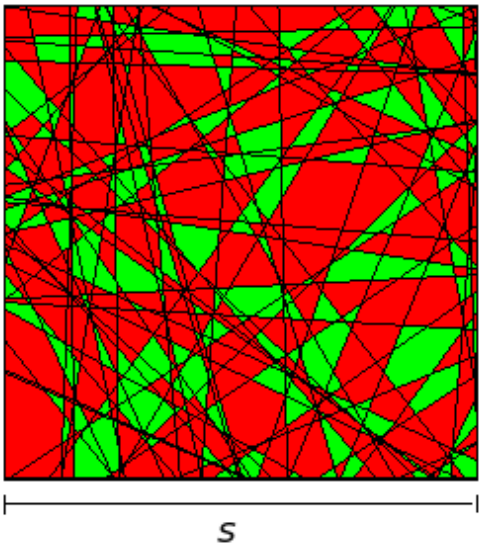

Case 1:

- deterministic configuration:
  $L = 1.27$ cm
- stochastic configuration:
  $\lambda = 2.84, \quad p = 0.32$

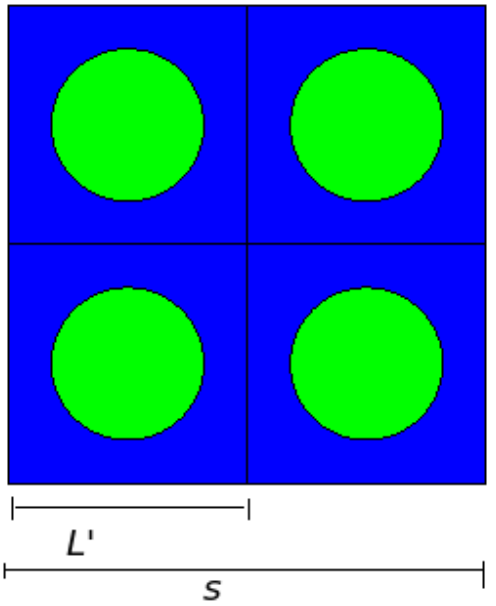

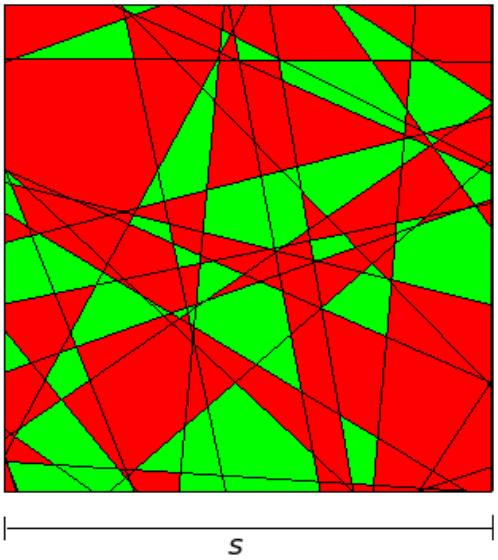

Case 2:

- deterministic configuration:
  $L = 2.560$ cm
- stochastic configuration:
  $\lambda = 1.419, \quad p = 0.32$

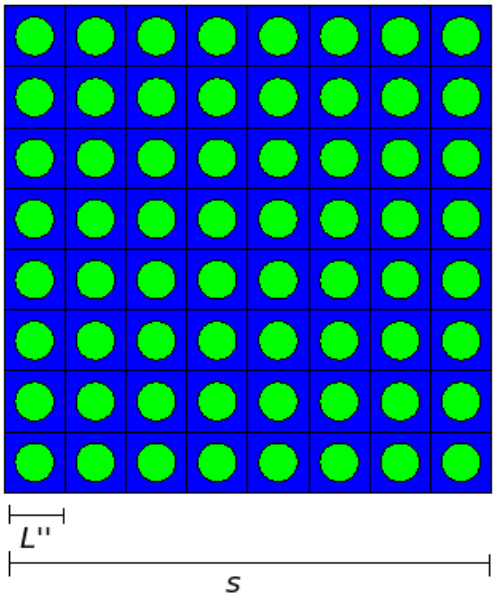

Case 3:

- deterministic configuration:

  $L = 0.638$ cm

- stochastic configuration:

  $\lambda = 5.676, \quad p = 0.32$

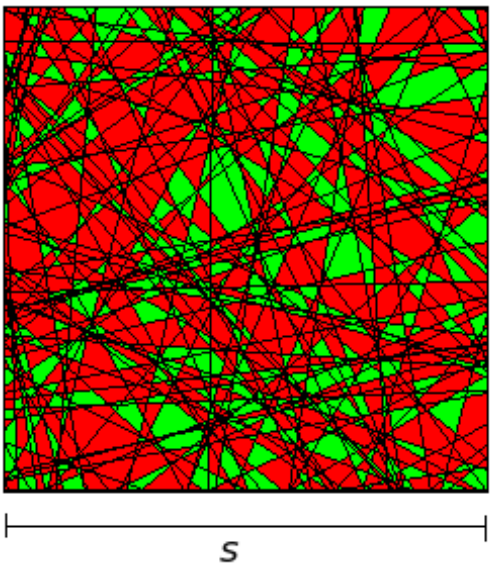

6.3 *Criticality calculations*

The steps are the same as for Suite I and Suite II calculations.

We generate a great number of stochastic geometries with the set parameters λ and Λ_0 for the different cases and then we launch the Monte Carlo code TRIPOLI-4® in the criticality mode to find the values of k_{eff}.

First, we perform different calculations in order to choose a value for s, the size of the domain.

We evaluate three different sizes: 20 , 50 and 100 cm and we analyse the convergence of the result.

At the end, we select a size s of 20 cm, because, even if the k_{eff} distribution is more picked for the largest dimension, the huge simulation time does not justify its choice (a single calculation requires about 60 hours). Moreover, the mean value is nearly the same, as we can see in the following histograms. Also between 20 and 50 cm, the selection is on the 20, since it allows to have a good distriubtion for the mean value and a narrow distribution for the corresponding error, with a reduced simulation time.

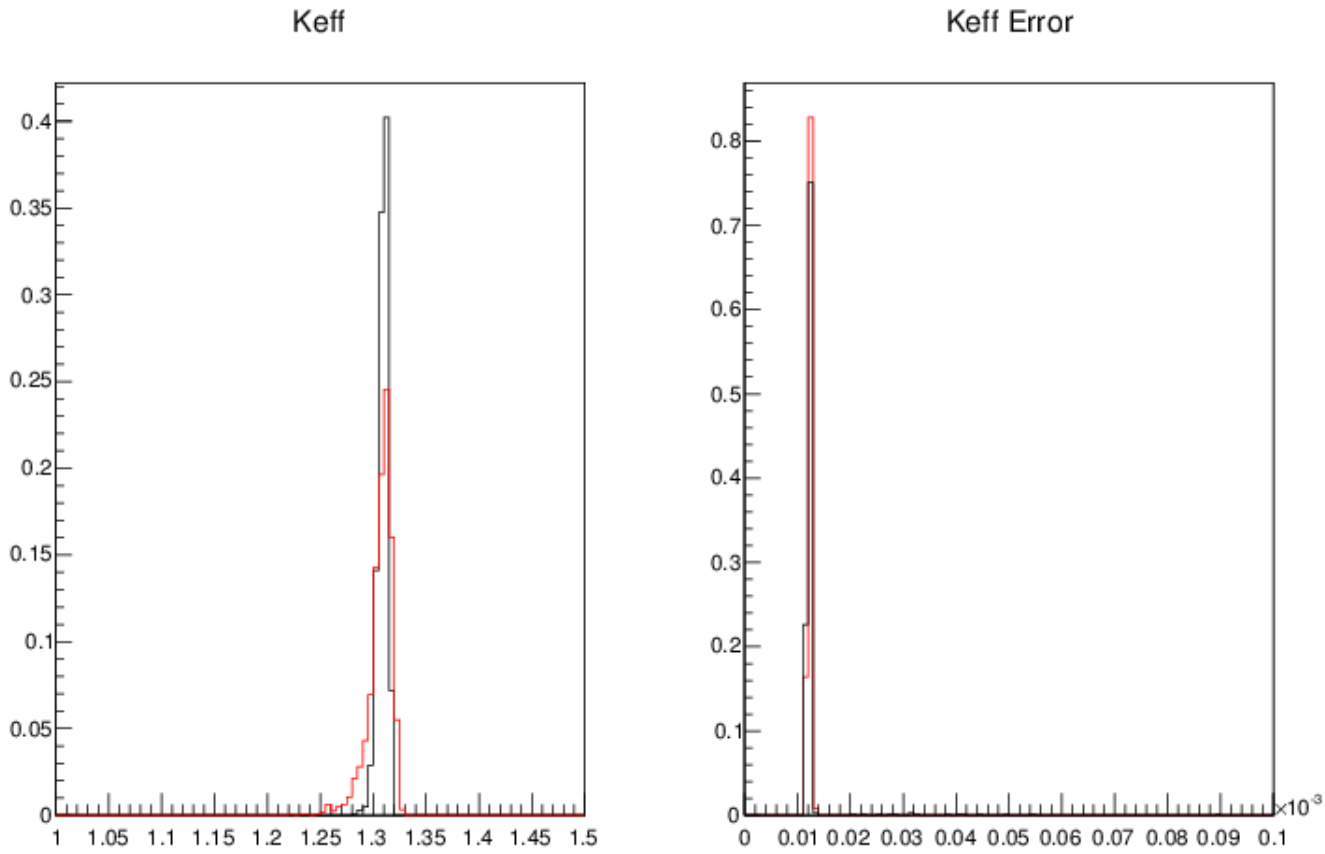

Fig. 6.3: k_{eff} mean value and error distribution for $s = 20$ (red) and $s = 50$ (black)

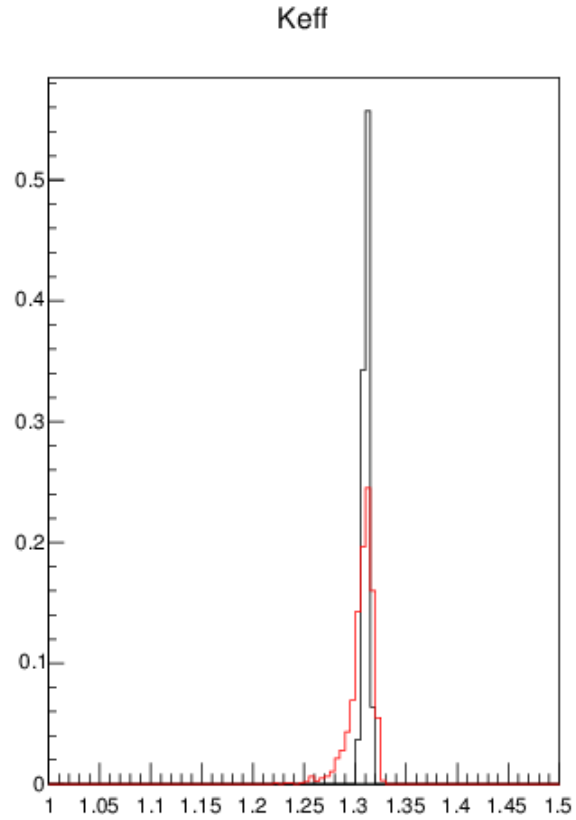

(a) k_{eff} distribution for $s = 20$ (red) and $s = 100$ (black)

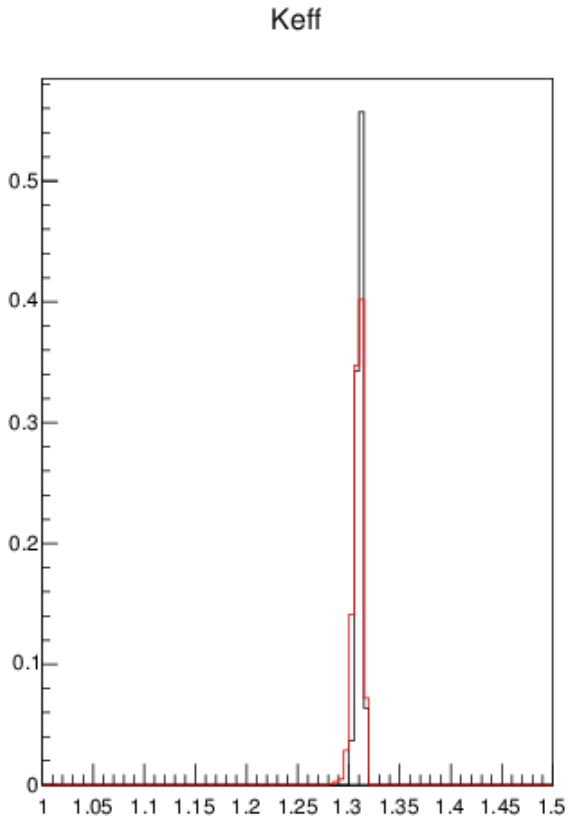

(b) k_{eff} distribution for $s = 50$ (red) and $s = 100$ (black)

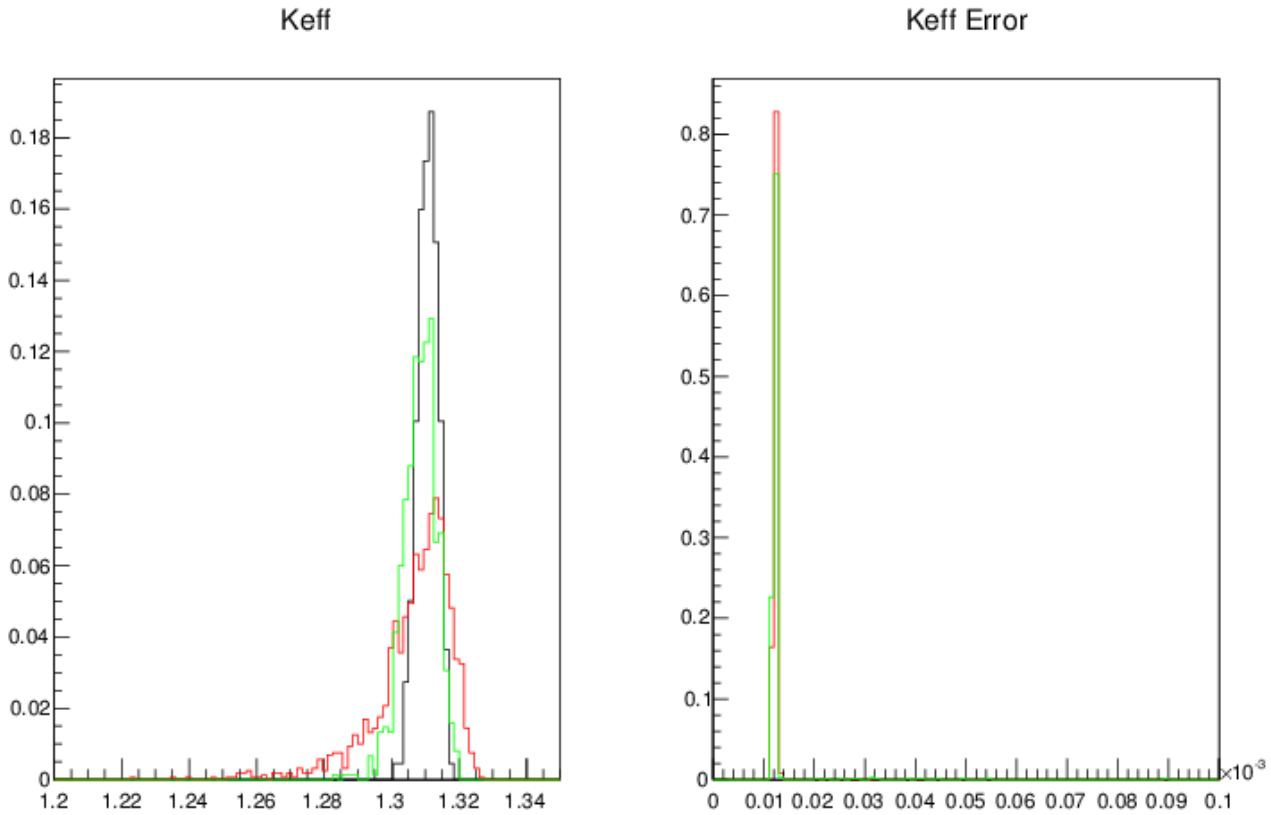

Fig. 6.4: k_{eff} and error histograms for three domain sizes: 20 (red), 50 (green) and 100 (black) cm

Chapter 7

Suite III results

This chapter is dedicated to the results obtained for the three cases of Suite III, for a domain size of 20 cm.
For each case, the value of the k_{eff} calculated with the standard deviation expressed in pcm and the relative histogram are reported.

7.1 *Case 1*

As we can see, the value of the k_{eff} for the stochastic configuration is statistically the same of the value for the deterministic configuration.
The distribution is peaked only with 1600 simulations (1600 geometries) and it includes the value of k_{det}.

CASE 1	
λ	2.84
k_{det}	1.3038
k_{eff}	1.3066

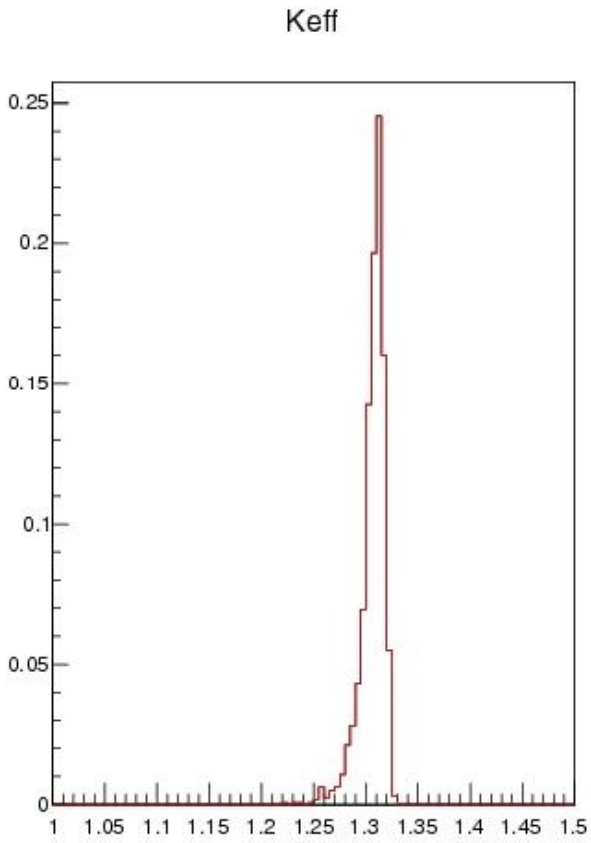

Fig. 7.1: k_{eff} distribution for Case 1; standard deviation : 1900 pcm

7.2 *Case 2*

The value of the K_{eff} in the stochastic configuration is lower than the one of the deterministic configuration, meaning maybe a consistent border effect. The distribution is very spread, meaning the need of more simulations. However, it is in accordance to Case 2 and 3 of Suite I and Suite II, where the smaller density λ implies a wider distribution of the mean value.

CASE 2	
λ	1.419
k_{det}	1.3491
k_{eff}	1.2337

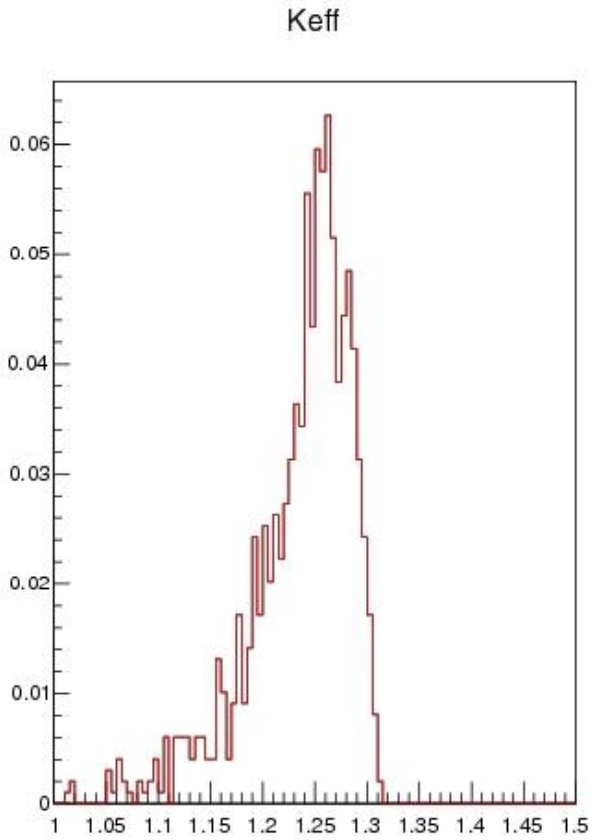

Fig. 7.2: k_{eff} distribution for Case 2; standard deviation : 6400 pcm

7.3 *Case 3*

For Case 3, the value of k_{eff} is much more smaller than k_{det} compared to other cases, whereas the deterministic value is not very different from the one of the first case.

The distribution is very picked, in accordance to those of Case 1 of Suite I and Suite II.

CASE 3	
λ	5.676
k_{det}	1.3094
k_{eff}	1.1145

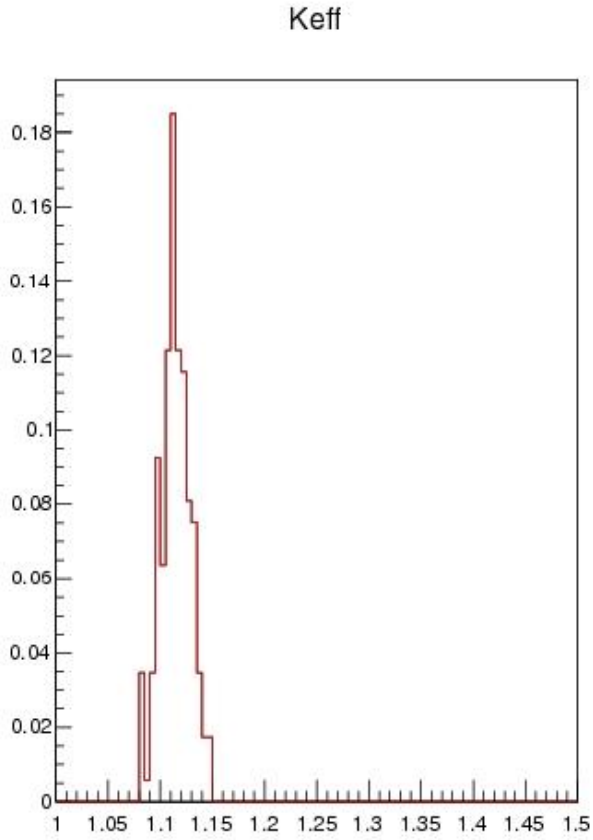

Fig. 7.3: k_{eff} distribution for Case 3; standard deviation : 3900 pcm

7.4 *Remarks and comparisons*

It is interesting to compare both the deterministic and the stochastic values of k_{eff} in the single case and the stochastic values between the three cases. Firstly, we notice that for Case 1 the value of k_{eff} is bigger than the value of k_{det}, whereas for the other cases there is an opposite behaviour, because the value of k_{eff} in the stochastic configurations is lower than that in the corresponding deterministic configuration.
However, the difference between the k_{eff} and the k_{det} in Case 1 is the smallest compared to Case 2 and Case 3, as we can see from the following tables.

Table 7.1: Differences between k_{eff} and k_{det} for the three cases

Case	$\Delta(k_{eff} - k_{det})$
1	0.28 %
2	11.54 %
3	19.49 %

Table 7.2: Differences between stochastic k_{eff} for the three cases

Δ	$k^1_{eff} - k^2_{eff}$ [pcm]	$k^1_{eff} - k^3_{eff}$ [pcm]	$k^2_{eff} - k^3_{eff}$ [pcm]
	8.29	19.21	10.92

From these data, the case in which the difference between the stochastic and the deterministic configuration is more pronounced is Case 3, the case with the higher Poisson density ($\lambda = 5.676$).
The geometric defined configuration gives a value of k_{eff} very different from the corresponding stochastic configuration, in which pieces of the two materials are randomly disposed in the domain; this latter configuration approaches the homogeneous one, because pieces are very small and really mixed, therefore the *atomic mix approximation* can fit quite well. So, in this case, we can see the influence of the core composition heterogeneity on the value of k_{eff}:

having a well defined core geometry gives a bigger k_{eff} than having materials with the same volume proportion but randomly (and quite homogeneous) distributed.

Case 3 shows this aspect very well because it is the only case in which the stochastic configuration approaches the homogeneous one and we can make a direct comparison between the heterogeneous and the homogeneous configuration of the core.

As concern the differences between the stochastic k_{eff} values, we remark that the values of Case 2 and Case 3 are smaller than the k_{eff} for Case 1, but, even if the densities are once the half and once the double of λ in Case 1, the differences do not show this proportion: k_{eff} of Case 3 is more little than the one of Case 2.

The last comparison that we have to do is the one between the value of k_{det} of Case 1 and the values of the stochastic k_{eff} for the three cases. We can see how the effective k modifies from the deterministic configuration depending on the way of mixing of the materials in the melted core.

Table 7.3: Differences between k_{det} of Case 1 and stochastic k_{eff} of the three cases

k_{det}	Δ	k^1_{eff}	0.28 %
		k^2_{eff}	7.01 %
		k^3_{eff}	18.93 %

Starting from the same deterministic configuration, we analyse three cases of mixing: the case in which the mean chord length is the same as the deterministic configuration, the case in which pieces are bigger (there are spots of the two materials where they concentrate) and the case characterized by small pieces (as the two materials strongly mix and create quite an homogeneous configuration).

If the fuel and the buffer clad mix in a way that maintains the same charac-

teristic chord length, the k_{eff} is bigger, but it does not change a lot. At the contrary, if they make a well mixed configuration, the k_{eff} is really reduced. The last case, the one that has a small Poisson density, shows a k_{eff} lower than the deterministic value, but not so different as for Case 3.

Chapter 8

Conclusions and perspectives

The present thesis deals with stochastic geometries applied to the neutron transport problem and it is divided into two steps.
The first one consists in performing Benchmark calculations for a well defined neutron transport problem, for which several cases have been already analysed using some different models and methods.
The second step concerns criticality calculations for a similar stochastic problem.
We performed Benchmark calculations in a real 2D Markovian geometry [1], constituted by a plane, made up of random intersecting lines, then extended in the vertical direction, for the 9 cases of two different suites. The goal is to compare the last results with those obtained with calculations in a 1D labelled planar Markovian geometry (*1D Benchmark*) and to analyse and/or validate the different stochastic geometry models.
From these more realistic results, we can see if and how much the 1D Benchmark calculations are less accurate in finding solutions for each case. Obviously, it is a simplified model of the real stochastic geometry, but we want

[1] constructed following the procedure described by Switzer, explained in Chapter 2

to see its convenience in terms of result precision and time saving compared with a more complete but complex model, the one we realized.

The other line of investigation concerns the theoretical models that can be used to solve the transport equation modelling stochastic geometries. We consider the so called *Markovian* model and the Monte Carlo algorithms A and B.

The Markovian model derives from a particular closure of the Levermore-Pomraning equation that describes the transport in stochastic geometries. It allows to have two coupled equations, each one including only one of the two material unknowns, that can be solved with deterministic codes. The stochastic nature of the geometry is included into the equations with the terms p_α and p_β (see Eqs. (2.33) and (2.34)).

The Monte Carlo algorithms can undergo the creation of the different several geometry realizations, seeking directly for the mean value of the ensemble-averaged quantity in just one simulation. The problem is that they do not provide information about the distributions, therefore more elaborated models will be needed to have this knowledge.

So, realising 2D Markovian geometries is a very long procedure, but it is necessary to validate simple models of stochastic geometries, like the *on the fly geometry* which is used in MC algorithms A and B.

From this point, the future evolution can involve the creation of a real 3D stochastic Markovian geometry, made up of an intersection of random planes, and the successive simulation with the Monte Carlo code TRIPOLI-4 ®. This kind of geometry is possible until now only in theory (the process is known on paper, [14] and [15]), but the implementation will need some work. Moreover, even if the geometry is created, simulations will require a very long time, considering that already in the 2D Markovian geometry for some cases

the necessary time for MC simulations is very high.
This increases the importance of finding an alternative method to solve this problem.
On one hand, it is possible to elaborate more complex and realistic models of stochastic geometries, whose accuracy can be evaluated thanks to the 2D Benchmark calculations.
On the other hand, we can think about a different kind of stochastic geometry, like a structured one: if we create a geometry divided into fixed cells, then populated by the two materials depending on the statistical probabilities p_0 and p_1, we could achieve a faster modelisation, taking however in account the stochastic nature of the problem. This way has not been studied yet, but it could be a valid successive step.
In conclusion, this work is a necessary intermediate step in the resolution of the neutron transport problem in stochastic geometries and it allows to analyse and compare previous ways of solution and also to choose the future direction of the studies.

Bibliography

[1] P.S. Brantley, *A benchmark comparison of Monte Calo particle transport alorithms for binary stochastic mixtures*, J. Quant. Spectrosc. Radiat. Transfer. (2011); 599-618 .

[2] G.C. Pomraning *Linear Kinetic Theory and Particle Transport in Stochastic Mixtures* , World Scientific, Singapore (1991)

[3] T. Lepage, L. Delaby, F. Malvagi and A. Mazzolo, *Monte Carlo Simulation of Fully Markovian Stochastic Geometries*, Progress in Nuclear Science and Technology, (2011); Vol. 2, pp.743-748

[4] O. Zuchuat, R. Sanchez, I. Zmijarevic , F. Malvagi, *Transport in Renewal Statistical Media: Benchmarking and comparison with model*, J. Quant. Spectrosc. Radiat. Transfer. (1994); 689-722

[5] R. Sanchez, *Linear Kinetic Theory on Stochastic Media*, J. Math. Phys. (1989); 2498

[6] G.B. Zimmerman, *Recent Developments in Monte Carlo Techniques*, Lawrence Livermore National Laboratory Report UCRL-JC-105616; (1990)

[7] N. McCOrmick, *Proposed Monte Carlo Calculation of a Binary Statistical Mixture*, unpublished (1998)

[8] G.B. Zimmerman, M.L. Adams, *Algorithms for Monte Carlo Particle Transport in Binary Statistical Mixtures*, Lawrence Livermore National Laboratory Report UCRL-JC-10810; (1991)

[9] G.L. Olson, D.S. Miller, E.W. Larsen, J.E. Morel, *Chord length distributions in binary stochastic media in two and three dimensions*, J. Quant. Spectrosc. Radiat. Transfer. (2006); 269-283

[10] M.L. Adams, E.W. Larsen, G.C. Pomraning, *Benchmark Results for Particle Transport in a Binary Markov Statistical Medium*, J. Quant. Spectrosc. Radiat. Transfer. (1989); 253-266

[11] P. Switzer *A random set process in the plane with a Markovian property*, Ann. Math. Stat. (1965); 1859-1863

[12] L. Delaby *Réalisation de géométries stochastiques bidimensionnelles en générant aléatoirement des droites selon le procédé formulé par Switzer en 1965*, Rapport de stage au DM2S, SERMA/LTSD(2009)

[13] A. Mazzolo *Probability of a one color stochastic geometry*, 2014

[14] A. Yu Ambos; G.A. Mikhailov *Statistical simulation of an exponentially correlated many-dimensional random field*, Russian Journal of Numerical Analysis and Mathematical Modelling (2001); Vol. 26, Issue 3, 263-273

[15] G.A. Mikhailov *Numerically Implementable Models of Exponentially Correlated Random Fields and Stochastic Problems of Particle Transport*, Doklady Mathematics (2011); Vol. 84, Issue 1, 535-538

Appendix A

From the Liouville master equation to the L-P model

A.1 *The Liouville master equation*

The Liouville equation describes an initial value problems in time and it was used in particle transport context for the first time by Vanderhaegen (1986). The description of a dynamical system with initial value in time is a Markovian problem: known the solution at any time $\bar{t}$, the solution is uniquely defined fo all times $t \geq \bar{t}$. That is, to obtain the solution for $t \geq \bar{t}$, we have only to know the solution at time $\bar{t}$; the solution prior $\bar{t}$ is irrelevant (it is a " memoryless " process).

Then, we consider a dynamic system which can be at any time in one of two states, namely, α and β. The process for knowing in which state the system is supposed to be Markovian. Thus, the probability of the system being, at time $t + dt$, in state $\beta \neq \alpha$, if it is in state α at time t, is given by:

$$Prob\,(\alpha \to \beta) = \frac{dt}{\lambda_\alpha(t)}, \quad k = \alpha, \beta, \quad \beta \neq \alpha \tag{A.1}$$

For any realization of the statistics, the dynamic system evolution is described by the equation:

$$\frac{d\xi(t)}{dt} + F(\xi, t) = 0 \quad 0 \leq t \leq \infty \tag{A.2}$$

where $F(\xi, t)$ is a nonstochastic function, provided that the state of the system is specified. For each state we have a $F_k(\xi, t)$ function,with $k = \alpha, \beta$. The nonstochastic initial condition assigned are:

$$\xi(0) = \begin{cases} \bar{\xi}_\alpha, & \text{if the system is in state } \alpha \text{ at } t = 0, \\ \bar{\xi}_\beta, & \text{if the system is in state } \beta \text{ at } t = 0, \end{cases} \tag{A.3}$$

In this case, being both the nonstochastic initial value problem and the transition between states Markovian, the process is called a *joint Markovian process*, for which we can use the Liouville master equation.

This equation describes, considering states as discrete, the joint probability density $P_k(\xi, t)$, defined such that $P_k d\xi$ is the probability that the system is in state k at time t and in the same time that the stochastic solution lies between ξ and $\xi + d\xi$.

For $k = \alpha, \beta$, the master equation is made by two coupled equations:

$$\frac{\partial P_\alpha}{\partial t} - \frac{\partial}{\partial \xi}(F_\alpha P_\alpha) = \frac{P_\beta}{\Lambda_\beta} - \frac{P_\alpha}{\Lambda_\alpha} \tag{A.4}$$

$$\frac{\partial P_\beta}{\partial t} - \frac{\partial}{\partial \xi}(F_\beta P_\beta) = \frac{P_\alpha}{\Lambda_\alpha} - \frac{P_\beta}{\Lambda_\beta} \tag{A.5}$$

with initial conditions:

$$P_k(\xi, t) = p_k(0)\, \delta(\xi - \bar{\xi}_k), \quad k = \alpha, \beta \tag{A.6}$$

Here $p_k(t)$ is the probability density of having system in state k at time t and its corresponding distribution function is $P_k(\xi, t)$. For definition, $p_k(t)$ satisfies:

$$p_k(t) = \int_{-\infty}^{\infty} d\xi \, P_k(\xi, t) \tag{A.7}$$

We can also write the coupled system in terms of simple differential equation for the $p_k(t)$ by integrating Eqs. (A.4) and (A.5) over all ξ, obtaining:

$$\frac{dp_\alpha}{dt} = \frac{p_\beta}{\Lambda_\beta} - \frac{p_\alpha}{\Lambda_\alpha} \tag{A.8}$$

$$\frac{dp_\beta}{dt} = \frac{p_\alpha}{\Lambda_\alpha} - \frac{p_\beta}{\Lambda_\beta} \tag{A.9}$$

which relate the probabilities $p_k(t)$ to the Markov transition functions Λ_k. Solving the equations (A.8) and (A.9), we have an expression for the $p_k(t)$:

$$p_k(t) = p_k(0) exp\left[-\int_0^t dt'' \frac{1}{\Lambda(t'')}\right] + \int_0^t dt' \frac{1}{\Lambda_l(t')} exp\left[-\int_{t'}^t dt'' \frac{1}{\Lambda(t'')}\right], \tag{A.10}$$

with $k \neq l$ and Λ expressed by Eq. (2.17).

The ensemble average of any function of the solution, say $H(\xi)$ is expressed by:

$$\langle H(\xi) \rangle = \int_{-\infty}^{\infty} d\xi H(\xi)[P_\alpha(\xi, t) + P_\beta(\xi, t)] \tag{A.11}$$

The Liouville master equation was first used to describe particle transport by Vanderhaegen in 1986.

He observed that the time independent, no scattering transport equation can be thought of an initial value problem, with initial values in space instead of

time. Thus, if the mixing statistics is Markovian, the transport problem is a joint Markovian process.

Considering the transport equation (1.6) and replacing ξ and t by, respectively, ψ and s, we have the expression for the function F in Eq. (A.2):

$$F(\psi, s) = \sigma(s)\psi - S(s) \tag{A.12}$$

and the general master eqation becomes:

$$\frac{\partial p_\alpha}{\partial s} - \frac{\partial}{\partial \psi}[(\sigma_\alpha \psi - S_\alpha)P_\alpha] = \frac{P_\beta}{\Lambda_\beta} - \frac{P_\alpha}{\Lambda_\alpha} \tag{A.13}$$

$$\frac{\partial p_\beta}{\partial s} - \frac{\partial}{\partial \psi}[(\sigma_\beta \psi - S_\beta)P_\beta] = \frac{P_\alpha}{\Lambda_\alpha} - \frac{P_\beta}{\Lambda_\beta} \tag{A.14}$$

with initial conditions given by:

$$\psi(0) = \begin{cases} \bar{\psi}_\alpha, & \text{if the boundary point } s = 0 \text{ is in material } \alpha \\ \bar{\psi}_\beta, & \text{if the boundary point } s = 0 \text{ is in material } \beta \end{cases} \tag{A.15}$$

where in this case they are initial condition in space, and boundary conditions given by:

$$P_k(\psi, 0) = p_k(0)\,\delta(\psi - \bar{\psi}_k) \tag{A.16}$$

for indices $k = \alpha, \beta$. As before, $P_k(\psi, s)d\psi$ is the joint probability density of finding material k at position s and a solution ψ lying between ψ and $\psi + d\psi$.

The relationship between the probability density $p_k(s)$ and the associated probability distribution function $P_k(\psi, s)$ is the same as for the preceding problem, but in this case the integral of Eq. (A.7) goes from 0 to infinity,

because there are no negative intensities of ψ:

$$p_k(s) = \int_0^\infty d\psi P_k(\psi, s) \tag{A.17}$$

Defining $\psi_k(s)$ as the conditional ensemble average of ψ, conditioned upon all the positions s being in material k, the definition of P_k gives the following relationship:

$$p_k(s)\,\psi_k(s) = \int_0^\infty d\psi \psi P_k(\psi, s) \tag{A.18}$$

We write also the expression for the ensemble average of the intensity $\langle\psi\rangle$, the unknown of transport equation we are interested in, which is the ensemble average of the intensity over all the physical realizations of the statistics.

$$\langle\psi(s)\rangle = p_\alpha(s)\,\psi_\alpha(s) + p_\beta(s)\,\psi_\beta(s) \tag{A.19}$$

The Eq. (A.19) has the same form of Eqs. (2.4) and (2.5), that express as well other ensemble-averaged variables.

Finally, we can note that, since $F(\psi, s)$ is linear in ψ, it is possible to write the two coupled equations (A.13) and (A.14) in ψ simply in a system in terms of the seeked unknown ψ_k.

Multiplying Eqs. (A.17) and (A.18) by ψ and integrating over $0 \leq \psi \leq \infty$ we have :

$$\frac{d(p_\alpha\psi_\alpha)}{ds} + \sigma_\alpha p_\alpha \psi_\alpha = p_\alpha S_\alpha + \frac{p_\beta\psi_\beta}{\Lambda_\beta} - \frac{p_\alpha\psi_\alpha}{\Lambda_\alpha} \tag{A.20}$$

$$\frac{d(p_\beta\psi_\beta)}{ds} + \sigma_\beta p_\beta \psi_\beta = p_\beta S_\beta + \frac{p_\alpha\psi_\alpha}{\Lambda_\alpha} - \frac{p_\beta\psi_\beta}{\Lambda_\beta} \tag{A.21}$$

Obviously, to find the corresponding initial and boundary conditions we have to multiply Eq. (A.16) by ψ and then integrate over $0 \leq \psi \leq \infty$:

$$\psi_\alpha(0) = \bar{\psi}_\alpha, \quad \psi_\beta(0) = \bar{\psi}_\beta \tag{A.22}$$

Thus, we have found a complete and exact description for the ensemble-averaged intensity $\langle\psi(s)\rangle$ for time independent, no scattering transport in binary Markovian mixture.

A.2 *The master equation for the case of non zero scattering*

As seen before, the Liouville master equation gives an exact description for the uncollisionless initial value transport problem. This is never the real case, in which scattering is present and important.

The master equation can not be used, in principle, when scattering is included, because it destroyes the Markovian nature of the basic transport problem: with scattering, the transport equation is a bounded value problem and thus it does not possess the properties of a Markov (initial value, " memoryless ") process.

Nevertheless, Liouville master equation is often employed, in an approximate way, to describe time independent, scattering transport problem in Markovian stochastic mixtures.

The problem with scattering included arises from the need of boundary conditions: the transport equation is mixed, through the integral scattering operator, for different direction. It is not possible to solve the problem for the

intensity in a given direction independently of the solution from the other; the single solution is dependent upon the boundary conditions for all other directions. Further, this type of problem can not be interpreted as an initial value problem, since the solution depends upon more than just one initial value: the boundary conditions are applied at two spatial positions, namely the two edges of the system.

Therefore, including scattering, the transport equation does not describe a Markov process and, when coupled with the mixing process (Markovian or not), the resulting joint process is not Markovian anymore.

Nevertheless, the use of the master equation can give a useful and simple, even if approximate, model for particle transport in scattering stochastic mixtures.

Considering the inscattering term of Eq. (1.1), namely

$$\text{Inscattering} = \int_0^\infty dE' \int_{4\pi} d\mathbf{\Omega}' \sigma_s(E' \to E, \mathbf{\Omega}' \to \mathbf{\Omega}) \psi(E', \mathbf{\Omega}'), \qquad \text{(A.23)}$$

in the same way as the internal source term $S(E, \mathbf{\Omega})$, we obtain two coupled equations:

$$\left(\frac{1}{v}\frac{\partial}{\partial t} + \mathbf{\Omega}\cdot\nabla\right) P_\alpha - \frac{\partial}{\partial \psi}\{[\sigma_\alpha \psi + (C_\alpha - \sigma_\alpha)\psi_\alpha - S_\alpha]P_\alpha\} = \frac{P_\beta}{\Lambda_\beta} - \frac{P_\alpha}{\Lambda_\alpha} \qquad \text{(A.24)}$$

$$\left(\frac{1}{v}\frac{\partial}{\partial t} + \mathbf{\Omega}\cdot\nabla\right) P_\beta - \frac{\partial}{\partial \psi}\{[\sigma_\beta \psi + (C_\beta - \sigma_\beta)\psi_\beta - S_\beta]P_\beta\} = \frac{P_\alpha}{\Lambda_\alpha} - \frac{P_\beta}{\Lambda_\beta} \qquad \text{(A.25)}$$

in which C_k is the collision operator for the transport equation written for the kth material, *i.e.*,

$$C_k = \sigma_k - \int_0^\infty dE' \int_{4\pi} d\mathbf{\Omega}' \sigma_{sk}(E' \to E, \mathbf{\Omega}' \to \mathbf{\Omega}) \tag{A.26}$$

and $\psi_\alpha(E', \mathbf{\Omega}')$ and $\psi_\beta(E', \mathbf{\Omega}')$ are the ensemble average of ψ over the continous states for which the system is in material α or β at any given $\mathbf{r}$ and t point.

The approximation made using the master equation for the case of non zero scattering is to replace the discete/continous random variable $\psi(E', \mathbf{\Omega}')$ in the inscattering term with a purely discrete two state random variable.

Again, $P_k(\psi, \mathbf{r}, E, \omega, t)d\psi$ is the joint probability of finding material k at space-time point $(\mathbf{r}, t)$ and having the intensity solution lying between ψ and $\psi + d\psi$, $\psi_k(\mathbf{r}, E, \mathbf{\Omega}, t)$ is the conditional ensemble average of ψ (averaged over the states for which the system is in material k at time t and position $\mathbf{r}$); similarly, relationships as (A.17) and (A.18) are still valid.

In the same way as before, we can derive, by multiplying Eqs. (A.24) and (A.25) for ψ and integrating over $0 \leq \psi \leq \infty$, the two coupled equation in function of the $\psi_k(\mathbf{r}, E, \mathbf{\Omega}, t)$:

$$\frac{1}{v}\frac{\partial(p_\alpha\psi_\alpha)}{\partial t} + \mathbf{\Omega} \cdot \nabla(p_\alpha\psi_\alpha) + C_\alpha(p_\alpha\psi_\alpha) = p_\alpha S_\alpha + \frac{p_\beta\psi_\beta}{\Lambda_\beta} - \frac{p_\alpha\psi_\alpha}{\Lambda_\alpha} \tag{A.27}$$

$$\frac{1}{v}\frac{\partial(p_\beta\psi_\beta)}{\partial t} + \mathbf{\Omega} \cdot \nabla(p_\beta\psi_\beta) + C_\beta(p_\beta\psi_\beta) = p_\beta S_\beta + \frac{p_\alpha\psi_\alpha}{\Lambda_\alpha} - \frac{p_\beta\psi_\beta}{\Lambda_\beta} \tag{A.28}$$

with initial and boundary conditions given by:

$$\psi_k(\mathbf{r}, E, \mathbf{\Omega}, 0) = \tilde{\psi}_k(\mathbf{r}, E, \mathbf{\Omega}) \tag{A.29}$$

and

$$\psi_k(\mathbf{r_s}, E, \mathbf{\Omega}, t) = \bar{\psi}_k(\mathbf{r_s}, E, \mathbf{\Omega}, t), \quad \mathbf{n} \cdot \mathbf{\Omega} < 0 \tag{A.30}$$

where $\mathbf{r_s}$ is a point on the surface of the system and $\mathbf{n}$ is a unit outward normal vector at $\mathbf{r_s}$.

Equations (A.27) and (A.28) are the equations for the standard model in case of scattering transport problem in Markovian stochastic mixtures. They represent the model from which the Levermore Pomraning model is derived.